"OPTIMIZATION ANALYSIS OF ORGANIC CARBON CONCENTRATION AND SEDIMENTATION RATE IN THE ANZA GRABEN, KENYA."

by

Cornel Sewe

A thesis submitted in partial fulfillment for the degree of Master of Science (Geology) in the University of Nairobi

1995

DECLARATION

This thesis is my original work and has not been presented for a degree in any other university.

Cornel Sewe

Cornel Sewe

This thesis has been submitted for examination with our knowledge as university supervisors.

Nyambok

Prof. Isaac O. Nyambok

BMboya.

B.G.O. Mboya

CONTENTS

LIST OF FIGURES

LIST OF TABLES

ABSTRACT

The Anza Graben is a major NW-SE structurally oriented sedimentary basin that lies in the northern part of Kenya roughly between the latitudes O° 30'N and 4°N, longitudes 36° 30'E and 41°E. Three basins: North, Central and South Anza define the graben and the main sub-basins comprise Chalbi in the northwest, the Yamicha in central and southeast and the Intermediate Tilted Blocks in the middle. The evolution, stratigraphy and environments of deposition of the sedimentary sequences of the basin, are discussed together with the post Gondwanaland break-up marine incursions in the graben.

Burial plots based on studies of five selected wells have been used to construct burial history curves for the named sub-basins and to calculate the TTI (Time-Temperature Index) indices. The results redefine maturity profiles and the hydrocarbon generation history of the basin. The oil window is determined from TTI in this study to occur from 2500 m to Total Depth (TD) for Bellatrix-1 and 1500 m to TD for Sirius-1 both of which are in the Chalbi sub-basin. In the Yamicha basin the window runs from 2500 m to TD (Ndovu-1) and 2550 m to TD for Anza-1 wells. The Intermediate Tilted Blocks area, Duma-1, has the window between 2500-3100 m depth.

The scope of heat flow in the basin is generally moderate. The average geothermal gradient for the graben is 24.9°C/km. Chalbi sub-basin, owing to its vicinity to the main Kenyan rift records a slightly higher value of 26.6-27.6°C/km. In the Yamicha area 22.2-24.0°C/km is observed while 23.9°C/km is noted in the Intermediate Tilted Blocks area.

Empirical relationships between the paleosedimentation rates and Total Organic Carbon values give optimum sedimentation rates of 30-90 m/M.Y for the Chalbi sub-basin with a corresponding T.O.C. value of 0.9 - 1.4% which is well above the 0.5% prospective threshold.

The central region of the Yamicha sub-basin gives 1.2% T.O.C. and an optimum paleosedimentation rate which is highest for the wells studied at 160-260 m/M.Y. Both the paleosedimentation rate and T.O.C. are, however, lower in the southeastern flanks of the Yamicha at 14-25 m/M.Y. and 0.3% T.O.C. The low T.O.C. percentage here is attributed to the low paleosedimentation rate and possible little or low availability of organic matter (source material).

The results of this study also show that in the entire graben, the optimum sedimentation rates and the corresponding T.O.C. are associated with shales, sandstones and limestones (in Sirius-1 only). In this regard, the role of shales and limestones as source rocks, and sandstones as possible reservoir rocks are noted. The overall pattern of these optimized empirical relationships, though applicable largely in specific individual sub-basin, do present an interesting hydrocarbon prospect in each of the three sub-basins of the graben when related to other hydrocarbon potential indicators namely Vitrinite Reflectance (R_o), Transformation Ratio and the temperature of maximum hydrogen generation during pyrolysis, (T_{max}).

There is an excellent match in the depth of the oil window as defined by TTI and the R_o in all the wells except for Duma-1. A close correlation between the TTI oil window and the Transformation Ratio is also observed in all the wells. They both give 2500 m to TD in Ndovu-1, and a T_{max} within the peak range at 421-483°C. In Anza-1 2480 m to TD is noted, with a relatively low T_{max} at 294-302°C possibly due to uplift and erosion. In Duma-1 2500 m to TD is recorded with a T_{max} of 469-483°C as compared to TTI result of 2500 to 3100 m. In both Bellatrix-1 and Sirius-1, the Transformation Ratio occurs slightly above that predicted by the TTI at 2620 m to TD with a T_{max} of 443-446°C and at 1900 m to TD with a T_{max} of 443-582°C in Bellatrix-1 and Sirius-1 respectively.

ACKNOWLEDGEMENTS

I am very grateful to Professor Isaac Nyambok for his patience and keen guidance during the entire phase of this work. It was indeed his initial suggestion that I undertake the research project in the country as opposed to an external scholarship in order to enhance the existing knowledge on the petroleum potential of Kenya.

I am also grateful to Mr. B.G.O. Mboya who as my second supervisor kindly assisted me in understanding many salient aspects of sedimentology.

Scholarship for this study was granted by Total CFP through Total Exploration and Production in Nairobi. I am extremely grateful to the company for both the award and for granting me leave to carry out the work. I wish to mention especially Dr. Mitchel Brun, (Regional Geologist), Pierre Six (Regional Manager) and Bruno Tixier (Technical Manager for North & East Africa) for their exceptional understanding, assistance, support and encouragement with this project. I am also indebted to Mr. Phillipe Biro, former Oil Exploration Advisor to the Kenya Government for his insight and valuable discussions during the initial stages of the project. Mr. Don Riaroh of the Ministry of Energy availed to me useful personal collection of petroleum journals, publications, reports etc. and also held helpful discussions with me on numerous occasions for which I am extremely grateful.

I am also thankful to the Geology Department for the opportunity to study at the department and for use of departmental facilities. Some part of the analysis and final bits of this work was done at the lab and office facilities of the National Oil Corporation of Kenya. I wish to acknowledge this assistance.

Lastly, I am grateful to the Office of the President for granting me permission to do research (Permit No. 283/2 of Oct. 1991) and to the Permanent Secretary, Ministry of Energy for permission to use exploration data held at the National Oil Corporation of Kenya.

Opinions and conclusions expressed in this study are those of the author and do not necessarily represent the official position of Total CFP, any of the oil companies and persons mentioned in this study, nor does it represent the official position of the Kenya Government, regarding hydrocarbon exploration in the country.

CHAPTER 1

INTRODUCTION

1.1 Position of the Study Area in Kenya

The Anza Graben defines a major NW-SE structurally oriented sedimentary basin that runs over the entire north and north-eastern Kenya. It lies roughly between the latitudes 0°30'N and 4°N and longitudes 36°30'E and 41°E (Fig. 1). The graben has similar trend and age with the Abu Gabra rift of the south Sudan (Beicip, 1984).

Owing to its favourable sedimentary formations, the basin has been the site of selective oil prospecting since 1984. Eleven oil wells have been sunk in the area to date with various amounts of gas and oil shows. No production, however, has been achieved.

1.2 Objectives and Scope of the Study

The main objectives of the study include the following:

(a) To study the concentration and pattern of organic carbon of the identified hydrocarbon bearing horizons in the basin through paleosedimentation rate analysis and their respective paleoenvironments using the method developed by Magara (1986), and to carry out quantitative evaluation of kerogen i.e Total Organic Carbon (T.O.C) where existing data is inadequate based on the procedure by Tissot and Welte (1978).

(b) To give an indication of the maturity of the organic matter through an analysis of burial plots using Lopatin's Time Temperature Index (TTI) of maturity.

(c) To relate sediment types with the optimum paleosedimentation rates and concentration of organic carbon.

(d) To attempt basinwide lithological correlations of the results obtained.

(e) To make any appropriate recommendation(s) on the status of hydrocarbon potential based on (a) to (d).

In order to achieve these objectives, five wells from the basins, namely, Bellatrix-1, Sirius-1, Ndovu-1, Anza-1 and Duma-1 were utilized in the study. It is also important to note that all the three techniques (a) to (c) have not been applied in the basin before.

1.3 The Study Concept / Literature Review

Studies on 25742 samples from the Russian Platform has shown that there is a significant difference between the petroliferous and non-petroliferous regions on the concentration of organic carbon which constitutes the main proportion of the organic matter (Ronov, 1958). Based on this data and other known evidence, an arbitrary empirical lower limit of the 0.4 weight % organic carbon (or 0.5 weight % organic matter) is generally accepted as the minimum kerogen concentration necessary for any significant hydrocarbon generation (Dow, 1978).

Since production, transportation and preservation or destruction of organic matter can be influenced or controlled by the environmental factors, an empirical relationship exists between depositional rate vis-a-vis environment and concentration of organic carbon (Magara, 1986). Where drilled data and seismic profiles are available, depositional environment, organic carbon concentration and respective rates of sedimentation can be determined and the empirical relationship between the sedimentation rate and organic carbon concentration established. An important application can be generated especially information on the best potential of organic carbon concentration from a plot of organic carbon versus sedimentation rate; where there is an optimum rate of sedimentation for the maximum concentration of organic carbon in sediments, as shown in Fig. 3 below (Dow, 1978; Selley, 1985). This method may also be used to compare the estimated potential of different prospects which would allow a petroleum geologist to rank these prospects.

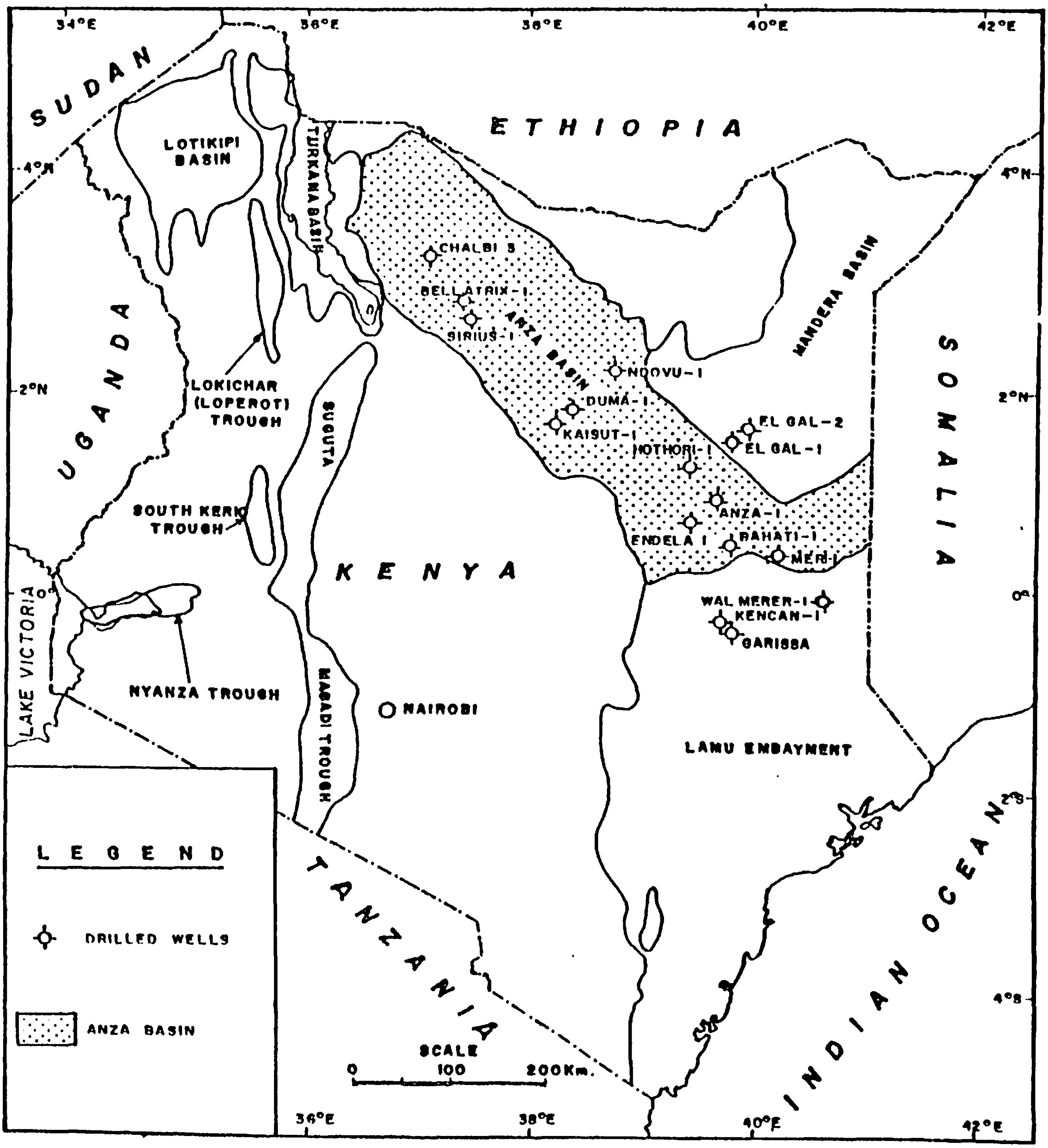

Fig. 1. Major sedimentary basins of Kenya including the Anza basin (shaded)

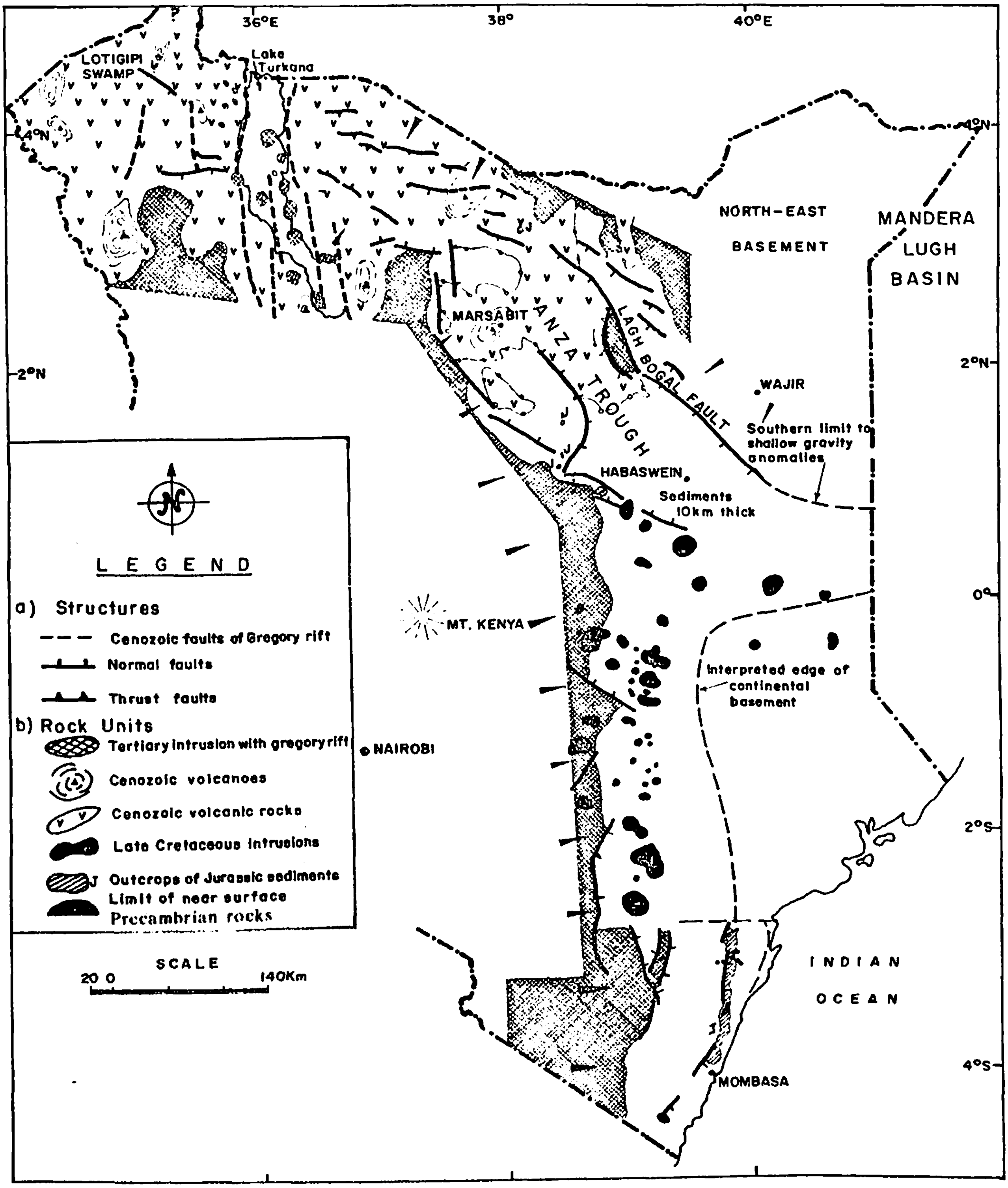

Fig. 2. Polyphase rifting in eastern and northern Kenya and the position of Anza Graben. (After Reeves et al, 1986).

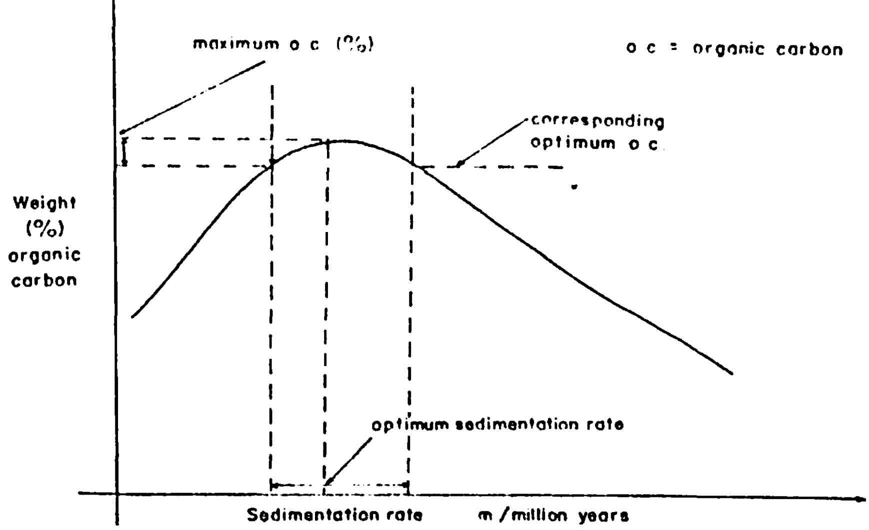

Fig. 3 - A typical carbon concentration vs Sedimentation rate curve.
(After Magara, 1986).

It should be noted that the average rate of sedimentation of a given geologic interval in an undrilled area may be estimated from the thickness of the interval and the corresponding geologic time, both of which can be estimated using seismic data or regional correlation. This gives the method an added advantage in that information on synclinal areas from which most petroleum is believed to be derived, and which is seldom available owing to lack of well data there, can be obtained. Such estimates of the best potentials of the organic carbon concentration can be quite valuable (Magara, 1986).

Having determined the presence of optimum organic matter, the the maturity of the sediments must be investigated. The major parameters controlling the generation of hydrocarbon are type and amount of organic matter in the source rock and its organic maturation evolution. Although the role of pressure is influential at low levels of organic maturation, it is now universally acknowledged that temperature is the most important parameter affecting hydrocarbon generation (Brooks,1981). The effects of temparature and time are recognized as essential parameters in evaluating maturation processes. Early efforts that took both time and temperature into account in studying the process of oil generation were developed by N.V. Lopatin (Waples 1981). In this method, the thermal maturity of organic material in sediments is calculated, and has been quantified as the Time Temperature Index (TTI). These factors are interchangeable; a high temperature acting for a short time can have the same effect on the maturation as low temperature

acting over a longer time. The dependence of maturity on time is linear. The implementation of this method is achieved through reconstruction of the depositional and tectonic history of the geologic section of interest.

By defining a factor which reflects the exponential dependence of maturity on temperature, the rate of maturation is taken to increase by a factor of 2 for every 10° C in reaction temperature. The length of time (in units of M.y.) is that time the sediments spent in each defined temperature interval (determined from geothermal gradient). Because maturation effects on organic material are additive the total maturity (or TTI) of a given sediment is equal to the sum of maturities acquired in each interval (Waples,1981). Thus

$$TTI = \sum_{n_{min}}^{n_{max}} 2^n \, T_n$$

Where n_{max} and n_{min} are the n-values of the highest and the lowest temperature intervals encountered. The TTI values in this study are correlated with the data obtained from other methods of evaluating the thermal maturity of organic material.

1.4 Previous Geologic Work

Lack of indigenous fuel resources, other than wood in Kenya, has led to the exploration for oil in the Mesozoic basin of north-eastern Kenya since the 1930's. A two year Oil Exploration Licence effective Feb. 1937 was granted to D'Arcy Exploration Co. Ltd. and the Anglo-Saxon Petroleum Co. Ltd covering about 195,000 sq. km in eastern Kenya, (Government Notice No. 167, 1937). It was however, relinquished after rapid geological reconnaissance.

The same area was examined a year later (Government Notice No. 613, 1938) by Kenya Oil Exploration Co. Ltd., employing the services of T. Dejean, W.G. Serra and J. Parkinson. The block was abandoned yet again in 1940. Joubert (1960) working in the area noted the occurrence of Didimintu Beds in north-eastern Kenya and suggested a marine link with Madagascar during the Toarcian times. He contended in his report that sea transgression with sea-level rise created the likelihood that at some stage in the sedimentation (given that the marine gulf in north-eastern

Kenya was somewhat restricted) favourable conditions for the formation of oil existed (Fig. 8). Indeed areas offering the highest chances of success are traditionally described as those areas of the earth where there are thick marine sediments containing in their sections dark shales and porous sands, where there are plenty of gentle folds but not violent fractures and where there is adequate impermeable cover.

Thompson and Dodson (1958) while working in area to the northeast of the study area noted in their report that on several occasions during the previous 20 years, the occurrence of oil deposits in north-eastern Kenya had been considered by both official and non-official bodies.

Two years later, Thompson and Dodson (1960) while noting no visible signs of the presence of oil, observed that the presence of Mansa Guda formation in the Bur Mayo-Tarby area (the equivalent of Matasade Formation in the study area) may be important indicators of the probable presence of pre-Jurassic marine sediments below parts of the basin further east.

During his survey of the western side of the Anza basin in the Garba Tula area, Matheson (1971) attributed the occurrence of Mesozoic sediments in northeastern Kenya and the Coast Province to a marine incursion. He observed that uplift and erosion were followed by a marine incursion in the Jurassic leading to deposition of sandstones. He cited the well-compacted fine-gained sandstones at Kubi Dakhara (Garba Tula area) - similar to Mansa Guda formation, Dogogicha and Duruma sandstones, as examples of this clastic deposition.

Miller (1973) in his geologic study of Garissa-Wajir area noted several occurrences of Jurassic formations northwest of Mado Gashi (Fig.9). These were mainly sandstones with local fossiliferous limestone intercalations. Although Pliocene and Quaternary sediments blanket the area (corresponding to the southern end of Anza) he noted that they are underlain by an extensive sedimentary section which, with several unconformities, span in time from Permian to Miocene. The late Triassic/early Jurassic to Cretaceous are singled out as being important for oil. He proposed that any feature that distinctly separated the Lamu Embayment from the shelf limestones to the north could, if active during the Jurassic, cause a profound change in the Jurassic section. Such a change, in his opinion, could be important for the occurrence of oil.

More recently, exploration activities of TOTAL in the mid 80's, in consortium with other oil companies in an area covering the middle of the Anza Graben has established the presence of several structural sedimentary units in several sub-basins namely: Kaisut basin, the Intermediate Tilted blocks and the Yamicha basin (Fig. 4). The northern parts of Anza, around Marsabit is covered by volcanics. The stratigraphy developed from these studies confirm marine influence in the lower Cretaceous and again in the upper Cretaceous. In the Yamicha basin, lower Cretaceous (Barremian-Hauterivian) rocks are found from about 4,000 m depth to 1500 m, giving way to Tertiary sediments. Although Kaisut basin is mostly barren and hence difficult to date, the adjoining basin with the Yamicha is composed of Quaternary, Mesozoic and Paleozoic sediments (beyond 3,000 m). Sandstone and siltstone formations with alternations of shale and clay were found to predominate in this intermediate basin. Both the Intermediate basin and the adjoining Yamicha basin are known to contain hydrocarbon occurrences in their profiles (Tepma, 1988).

Investigations by Amoco Kenya (1988) in the Hothori-Desert, south-eastern part of Yamicha basin, revealed upper Cretaceous strata at about 4700 m. Considerably thick (ca 3400 m) Tertiary rift-fill sandstone sequences interbedded with minor claystone/clay and shale intercalations were encountered. Although the sediments were mainly of continental facies, some marine facies were encountered in the section suggesting minor marine transgressions. Below the sandstones were Cretaceous fluvial-lacustrine shale/sandstone sequences. Hydrocarbon gases were detected from 2,200 m to 4,700 m, including weak shows of liquid hydrocarbons or condensates at about 2852 m.

Towards the south-eastern end of Anza Graben, investigations revealed, in gross aspects, sand dominated profiles with negligible shale (Miller, 1973). The continental sands rest on lower Cretaceous. Although the sands display good porosity, they were found to be devoid of hydrocarbon indications other than small methane shows. Diorite intrusions in the 3047-3053 m were observed, dating 8.8 - 10.9 Ma. Pertinent lab reports suggest that owing to the small amount and the continental type of organic matter, the whole section of Anza-1 well should be considered as of very poor or non-source rock.

Exploration ventures by Amoco Kenya in the north-west end of the Anza Graben, 50 km NW of Marsabit, in the Horr area, has added to our knowledge of the Chalbi sub-basin. Thick Tertiary sand overlie interbedded sandstone and shale sequences of Cretaceous age. Massive good reservoir quality sandstone underlie the sequences. This section has been proposed as a possible target for future exploration. Dolomite and dolomitic limestone section overlying the basement (Mozambique Belt rocks) were noted. Gas and oil shows have been reported after the 1,180 m depth, with good visible oil show within an interbedded sandstone at 2,300 m. Geological setting of the region is believed to be similar to the Abu Gabra Rift in the southern Sudan where Chevron has made oil discoveries from Lower Cretaceous sandstones (Fig. 6).

The profile described above (Bellatrix-1 well) is repeated somewhat in an area about 20 km slightly to the south, where Sirius-1 well was sunk, thus emphasizing the regional extension and similarity of the graben sedimentology within the Chalbi sub-basin (Fig. 4). Here the surface volcanics overlie the thick Tertiary sands, followed by interbedded sand/sandstone, siltstone and clay/claystone sequence of possible upper Cretaceous age. Interbedded sandstone/shale/coal seam sequence of about 50 m follows. A quartzitic section that is possibly a diagenetically altered sandstone overlie the basement.

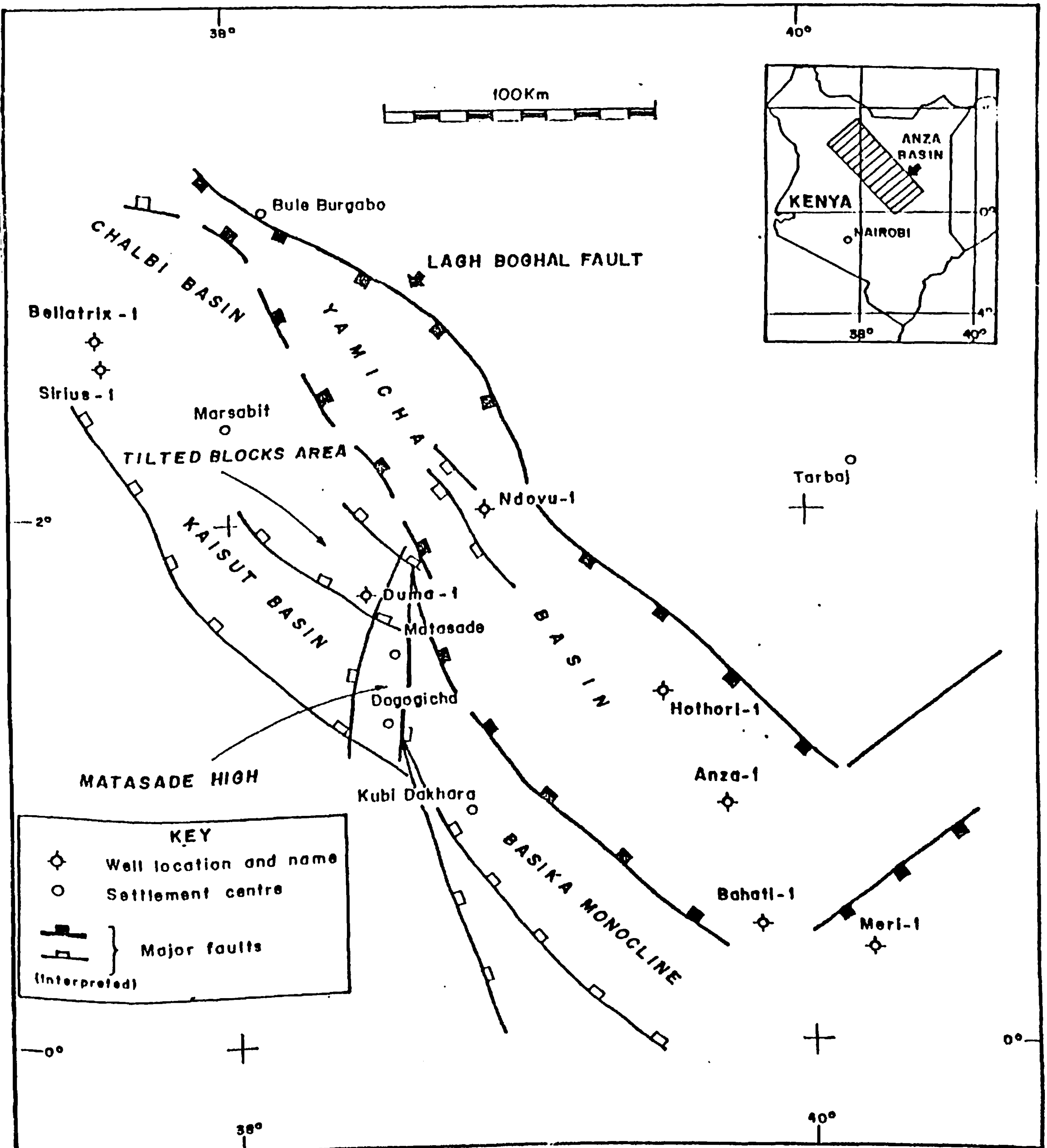

Fig. 4. Structural configuration of the Anza Graben showing the sub-basins and the five wells under study : Sirius-1 and Bellatrix-1 (Chalbi sub-basin), Ndovu-1, and Anza - 1 (Yamicha sub-basin) and Duma - 1 (Intermediate Tilted Blocks).

CHAPTER 2

EVOLUTION OF THE ANZA BASIN

2.1 The Anza Graben

The Anza graben is separated from the Mandera basin by the major NW-SE trending Lagh Boghal fault, which also marks the flank of its north-western half graben end (Figs. 2 and 4). Its southern part, is terminated in the Meri area, by a large ENE-NSW striking syncline, with step faulted flanks.

2.2 Origin of the Graben

Epeirogenic movements associated with the Gondwanaland break-up at the end of Jurassic time affected the borders of Kenyan basins, initiating rifting in early Cretaceous/late Jurassic time in the Anza region. NE-SW tensional forces created the NW-SE trending graben after an initial rifting phase and developed during the Cretaceous and Tertiary times into a failed rift (Fig. 8). The existence of Karroo sequence in the Wajir area, established from field outcrops and based on seismic interpretations, point to the presence of the Karroo in the southern part of the Anza Graben. This means that this area was part of the rift sedimentation in Karroo time (Beicip, 1984).

According to studies by Beicip (1984), the initial rifting activity has been confirmed by the presence of a thinned lithosphere beneath the Anza graben as shown in Fig. 5. Similar interpretations have been given by other authors to explain the origin of the grabens in the southern Sudan (Abu Gabra), Chad and Niger, which developed during the same period (Schull, 1988). Beicip (1984) noted that regional rifting activity at that time may have been related to the opening of the South Atlantic and Indian Oceans.

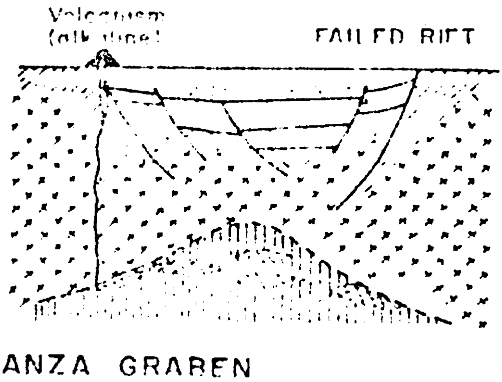

Fig. 5 - Thinned lithosphere beneath the Anza Graben.
(After Beicip, 1984).

2.3 Regional Setting

Recent studies (Bosworth and Morley, 1992; Reeves *et al*, 1986) suggest that the Anza Graben represents an arm of a failed rift or (aulocogen) extending through Marsabit towards Lake Turkana (Rabinowitz and Favey, 1982). Based on the results of these studies, and others (Beicip, 1984; Bossellini, 1986; Chenot, 1988; Dindi, 1992) which are largely derived from the interpretation of available aeromagnetic survey data for Kenya together with gravity data, the existence of a paleo-tripple junction of Jurassic age in Eastern Kenya is established (Fig. 7). Two arms, represented by the Mombasa coast and the Somalia coast respectively, developed into a part of the Indian ocean. The third arm, represented by the Anza Graben, now concealed by Quaternary sediments and volcanic rocks, remains a rifted, sediment-filled trough extending at least as far northwest as the presently active East Africa Rift in the Lake Turkana area. It appears that the first arm, along the Mombasa coastline (Fig. 7), is a rejuvenation of the older, possibly Karroo, rift initiated during the late Carboniferous times and continued with subsequent deposition to Jurassic times.

Fig. 6 is an attempt to show the pre-break-up polyphasic rifting during the Mesozoic times. In this illutration the southern terminus of the exposed basement of northeastern Kenya represents the second arm. This extends to Bur Acaba region of Somalia, (Fig. 6 and 7). It became active in Jurassic following the failure of an earlier parallel rift to the north, now preserved as Mandera Lugh Basin (Reeves *et al*, 1986). The rifting is thought to have developed into ocean-floor spreading and the departure of some other fragments of Gondwanaland from Kenya-Somalia coastline, which shows marine sedimentary conditions throughout the Jurassic. Some evidence exists of a major delta prograding southwards into the proto-Indian ocean in the vicinity of Lamu Embayment (Cannon *et al*, 1984; Reeves *et al*, 1986; Dindi, 1992).

A hingeline to the north of Lamu Embayment, perhaps a subsurface extension of Bur Acaba basement is thought to separate coastal/deltaic conditions from a fluvio-lacustrine environment in the trough itself (Reeves *et al*, 1986). Recent basin analysis work by the staff of NOCK have since confirmed this change-over position (Biro, 1991, per. comm.). The Anza Graben may be traced with certainity for 600 km to the northwest, as far as Lake Turkana on a NW-SE trend.

2.4 Marine Influence in the Basin

Geological evidence shows that the entire Graben was subjected to an extensive marine transgression during the Upper Jurassic time, (Joubert, 1963; Cannon *et al*, 1980; Beicip, 1984; Reeves *et al*, 1986; Tepma Kenya, 1988; 1989). Jurassic outcrops, for instance in the west of the Graben (Matasade and Dogogicha, Figs. 4 and 7) are part of a late Jurassic marine transgression over the basement which took place within the platform-type environment that developed here at the time (Beicip, 1984). This development is thought to have resulted from the failure of the northern arm (Mandera-Lugh basin) to fully develop when the southern arm of the rift between Africa and Madagascar gave birth to the proto-Indian ocean (Cannon *et al.*, 1982; Beicip, 1984).

According to Reeves *et al* (1986), Cretaceous marine regression to the region of Lamu Embayment marked the return of continental conditions, and tectonic events led to marked deposition in the Anza Graben. This pattern continued into the Tertiary, with Lamu Embayment experiencing large-scale subsidence, causing the prograding delta of the tripple

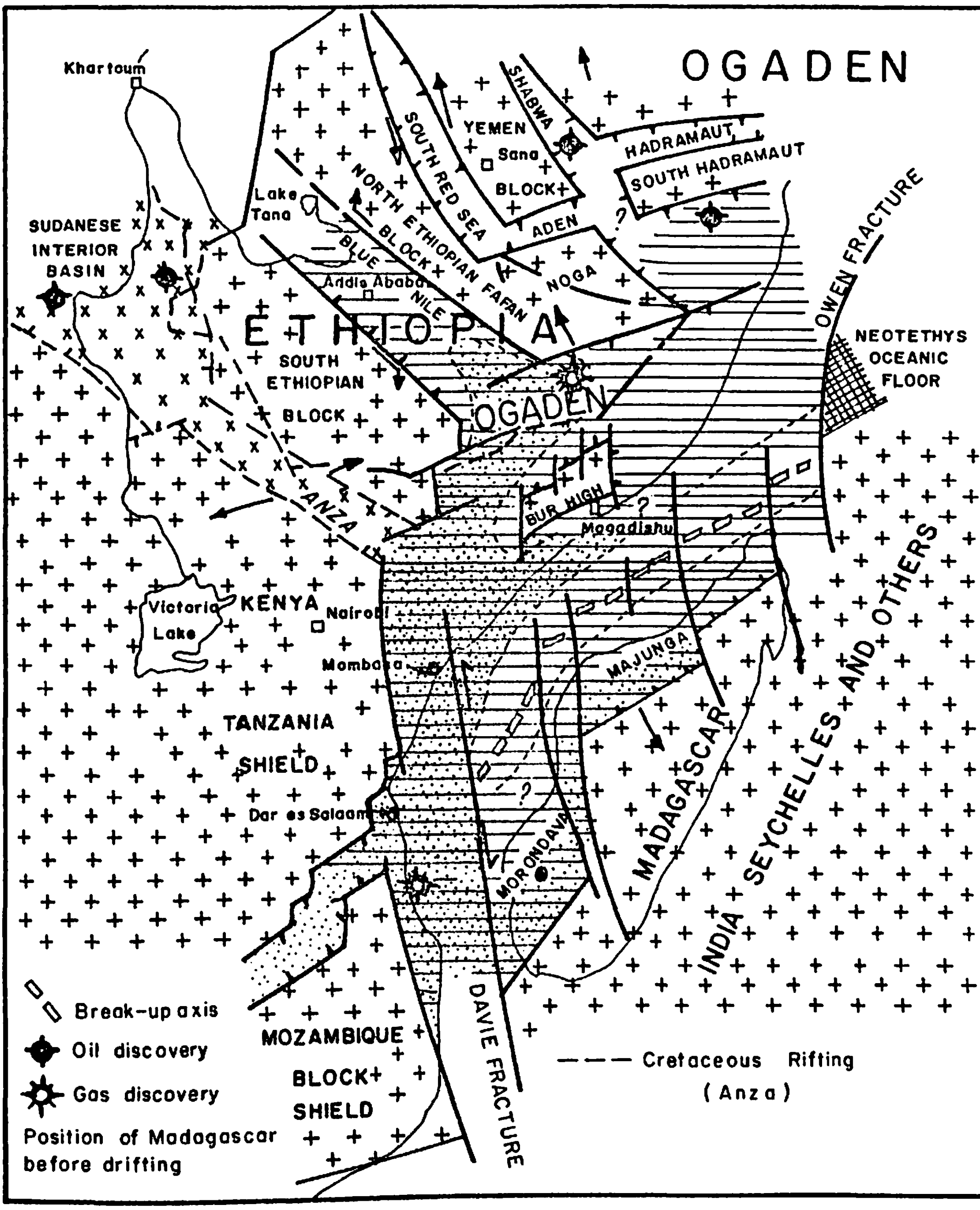

Figure 6. Polyphasic rifting in East Africa during the Mesozoic and the Karroo-Jurassic hydrocarbon occurrence in the region (*After Beicip, 1984*).

junction to become so large as to occupy the whole of the coastal Kenya. The Anza Graben continued to receive continental fluvio-lacustrine sediments during the same period. Investigations carried out by Matheson (1971) in the central part of the area indicated that after a long period of uplift and erosion, there was a marine incursion in the early Jurassic which led to the deposition of sandstones. He noted further that this incursion is probably responsible for the occurrence of the Mesozoic rocks in north-eastern Kenya and the Coast province, although these are largely covered by later deposits in the present area of study. The Jurassic shallow water carbonates on the Matasade High (Fig. 4) is thus considered as an important evidence (demonstrates the presence of a seaway connection) linking the Jurassic marine incursion with continental rifting which led to the separation of Madagascar from East Africa in the middle Jurrasic (Bosworth and Morley, 1992).

2.5 Sediment Thickness

Based on the interpretation of reflection seismic data carried out as a supplement to this study, the maximum thickness of the sediments in the Anza graben is about 6,000 - 8,000 m. It is filled with continental sediments with lacustrine intercalations (Beicip, 1985; Tepma, 1988; 1990). Of significance is the observation that gravity interpretation, supported by that of the magnetics, indicate the graben to be somewhat asymmetrical, being generally deeper to the northeast against Lagh Boghal fault (Reeves *et al*, 1986).

2.6 Structures

Tensional forces in the Graben resulted in listric faulting with its associated roll-over structures and compensation faults (Bosworth and Morley, 1992). The roll-over structures are expressed in the sediments along the borders of the graben whereas there is evidence of shale diapirs in central part (Beicip, 1984). NW-SE trending faults define three main structural sub-basins of the graben: Chalbi basin (Bellatrix & Sirius wells), Yamicha basin (Ndovu and Anza wells) and the Intermediate Tilted blocks basin where Duma well is located (Fig. 4).

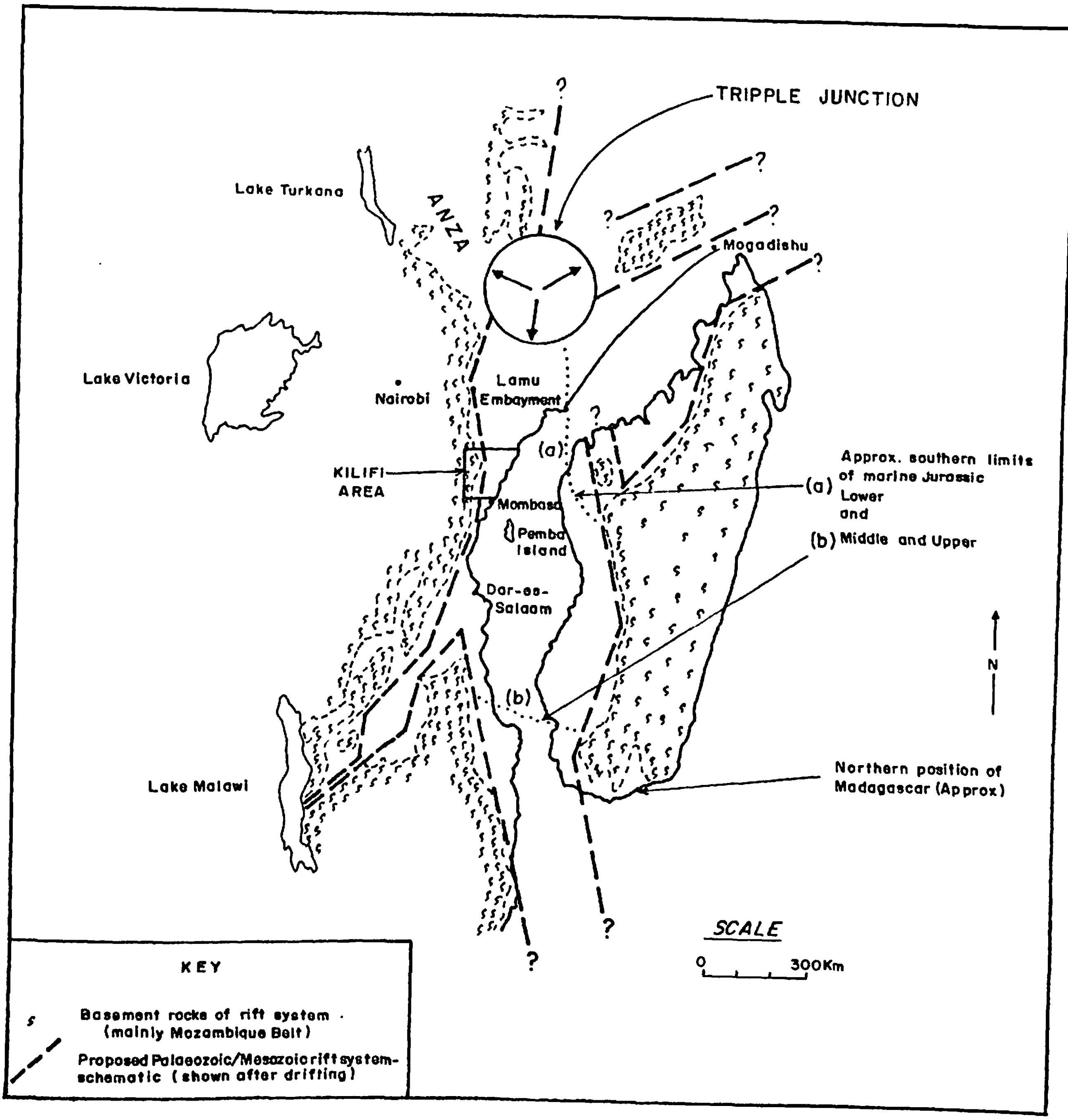

Fig. 7. Sketh map of the Paleozoic/Mesozoic triradial rift system in E.Africa and the marine Jurassic. (After Tectonic map of Africa, UNESCO/C.C.G.M., 1971 : Cannon et al, 1981).

2.7 Influence of the East African Rift

The initiation of the East African Rift System in the Miocene times (Reeves *et al*, 1986), resulted in the uplift and erosion of the Marsabit-Turkana region in the vicinity of the present day Lake Turkana, and reactivated block-faulting in the Mesozoic troughs further east, allowing them to continue receiving sediments during the Tertiary times. This is also suggested in the burial curves for Bellatrix-1 and Sirius-1 wells (Figures 23 and 27 respectively) that are sited in the area.

The sequence of events related to the Graben is summarized in (Fig. 8), which is adapted from Beicip (1984) and Reeves *et al* (1986).

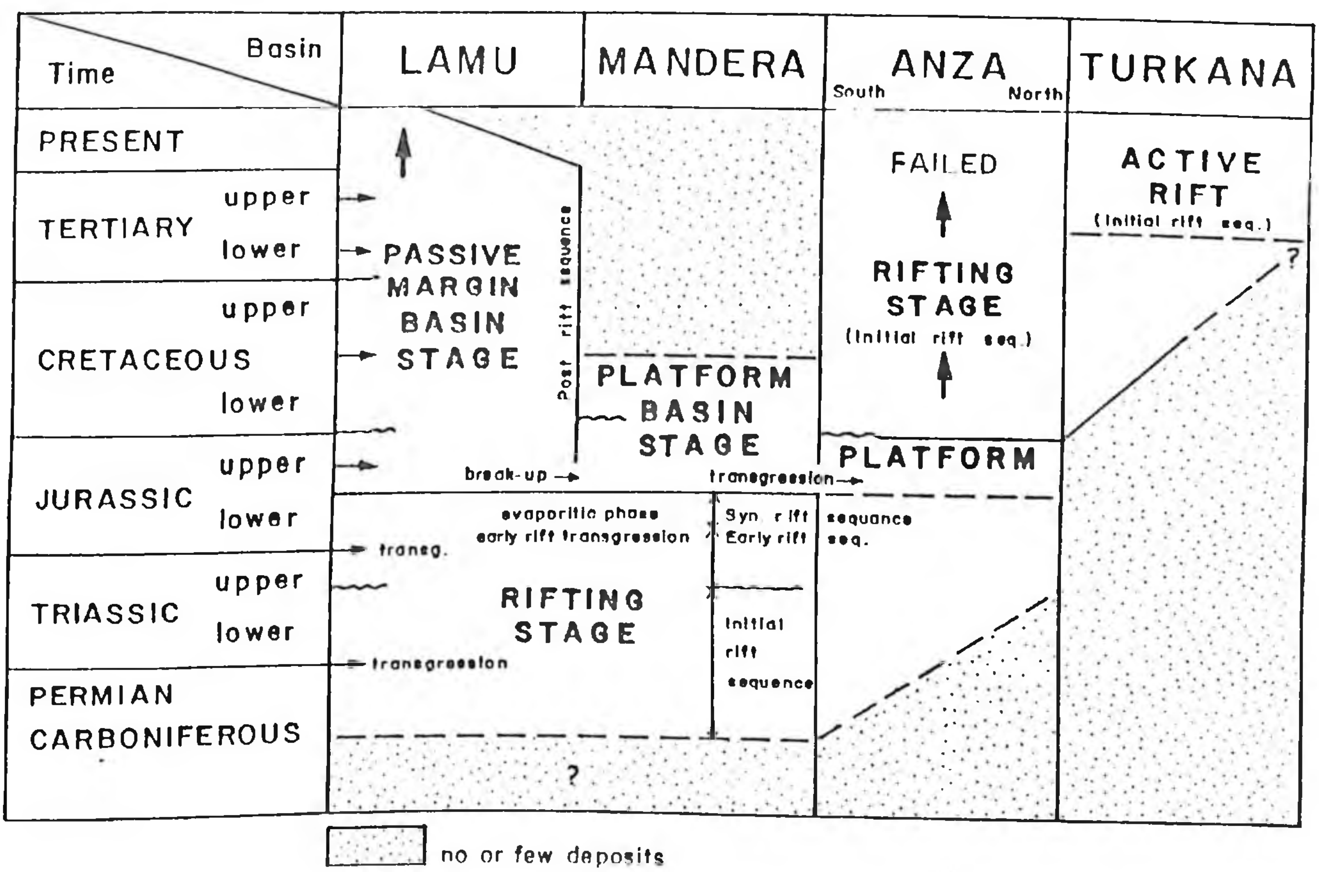

Fig. 8 Evolution of the sedimentary basins of Kenya (Lamu, Mandera Lugh, Anza and Turkana basins), *(After Beicip, 1984, Reeves et al, 1986)*.

CHAPTER 3

METHODOLOGY AND RESULTS

3.1 Overview on Data Generation/Collection

Acquisition methods and the extent to which parameters (i.e. environment of deposition, T.O.C., sedimentation rates etc) are determined, are explained in the following respective subheadings. The results obtained accompany the text and are also partly indicated in the appendix listing at the end of the report.

3.2 Stratigraphy and Environments of Deposition

Results of palynostratigraphic studies of well cutting and core samples combined with wireline logs and well completion reports have been amalgamated in this study to outline stratigraphy and the various basic paleoenvironments penetrated by the well bores (Figs. 11 to 15) whose general locations in the Anza basin are illustrated in Fig. 10. The legends for the lithological profiles is shown in Fig. 33. A synthesized stratigraphic sequence based on the palynological results of the 5 wells are summarized in (Fig 9), which is modelled after Bosworth and Morley (1992). Although crystalline basement is indicated in the suggested sequence, it has not been penetrated by any of the five wells and has only been shown for completion purposes as deduced from known stratigraphy. A tentative regional stratigraphic correlation for the whole basin is presented (Fig. 33).

It is observed that whereas marine environment predominated the Cretaceous in the southern Anza Graben, this is less specific in the north, where the sediment profile (Bellatrix and Sirius wells) are mainly of fluvial/lacustral deposition (Fig. 11 to 15). The sea invasion and regression phenomena following the Gondwanaland break-up probably never had a pronounced effect on areas beyond Marsabit along the failed Anza trough. Variability in the sub-basin geometries related to tectonism and subsidence within the graben where the wells have been sunk is invoked to explain the thickness variations of say marine environment over the different profiles (Section 3.9).

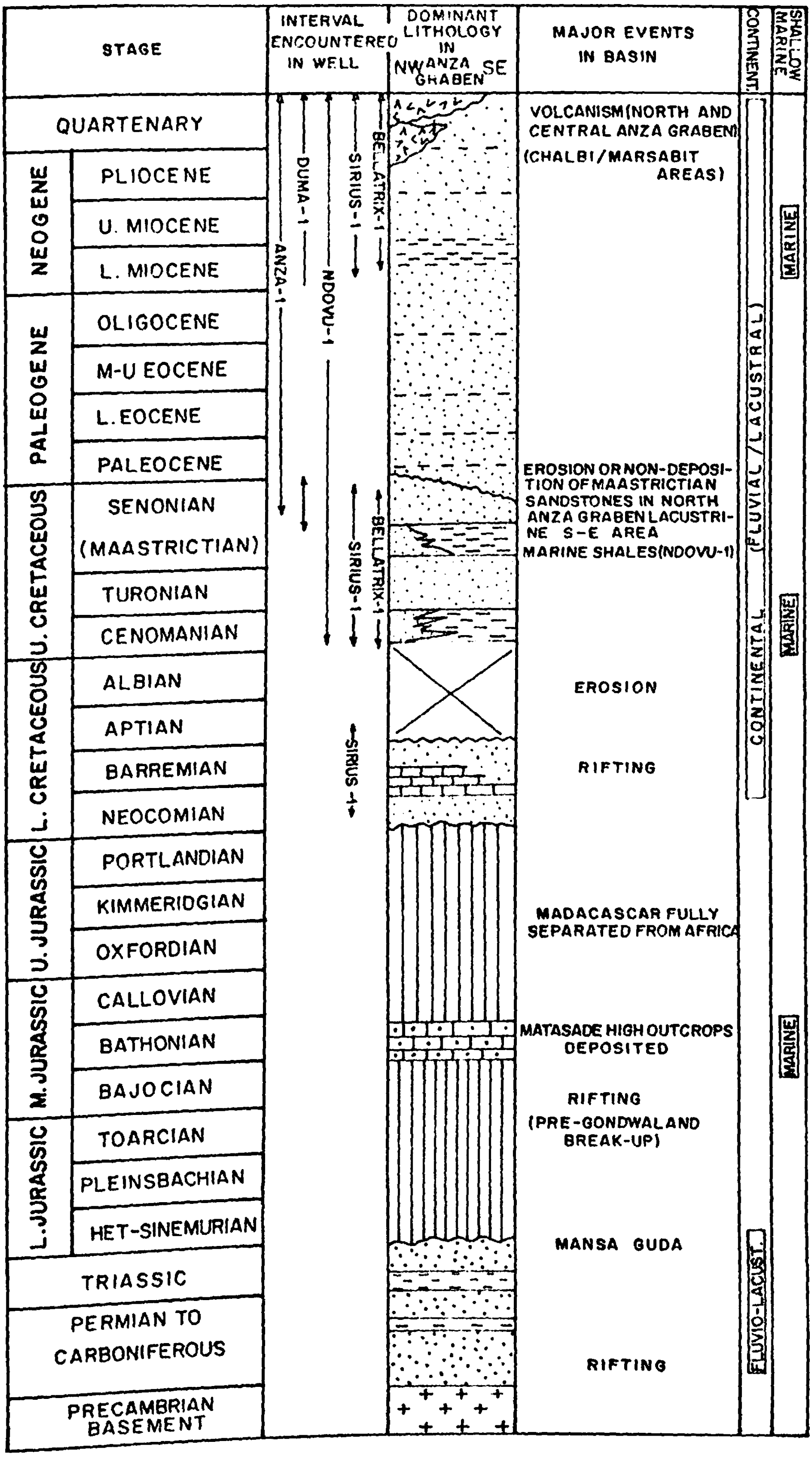

Fig. 9 – Summary of the stratigraphy, depositional environments and major events of the Anza Graben.

Fig.10. General location map for Anza Graben wells and the adjacent areas

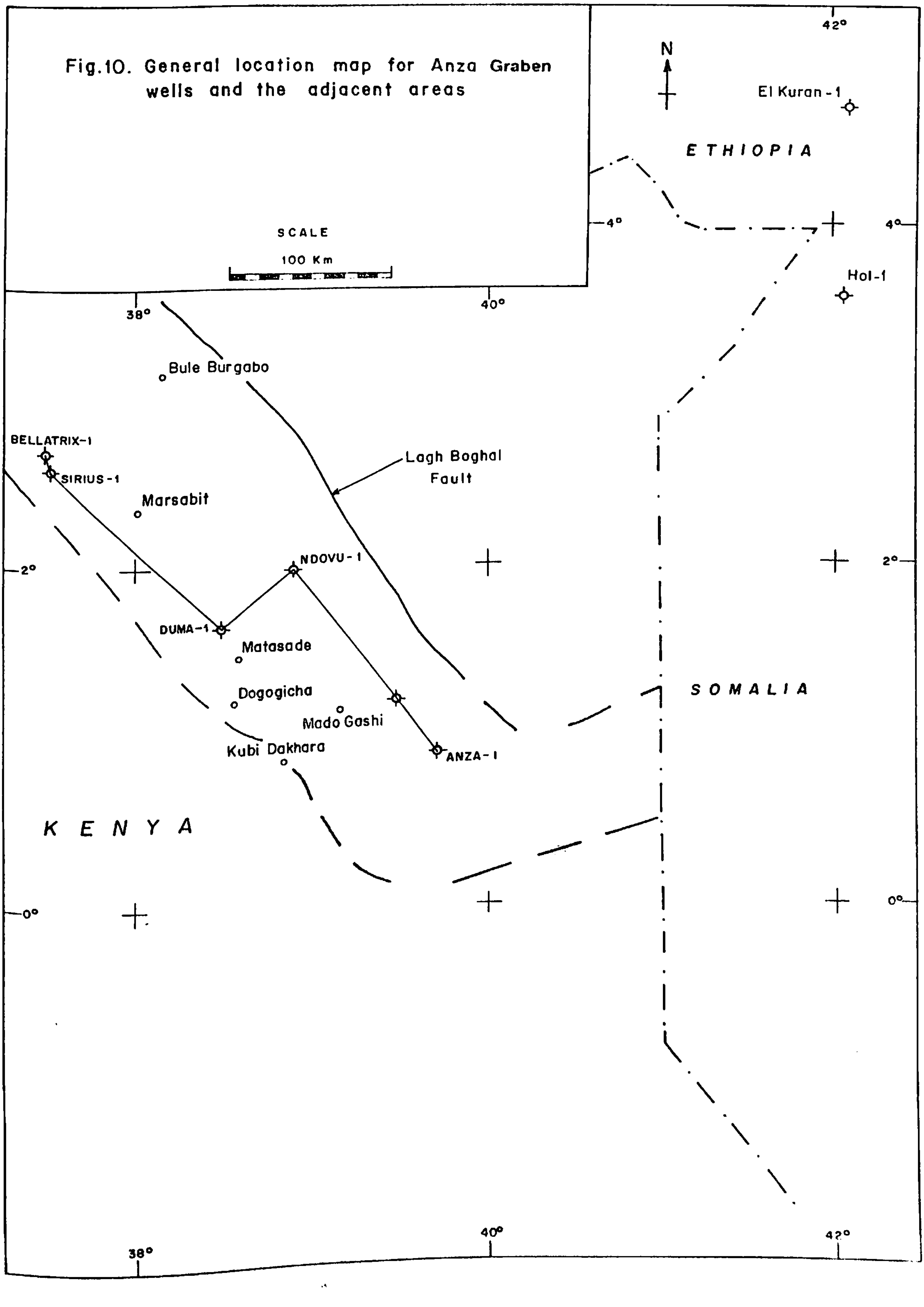

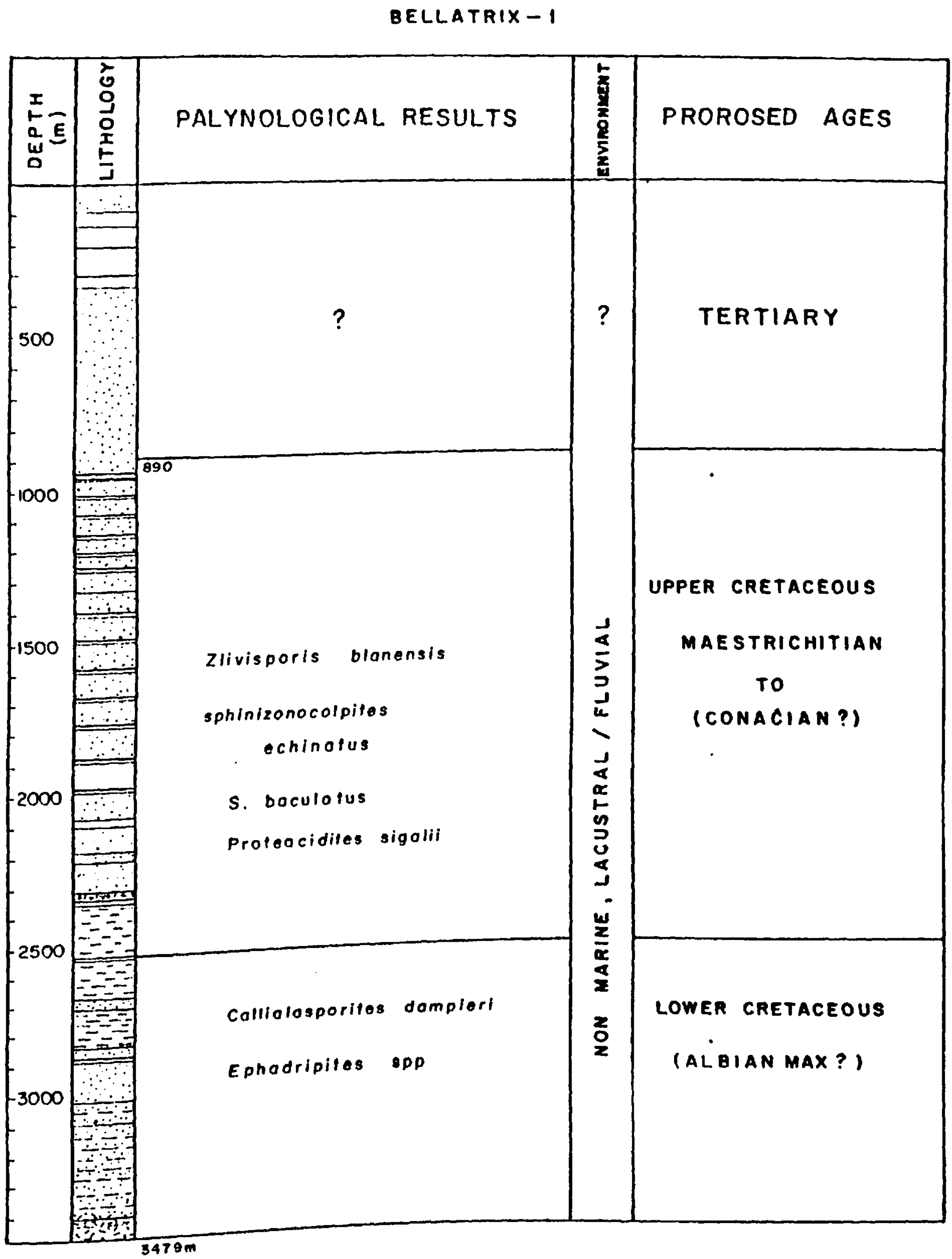

Fig. 11. Stratigraphy and environments of deposition, Ballatrix -1 (Chalbi sub-basin) .

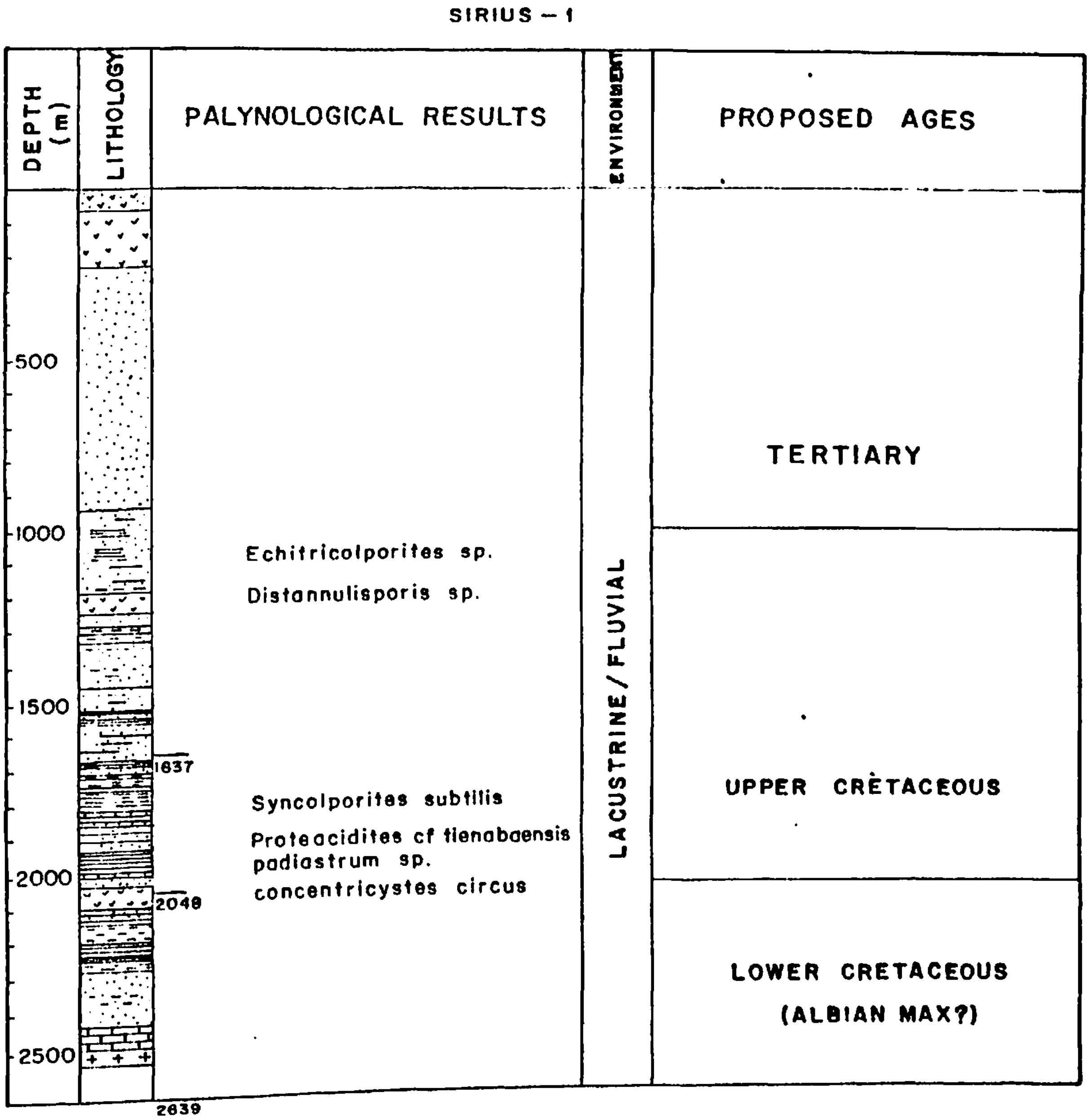

Fig. 12. Stratigraphy and environments of deposition, Sirius -1 (Chalbi sub-basin) .

DUMA - 1

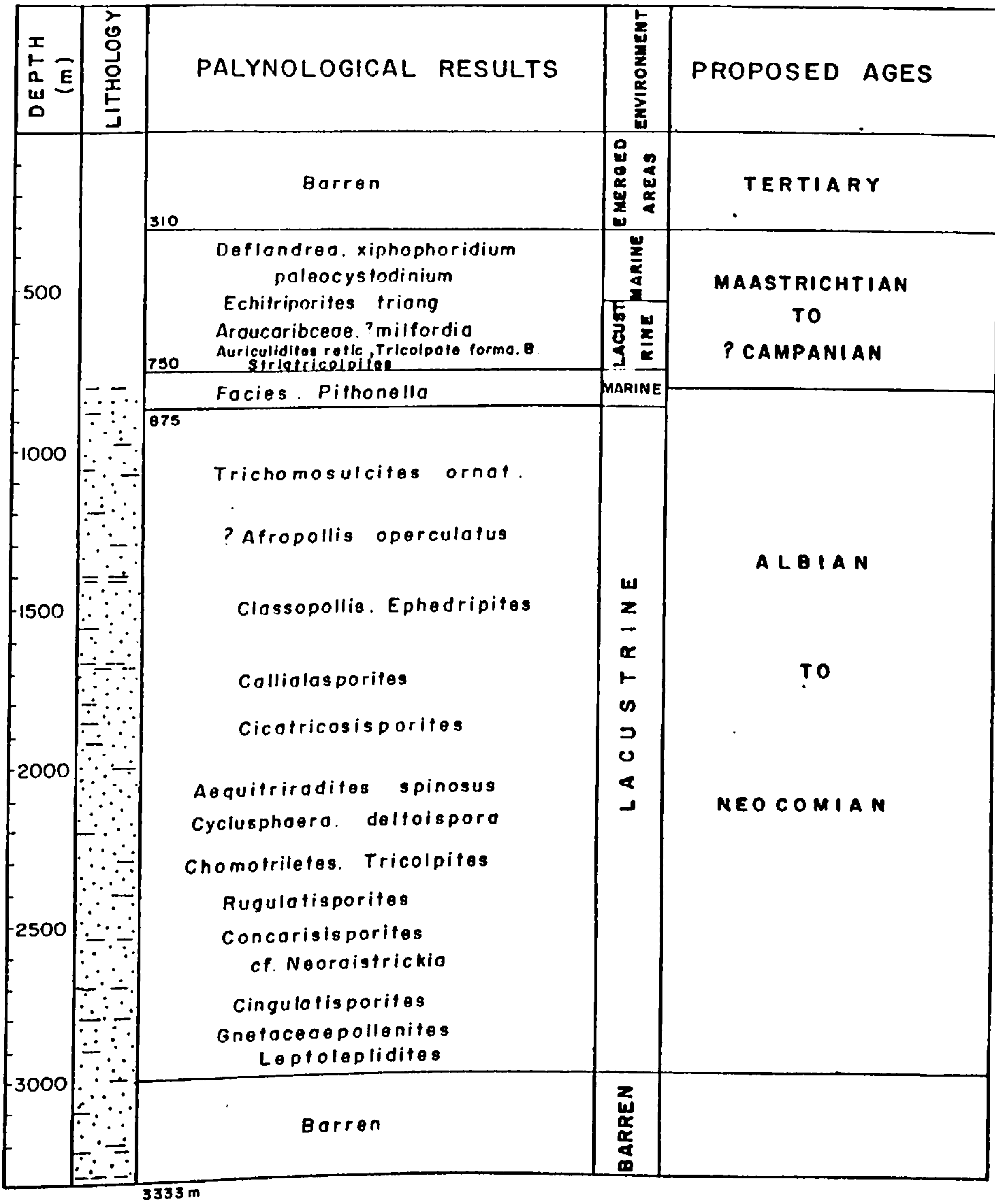

Fig. 13. Stratigraphy and environments of deposition, Duma - 1 (Intermediate Tilted Blocks sub-basin) .

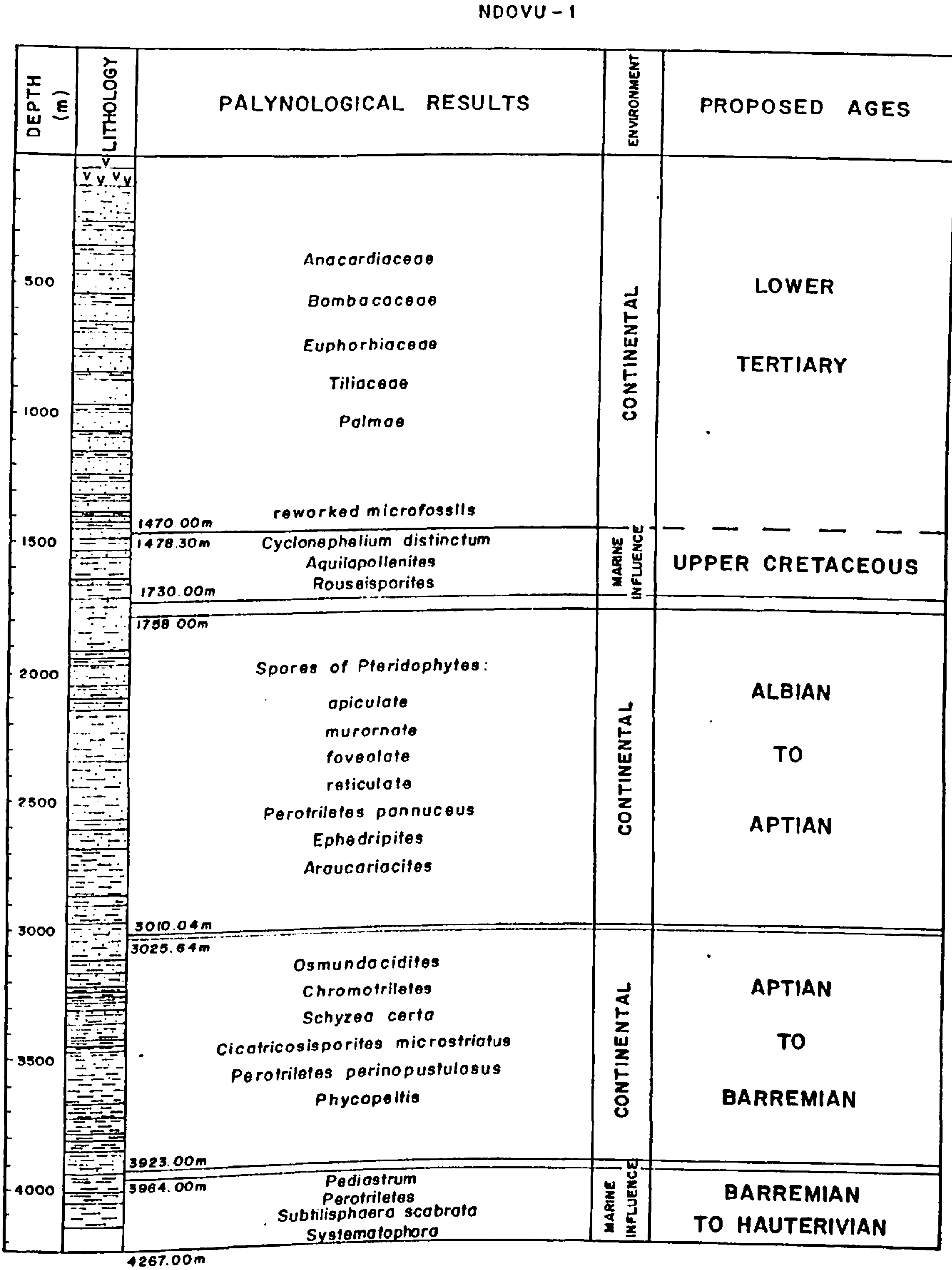

Fig. 14 :- Stratigraphy and environments of deposition, Ndovu-1(Yamicha sub-ba
(After DeCruz, M and P. Milleped, 1988).

ANZA - 1

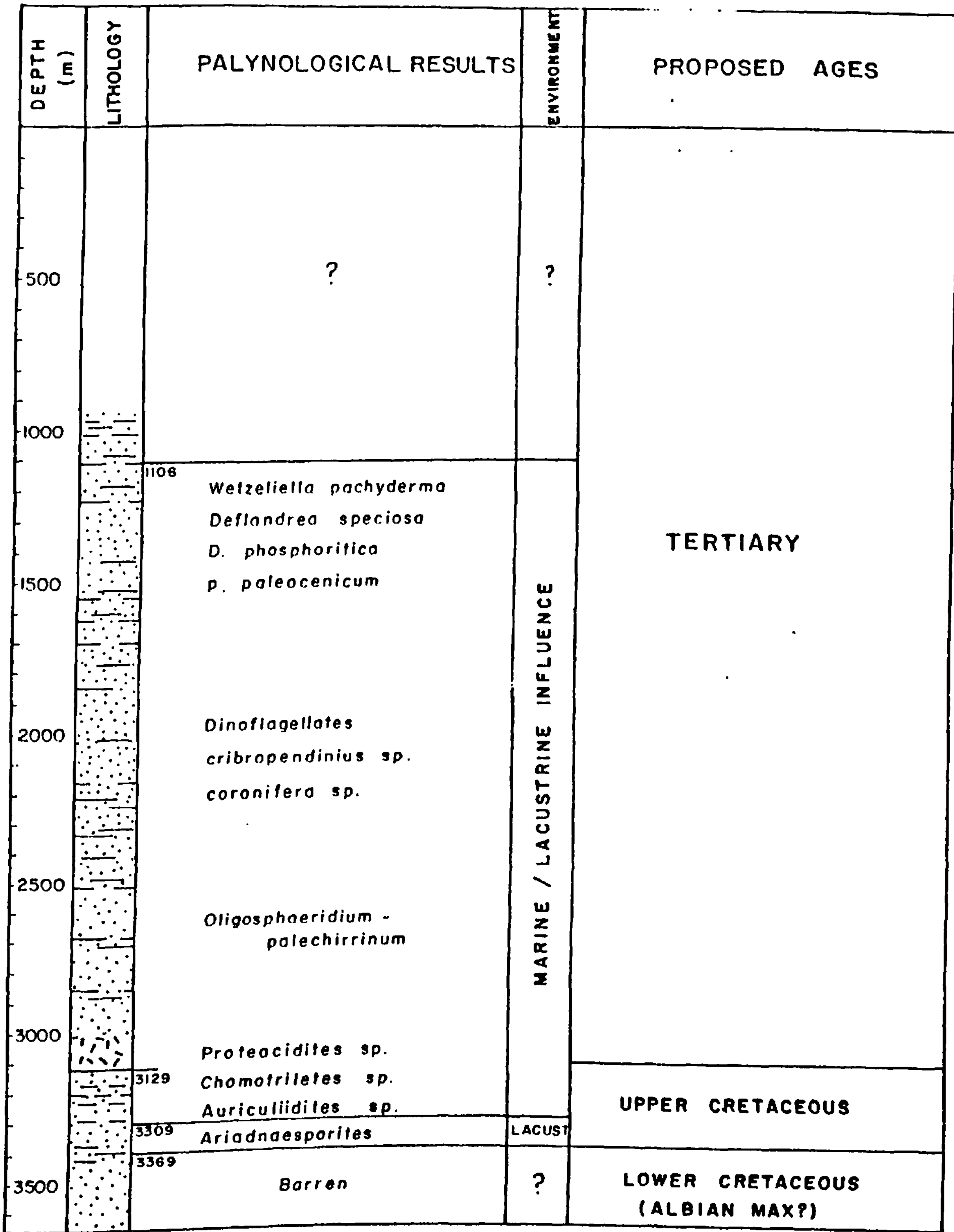

Fig. 15. Stratigraphy and environments of deposition, Anza-1 (Yamicha sub-basin).

3.3 Geothermal Gradients

The increase in temperature with burial depth is mainly a consequence of the transfer of thermal energy from the interior of the earth to the surface where it is dessipated (Tissot and Welte, 1978). Physical and chemical conditions of the source rock which consequently determine hydrocarbon accumulations, change with depth of burial, notably temperature and pressure. Geothermal gradient defines this change in temperature with depth (°C/km). Its value depends on the thermal conductivity of different lithologic units, proximity to the surface, and by subsurface water flow. Although these details are not delved into in this study, existing subsurface temperature data have been synthesized, and all the geothermal gradients for the five wells have been determined and a geothermal interpretation for the basin presented. In constructing the geothermal gradients only the calculated stabilized bottom hole temperatures (BHT) are utilized, noting that the mud at the bottom of the hole takes hours to warm up to the ambient reservoir temperature (Fig. 16).

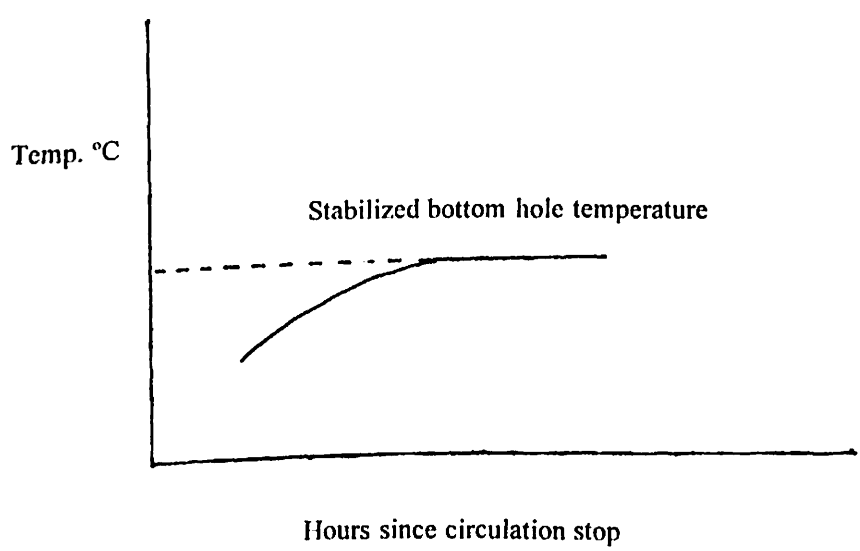

Fig. 16 Model curve for the determination of true BHT taken hours apart.

These different BHT, from different log runs obtained at different depths, were then used to determine the geothermal gradient for each well as illustrated below.

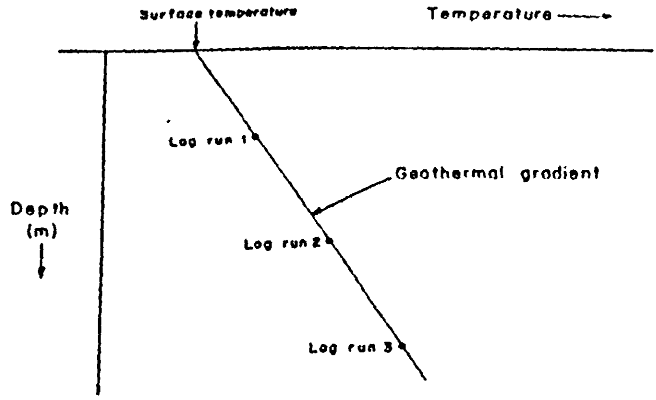

Fig. 17 A sketch of determination of geothermal gradient from two or more BHT taken at different log runs. (After Selley, 1985).

Figures 18 to 22 illustrate the results obtained for the geothermal gradients in the basin. They are summarized in Table 1.

Table 1. Summary of geothermal gradients for the five wells.

Well Name		Sub-basin	Geothermal Gradient °C/km
1.	Sirius	Chalbi	26.6
2.	Bellatrix	Chalbi	27.6
3.	Duma	Intermediate T. Blocks	23.9
4.	Ndovu	Yamicha	22.2
5.	Anza	Yamicha	24.0

3.3.1 Assumptions and Explanation

These determinations are based on the assumption that the present-day gradient and surface temperatures have remained constant throughout the rocks history enabling us to use these present-day data. The assumption is largely justified because of the basin's large sedimentary cover that ultimately reduces heat dessipation, and the absence of lavas which suggest no shallow heat sources. Additional discussion is offered in section 4.1 under Thermal Maturity.

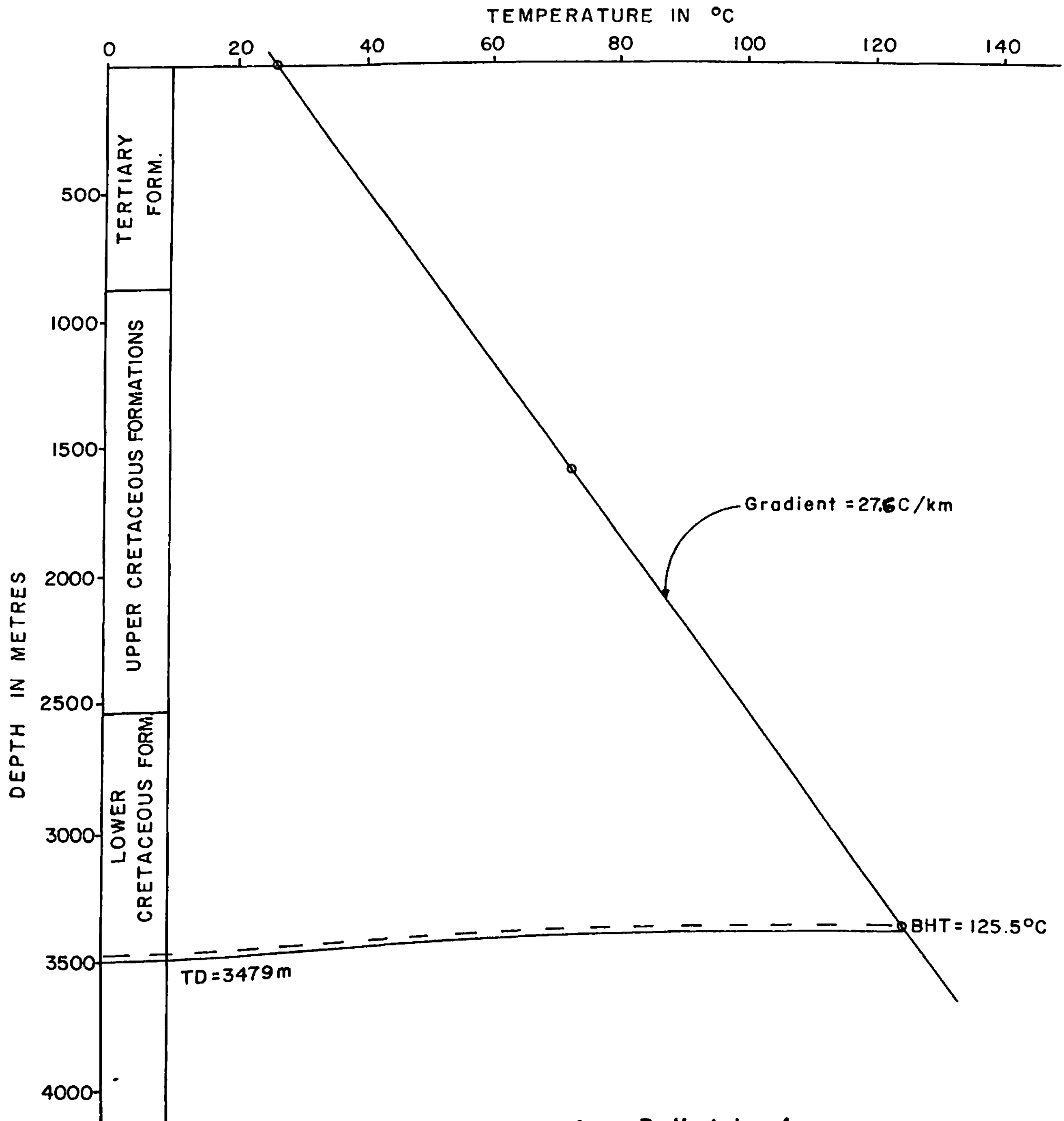

Fig.18. Geothermal gradient for Bellatrix-1

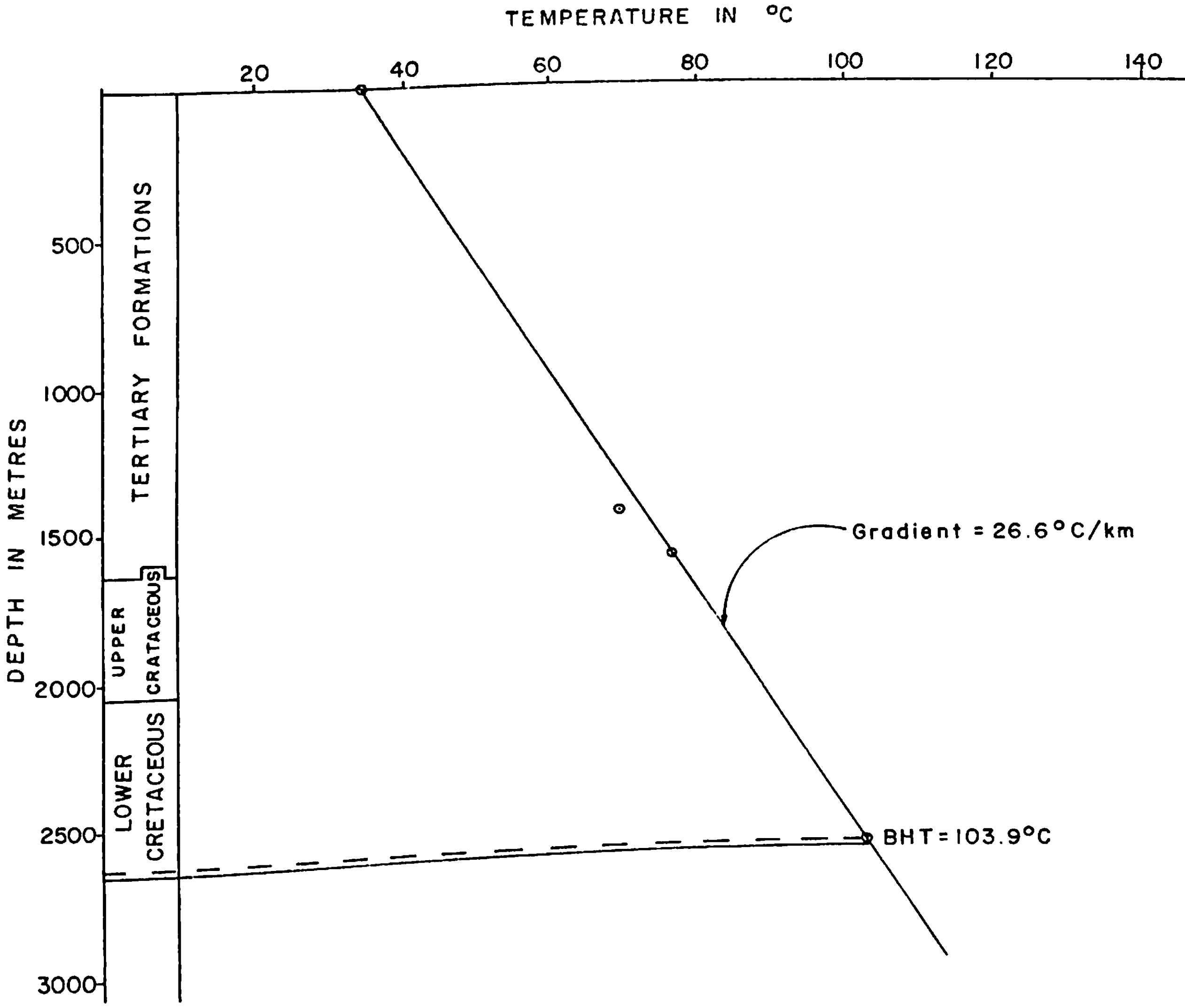

Fig.19. Geothermal gradient for Sirius - 1

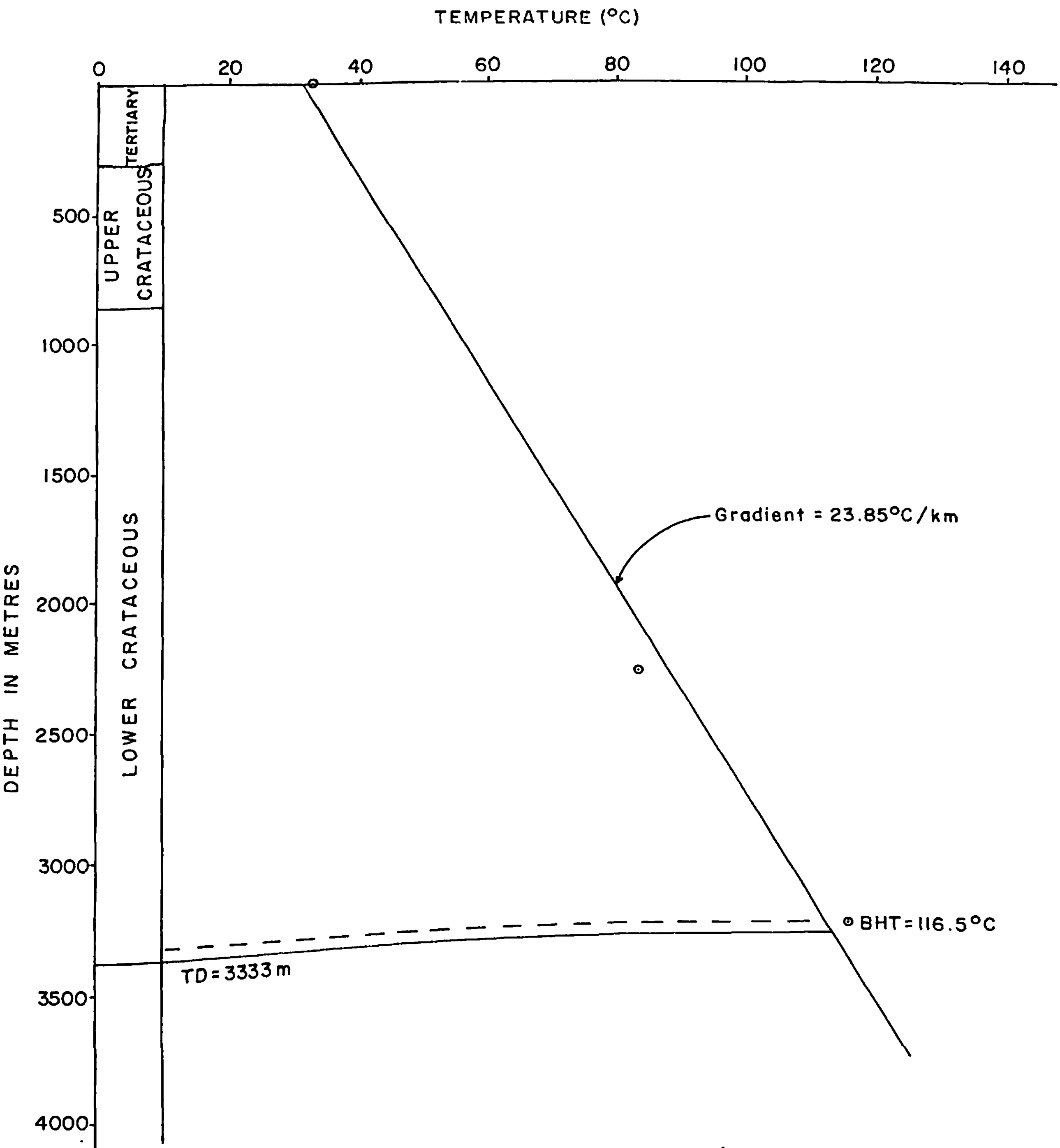

Fig.20. Geothermal gradient for Duma-1

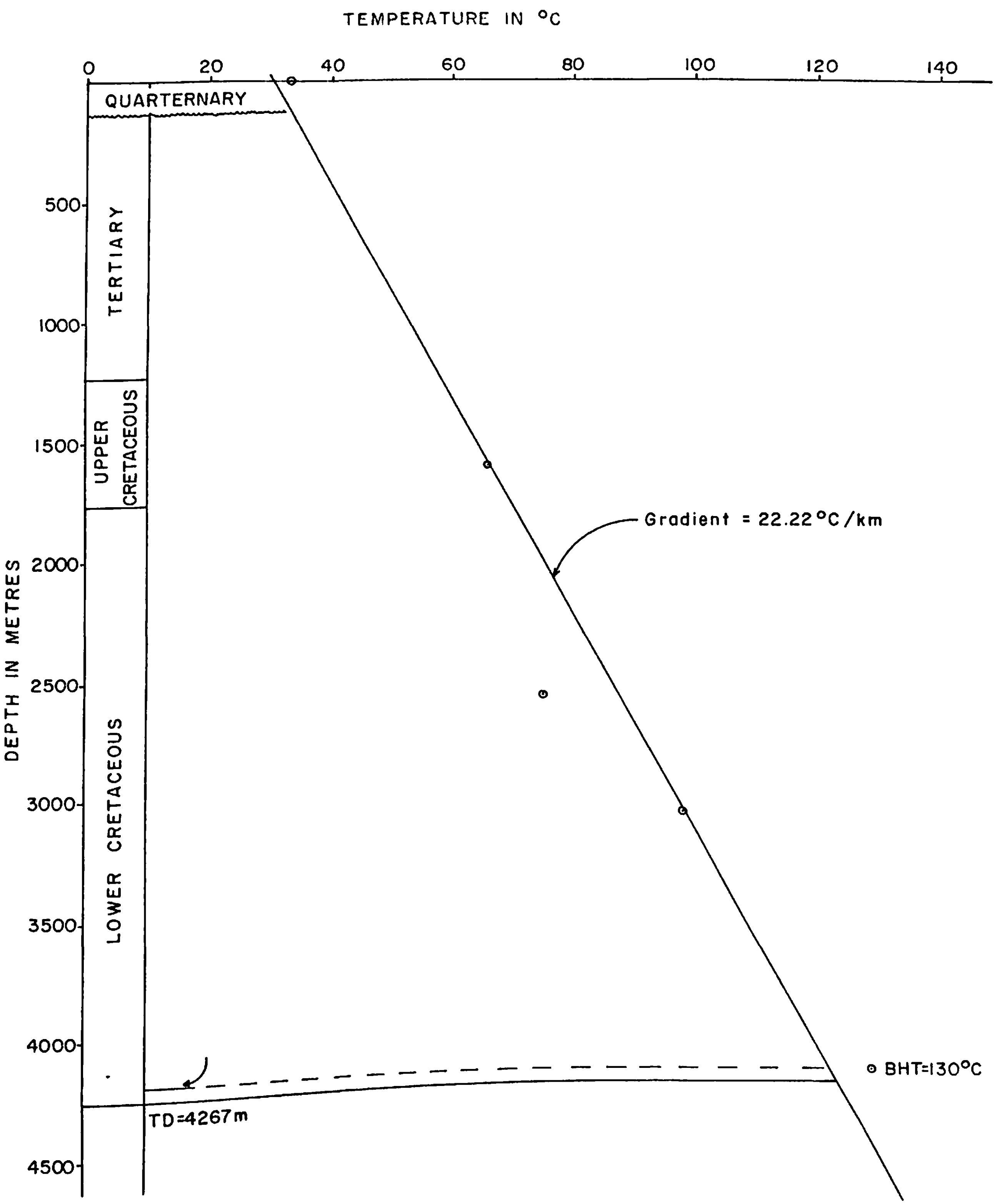

Fig. 21. Geothermal gradient for Ndovu-1

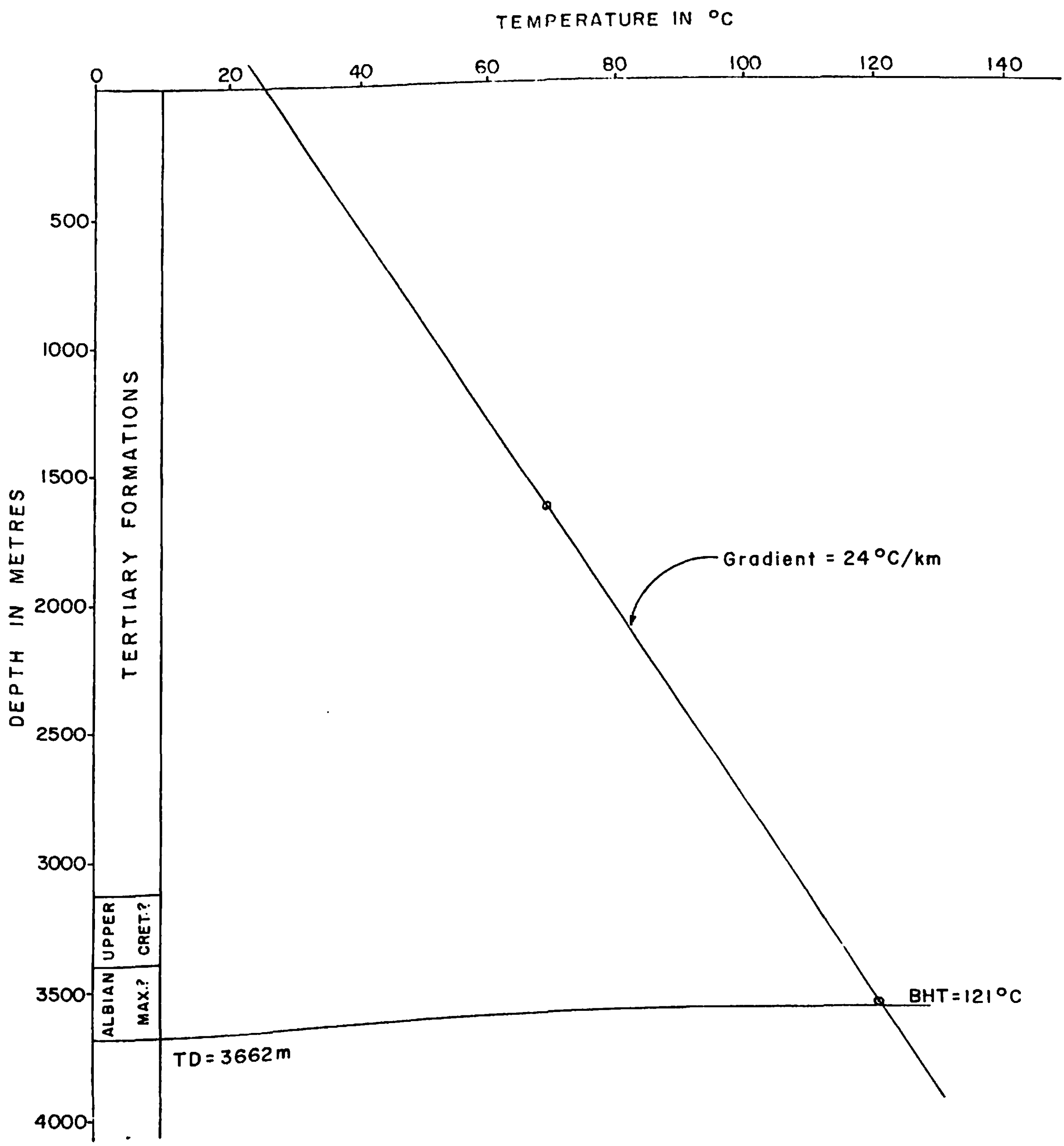

Fig. 22 Geothermal gradient for Anza-1

3.4 Burial & Thermal History: Lopotin's TTI Technique

3.4.1 Burial-History Curves

Data on formation tops (from well reports) and ages obtained by biostratigraphic analysis (section 3.2) were synthesized for each well to form a time-stratigraphic data (Table 2). The burial-history curves were constructed by first choosing the points that represent the initial deposition (age at total depth) of the sediment and their position today on an age-depth plot (Figures 23 to 27). The difference between the depth of the next-in-age formation top and the TD were plotted against the formation age to represent the sediment accumulation (burial) during that time span (initially ignoring the compaction effect). This procedure was repeated for each identified formation top in each age interval as was necessary. The burial-history curve was obtained by connecting the plotted points as shown in each of the five wells, where allowance has also been made for compaction effects (Magara, 1986). All the shallower and younger horizons normally have burial-history curves with segments being parallel to those of the oldest horizon as Figures 23 to 27 illustrate.

A temperature-history was also constructed to accompany the burial-history curves. Using the computed present day geothermal gradient, in each well it was assumed (for determinative purposes) that the gradient and surface temperature have remained constant throughout the rocks history, the present-day data (Figures 18 to 22) used in each respective case to construct the temperature grid as shown in each well (Figures 23 to 27). In each of the five wells, a simple temperature-history model was assumed.

Table 2. Time-stratigraphic data (Formation tops).

Bellatrix-1 well

	Tertiary	Upper Cretaceous		
Age (M.Y.)	0	65	75	97
Depth (m)	0	890	2300	3470

Sirius-1 well

	Tertiary	Upper and Lower Cretaceous		
Age (M.Y.)	0	65	100	120
Depth (m)	0	960	2040	2640

Ndovu-1 well

	Tertiary		Upper and Lower Cretaceous		
Age (M.Y.)	0	65-75	100	120	125
Depth (m)	0	1500	1750	3000	4267

Anza-1 well

	Tertiary		Upper and Lower Cretaceous	
Age (M.Y.)	0	25-38	65-73	113
Depth (m)	0	1800	3129	3662

Duma-1 well

	Tertiary		Upper and Lower Cretaceous	
Age (M.Y.)	0	65	100	125
Depth (m)	0	300	800	3300

3.4.2. Procedure for the determination of maturity (TTI) and the results obtained.

Having determined the burial-history curves (Figures 23 to 27), temperature grids were constructed and superimposed on the curves for each of the five wells. Where the burial-history curve intersects each isotherm (marked with circles) defines, between them, the time and temperature intervals. Temperature intervals are defined by isotherms spaced 10°C apart (Waples, 1981). Time interval on the other hand is the length of time expressed in units of millions years that the rock spent on in that particular temperature interval. By summing the incremental maturity added in each succeeding temperature interval, we obtain the Total Maturity. The interval 100-110°C is chosen as the base and is assigned an index n=0, and the rate of reaction assumed to double with every 10°C rise in temperature (Waples, 1980; 1981; 1985). Index values decrease or increase regularly at higher or lower temperatures (Tables 3 to 7). The rate of maturation is assumed to increase by a factor of 2 (Waples, 1980; 1981; 1992) for every rise of 10° temperature rise, thus defining a temperature factor which Lopatin called γ. The γ given by the equation $\gamma = 2^n$ reflects the exponential dependence of maturity on temperature. Time and temperature factors are infact interchangeable: a high temperature acting over a short time can have the same effect on maturation as a low temperature acting over a longer period (Waples, 1985).

By multiplying the time factor for any temperature interval by the appropriate γ-factor for the temperature interval, we obtain the thermal maturity index or Time-temperature Index of maturity (TTI) for that interval (Tables 3 to 7). The interval TTI is the maturity acquired by the rock in a particular temperature interval, and summing up all the interval-TTI values gives the total maturity for the rock upto that time (Waples, 1981; 1985; 1992).

Table 3. TTI calculations for Duma-1.

Temperature Interval (°C)	Temp Factor 2^n	Time Factor (M.Y) Δt	Interval TTI $\Delta t.2^n$	Total TTI $\sum \Delta t.2^n$	Time (M.Y.B.P.)
30-40	2^{-7}	1.5	0.01	0.01	122.5
40-50	2^{-6}	1.5	0.02	0.03	121.0
50-60	2^{-5}	2.0	0.06	0.09	119.0
60-70	2^{-4}	2.0	0.13	0.22	117.0
70-80	2^{-3}	2.0	0.25	0.47	115.0
80-90	2^{-2}	2.0	0.50	0.97	113.0
90-100	2^{-1}	2.0	1.00	1.97	11.0
100-110	2^{0}	18.0	18.00	19.97	93.0
110-120	2^{1}	28.0	56.00	75.97	65.0
120-130	2^{2}	65.0	260.00	335.97	0

a. Lower Cretaceous (Albian to Neocomian).

30-40	2^{-7}	35.0	0.27	0.27	45.0
40-50	2^{-6}	45.0	0.07	0.34	0

b. Upper Cretaceous (Maestritchtian to Campanian?)

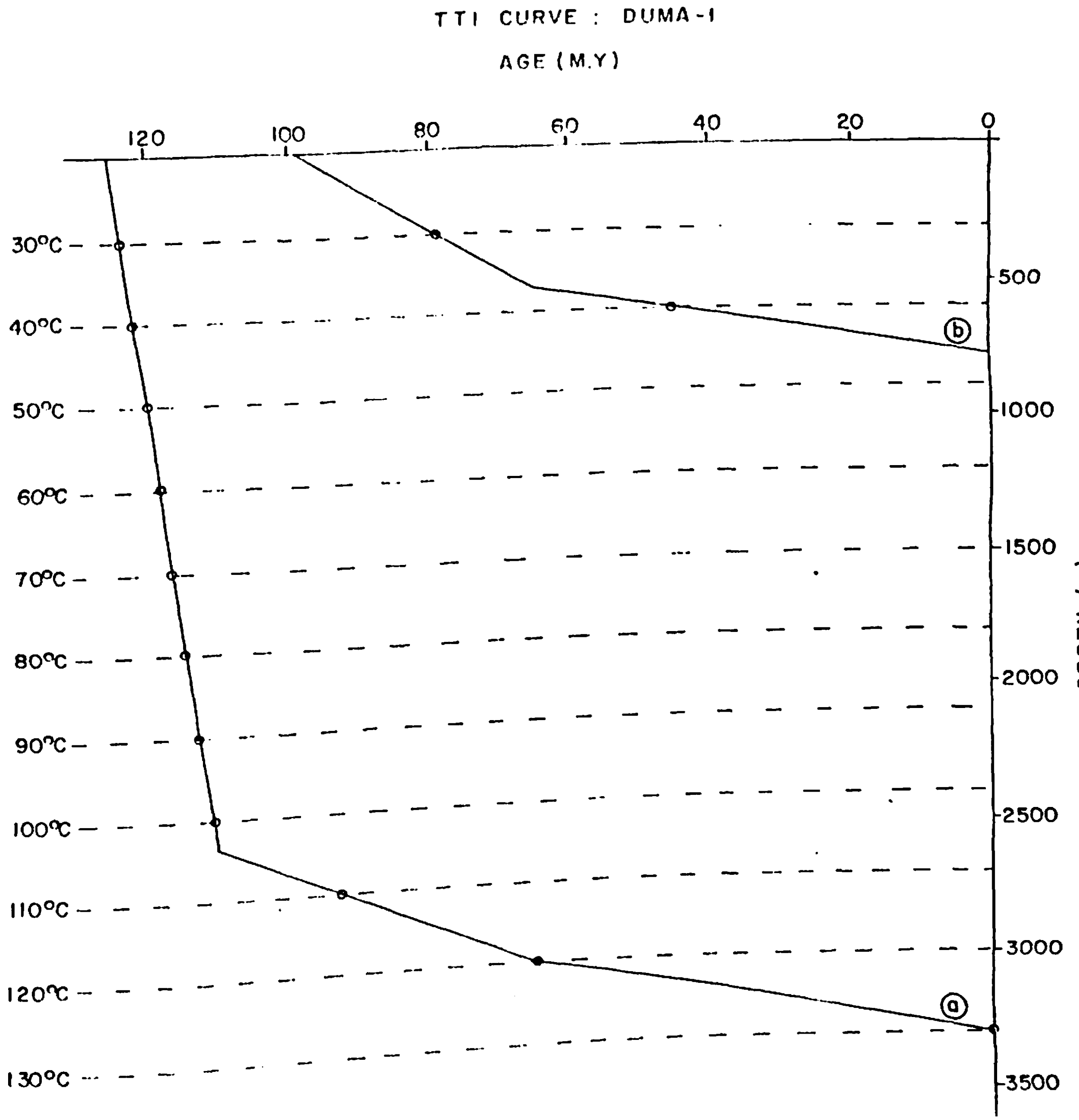

Fig. 23. Burial-history curve and subsurface temperature grid (TTI curve) for Duma-1.

Table 4. TTI calculations for Anza-1.

Temperature Interval (°C)	Temp Factor 2^n	Time Factor (M.Y) Δt	Interval TTI $\Delta t.2^n$	Total TTI $\sum \Delta t.2^n$	Time (M.Y.B.P.)
30-40	2^{-7}	7.0	0.05	0.05	54.5
40-50	2^{-6}	7.0	0.11	0.16	47.5
50-60	2^{-5}	7.0	0.22	0.38	10.5
60-70	2^{-4}	19.0	1.19	1.57	21.5
70-80	2^{-3}	4.5	0.56	2.13	17.0
80-90	2^{-2}	5.0	1.25	3.38	12.0
90-100	2^{-1}	5.0	2.50	5.88	7.0
100-110	2^{0}	2.5	5.00	15.38	2.5
110-120	2^{1}	2.5	5.00	15.38	0

Anza-1. Lower Cretaceous (Albian Max.)

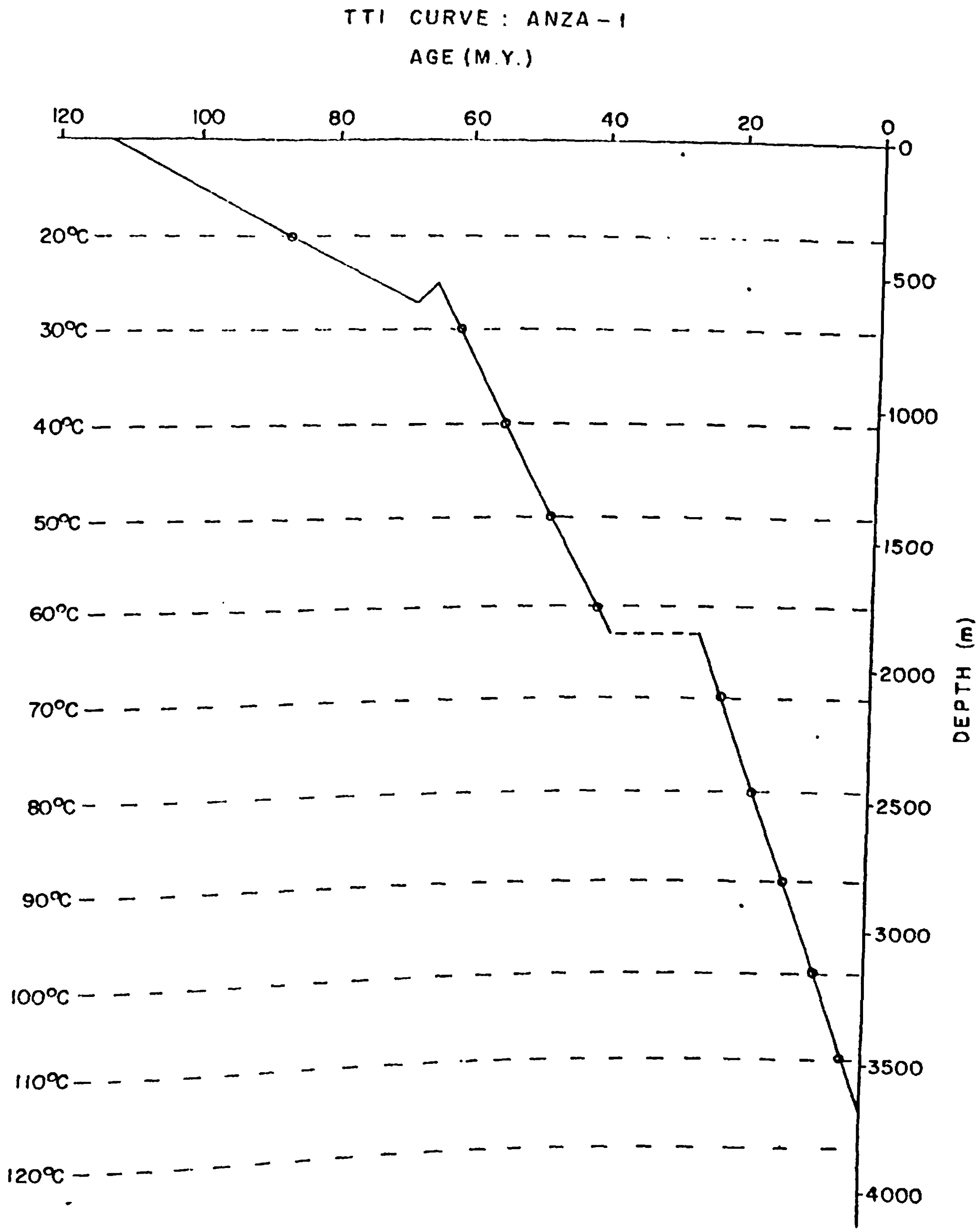

Fig. 24. Burial-history curve and subsurface temperature (TTI curve) for Anza-1.

Table 5. TTI calculations for Ndovu-1.

Temperature Interval (°C)	Temp Factor 2^n	Time Factor (M.Y) Δt	Interval TTI $\Delta t.2^n$	Total TTI $\sum \Delta t.2^n$	Time (M.Y.B.P.)
30-40	2^{-7}	4.0	0.03	0.03	117.0
40-50	2^{-6}	4.0	0.06	0.09	113.0
50-60	2^{-5}	4.0	0.13	0.22	109.0
60-70	2^{-4}	4.0	0.25	0.47	105.0
70-80	2^{-3}	4.0	0.50	0.97	101.0
80-90	2^{-2}	38.5	9.63	10.60	62.5
90-100	2^{-1}	17.5	8.75	19.35	45.0
100-110	2^{0}	17.5	17.50	36.85	27.5
110-120	2^{1}	17.5	35.50	72.35	10.0
120-130	2^{2}	10.0	40.00	112.35	0

a. Lower Cretaceous (Aptian to Hauterivian)

30-40	2^{-7}	7.0	0.05	0.05	105.5
40-50	2^{-6}	8.0	0.13	0.18	97.5
50-60	2^{-5}	38.0	1.19	1.37	59.5
60-70	2^{-4}	17.5	1.09	2.46	42.0
70-80	2^{-3}	17.5	2.19	4.65	24.5
80-90	2^{-2}	17.0	4.25	8.90	7.5
90-100	2^{-1}	7.5	3.75	12.65	0

b. Lower Cretaceous (Albian to Aptian)

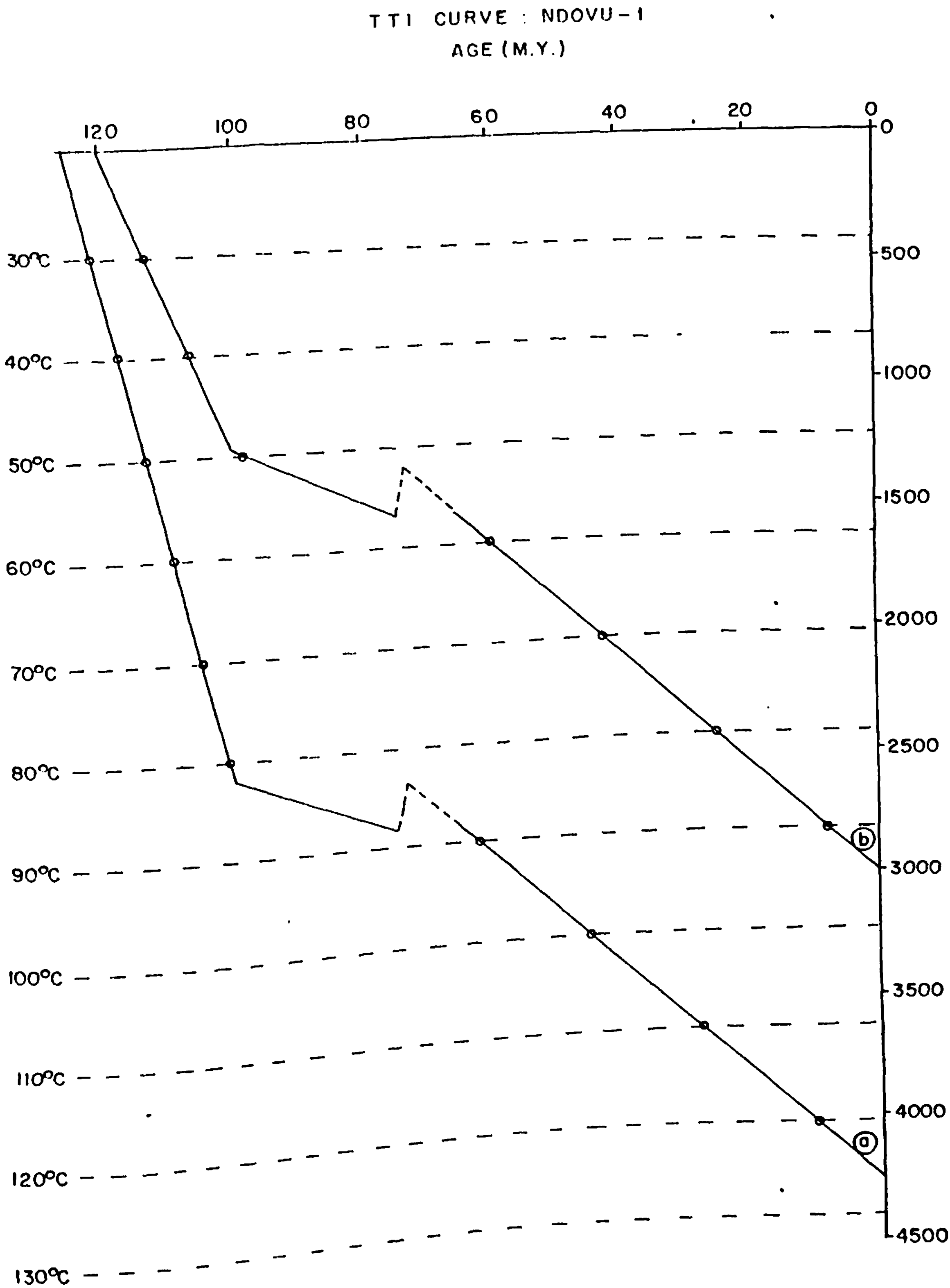

Fig. 25 Burial-history curve and subsurface temperature grid (TTI curve) for Ndovu-1 .

Table 6. TTI calculation for Bellatrix-1

Temperature Interval (°C)	Temp Factor 2^n	Time Factor (M.Y) TTI Δt	Interval TTI $\Delta t.2^n$	Total $\sum \Delta t.2^n$	Time (M.Y.B.P.)
30-40	2^{-7}	7.0	0.05	0.05	85.5
40-50	2^{-6}	6.5	0.10	0.15	79.0
50-60	2^{-5}	6.0	0.38	0.53	73.0
60-70	2^{-4}	2.0	0.13	0.66	71.0
70-80	2^{-3}	2.0	0.25	0.91	69.0
80-90	2^{-2}	2.0	0.50	1.41	67.0
90-100	2^{-1}	2.5	1.25	2.66	64.5
100-110	2^{0}	24.0	24.00	26.66	40.5
110-120	2^{1}	24.0	48.00	74.66	16.5
120-130	2^{2}	16.5	66.00	140.66	0

a. Lower Cretaceious (Albian Max.)

30-40	2^{-7}	2.0	0.02	0.02	67.5
40-50	2^{-6}	2.0	0.03	0.05	65.5
50-60	2^{-5}	2.0	0.06	0.11	63.5
60-70	2^{-4}	15.5	0.97	1.08	48.0
70-80	2^{-3}	24.0	3.00	4.08	24.0
80-90	2^{-2}	24.0	6.00	10.08	0

b. Upper Cretaceous (Maestrichtian)

TTI CURVE : BELLATRIX - 1

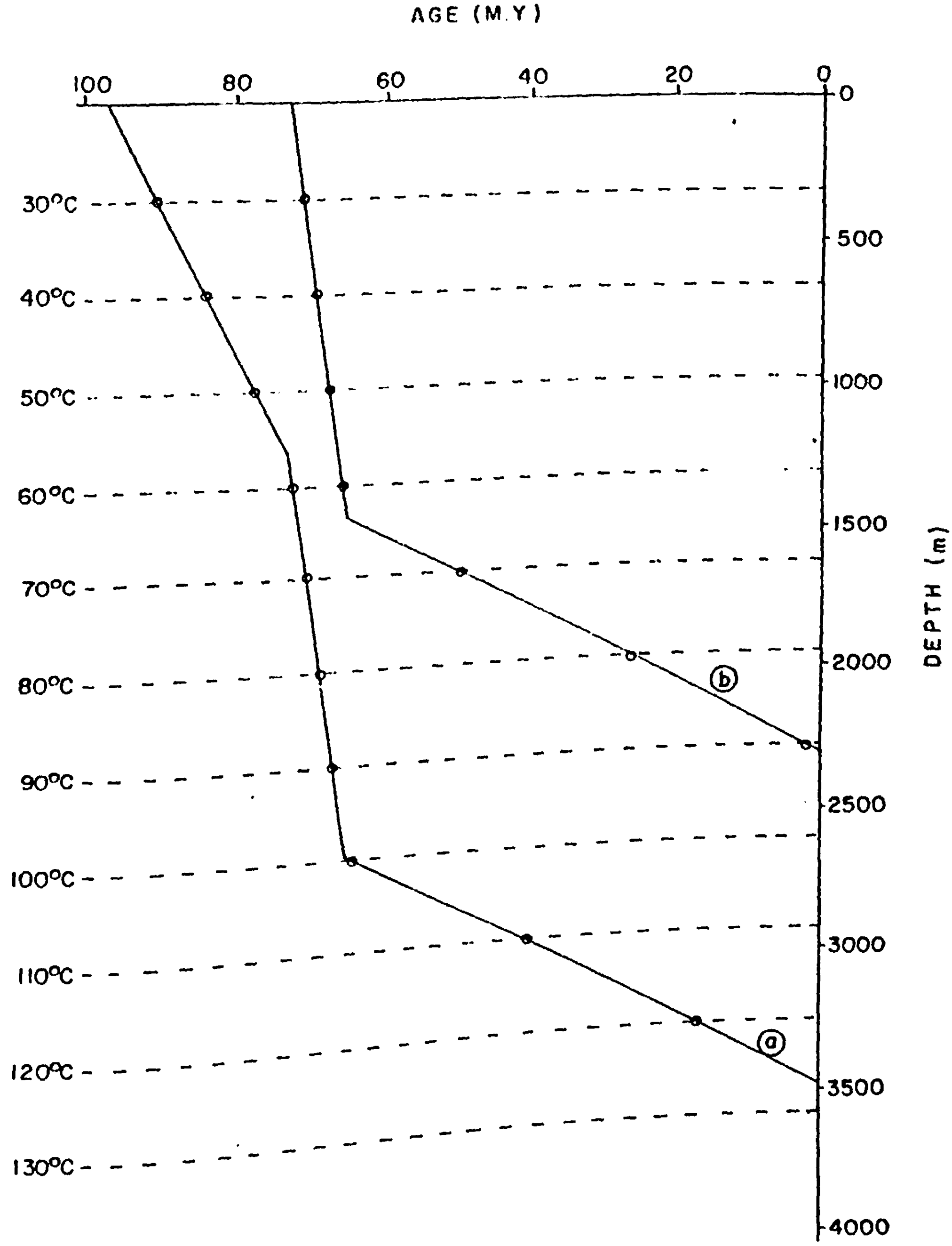

Fig. 26. Burial - history curve and temperature grid ⊕ (TTI curve) for Bellatrix-1 .

Table 7. TTI calculations for Sirius-1

Temperature Interval (°C)	Temp Factor 2^n	Time Factor (M.Y) TTI Δt	Interval TTI $\Delta t.2^n$	Total $\sum \Delta t.2^n$	Time (M.Y.B.P.)
30-40	2^{-7}	20.0	0.16	0.16	100.0
40-50	2^{-6}	10.0	0.16	0.32	90.0
50-60	2^{-5}	10.0	0.31	0.63	80.0
60-70	2^{-4}	10.0	0.63	1.26	70.0
70-80	2^{-3}	14.5	1.81	3.07	55.5
80-90	2^{-2}	20.5	5.13	8.20	35.0
90-100	2^{-1}	20.0	10.00	18.20	15.0
100-110	2^{0}	15.0	15.00	33.20	0

a. Lower Cretaceous

30-40	2-7	10.0	0.08	0.08	80.0
40-50	2^{-6}	10.0	0.16	0.24	70.0
50-60	2^{-5}	13.5	0.42	0.66	56.5
60-70	2^{-4}	20.0	1.25	1.91	36.5
70-80	2^{-3}	20.0	2.50	4.41	16.5
80-90	2^{-2}	16.5	4.13	8.54	0

b. Upper Cretaceous (Maestrichtian)

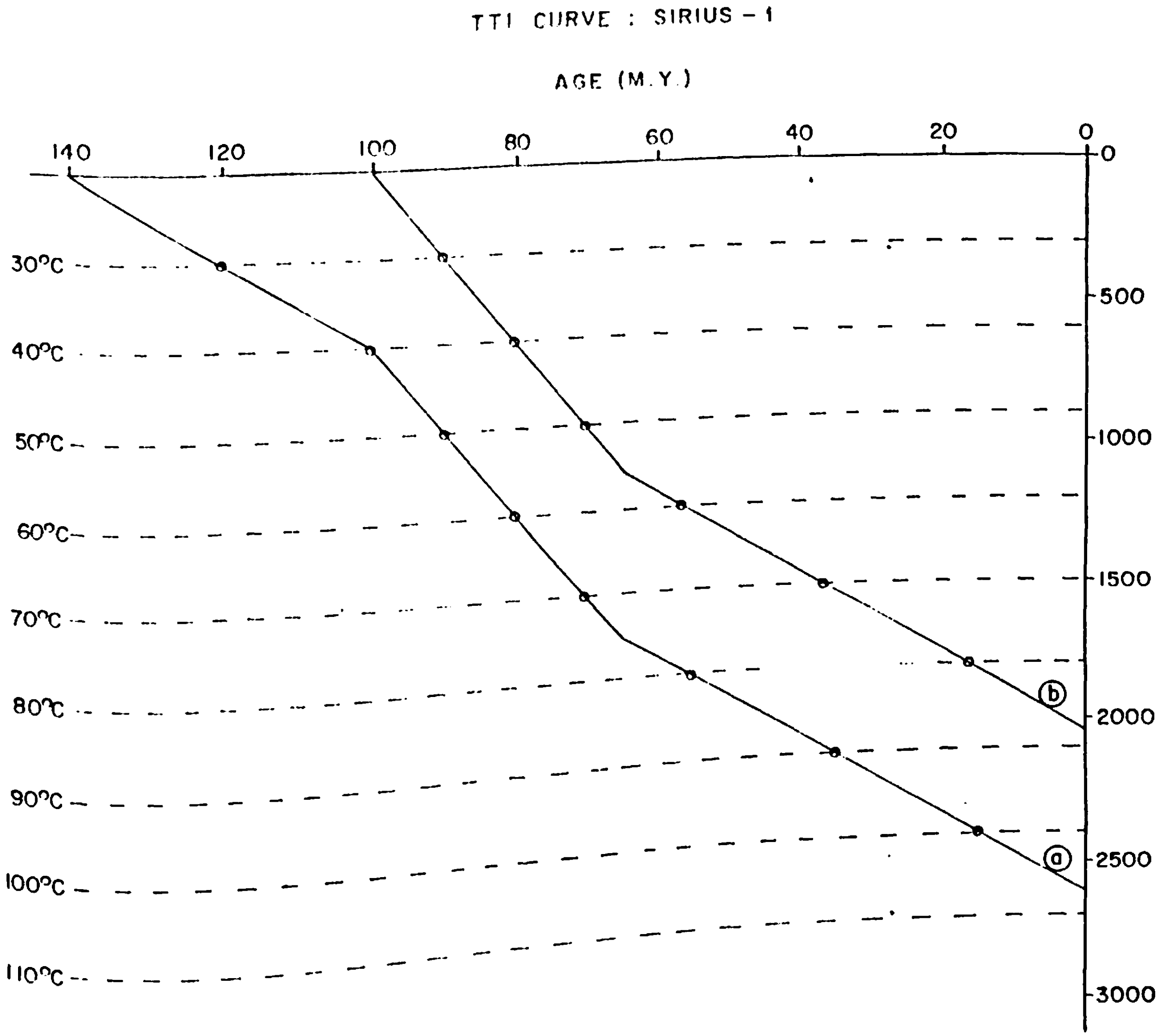

Fig. 27. Burial-history curve and subsurface tempature grid (TTI curve) for Sirius-1.

3.5 Sedimentation Rates and Trends

Where each well is sited is taken to generally represent the sedimentation style of the sub-basin. This assumption has been necessary even in the case of Sirius and Bellatrix which were sunk in the flanks of an anticline (Amoco, 1988). Using time-stratigraphic data and burial curves, sedimentation rates over each basin have been calculated as shown in Table.8. In each case, marginal compaction and erosional effects were assumed (Magara, 1987). Significant uplift and subsequent erosion as recorded in Anza-1 and Ndovu-1 wells were, however, treated as shown in Figures 24 and 25. Well logs and geologic completion reports have been used to precise the formation tops for these determinations. The results obtained for all the wells are presented in Table 8.

3.6 Organic Carbon Concentration over the Well Profiles

The organic carbon concentration data have been obtained and synthesized mainly from existing T.O.C data, S_1, S_2, PI and T_{max} (these standard notations carry the meaning as contained in the Legend to the Appendix) data base for representative wells sunk in the various sub-basins within the Anza graben. Whereas the existing TOC and other database are sampled at roughly 3 metre intervals, for the purposes of this study all the data were recalculated and averaged at a 20 m interval to obtain 3,199 units of data which are listed in Appendix A to E. It is considered that this synthesis has yielded more representative downhole profiles in each well and hence more consistent with sedimentation rate calculations.

In the Sirius and Bellatrix profiles, quantitative laboratory analysis of kerogen was carried out to supplement the available data.

Table 8. Sedimentation Rates and Trends.

a) Bellatrix-1

Depth Range (m)	Thickness (m)	Age Interval (M.Y.B.P.)	Time (M.Y.)	Sedimentation Rate m/M.Y.
3479-2300	1179	97.5-73.0	24.5	48.1
2300-890	1410	73.0-63.0	10.0	141.0
890-0	890	63.0-0	63.0	14.0

b) Sirius-1

2639-2040	599	125.0-97.5	27.5	21.8
2040-960	1080	97.5-65.0	32.5	33.2
960-0	960	65.0-0	65.0	14.8

c) Duma-1

3333-800	2533	125.0-100.0	25.0	101.3
800-300	500	100.0-65.0	35.0	14.3
00-0	300	65.0-0	65.0	4.6

d) Ndovu-1

4267-3000	1267	125.0-1200	5.0	253.4
3000-1750	1250	120.0-100.0	20.0	62.5
1750-1500	250	100.0-75.0	25.0	10.0
1500-1500	0	75.0-65.0	10.0	0
1500-0	1500	65.0-0	65	23.1

e) Anza-1

3662-3129	533	113.0-73.0	40.0	13.3
3129-3129	0	73.0-65.0	8.0	0
3129-1800	1329	65.0-38.0	27.0	49.2
1800-1800	0	38.0-24.6	13.4	0
1800-0	1800	24.6-0	24.6	73.2

3.7 Chemical Isolation of Kerogen: Laboratory Analysis

The procedure by Tissot and Welte (1978) was adopted. Samples were ground to about 200 mesh size and treated with a benzene/methanol mixture at a ratio of 3:1 to remove soluble organic matter (bitumen) after which it was treated with 3M hydrochloric acid at 70°C for 1 hour to destroy the carbonate material. The product was then treated with 1:1 mixture of 50% hydrofluoric acid (HF) and 3M HCl to destroy the carbonate material. The mixture was subsequently centrifuged, decanted, washed, recentrifugated and decanted to obtain a residue which is kerogen. It was weighed and compared to original sample weight. The percentage of kerogen in the original sample was thereafter calculated, and the procedure repeated for the samples from the depths (horizons) sampled. The results obtained are incorporated with existing data and listed in appendix A to E.

3.8 T.O.C. Versus Sedimentation Rate Curves

Data from 457 samples and readings from five wells (Appendix A to E) in the Anza Graben have been used to construct the T.O.C. - sedimentation rate curves shown in Figures 29 to 33 and summarized in Table 9. The width of the optimum sedimentation rate is chosen based on the optimum balance between each side of the curve against the "maximum" TOC for the curve as illustrated in each case.

Table 9. Summary of T.O.C.-optimum paleosedimentation rate curves.

Well Name	Sub-basin	Optimum sedimentation (m/M.Y)	Corresponding T.O.C. value (%)
Bellatrix	Chalbi	51-90	0.9
Sirius	Chalbi	39-70	1.4
Ndovu	Yamicha	160-260	1.2
Anza	Yamicha	14-25	0.3
Duma	Intermediate T. Blocks	35-65	0.9

It is observed that in the central part of the Yamicha basin (Fig. 4), where Ndovu well is situated, is characterized by the highest optimum sedimentation rate of 160-260 m/M.Y (Fig.30) for the whole Graben. Both the Chalbi sub-basin (North Anza) and the Intermediate Tilted Blocks have optimum rates in between 35 and 90 m/M.Y with all having corresponding T.O.C. values above the minimum 0.5%. The southern parts of the Yamicha (Anza well) witnessed the lowest optimum sedimentation rates in the basin at 14-25 m/M.Y and a corresponding T.O.C. values of 0.3% which is below the minimum 0.5%.

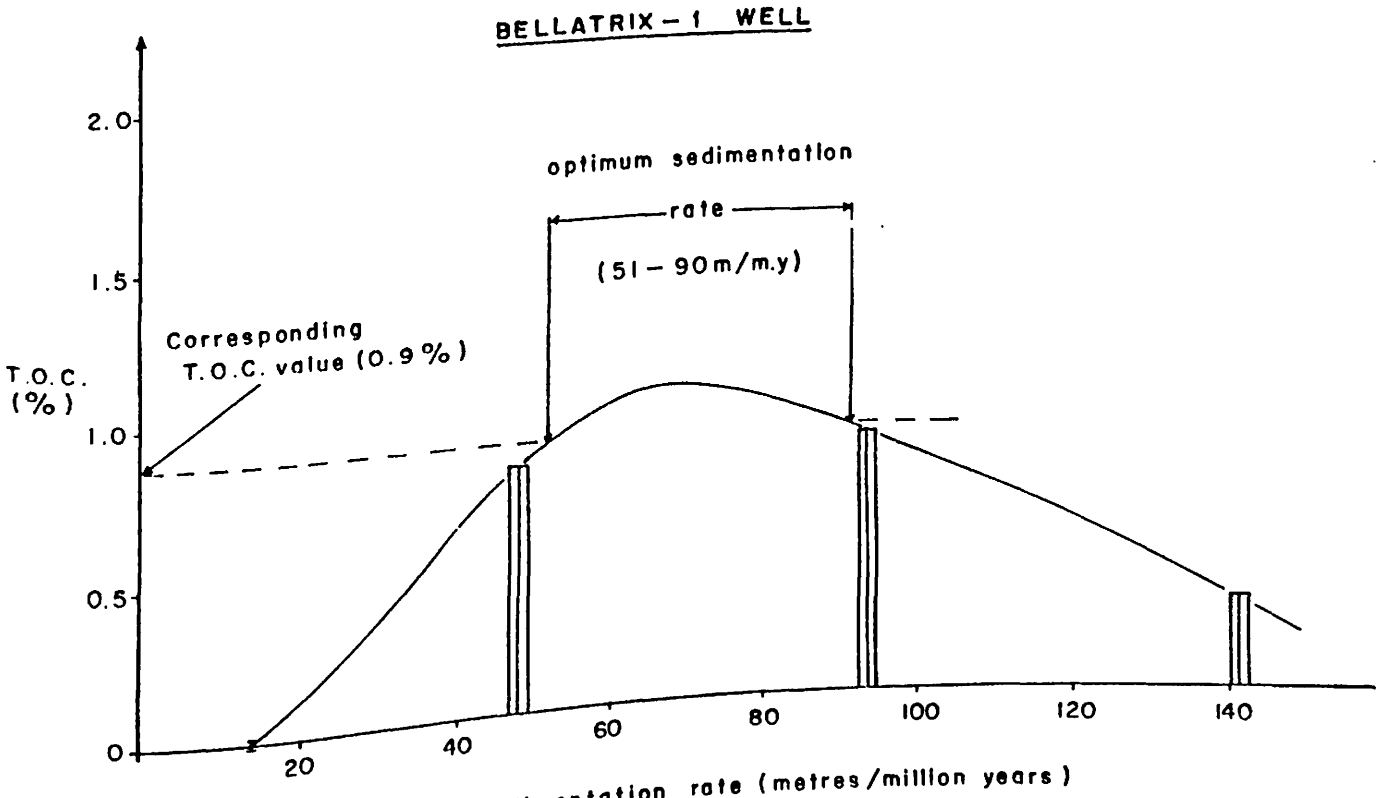

Fig. 28. T.O.C. - Sedimentation rate curve for Bellatrix-1 well.

SIRIUS – 1 WELL

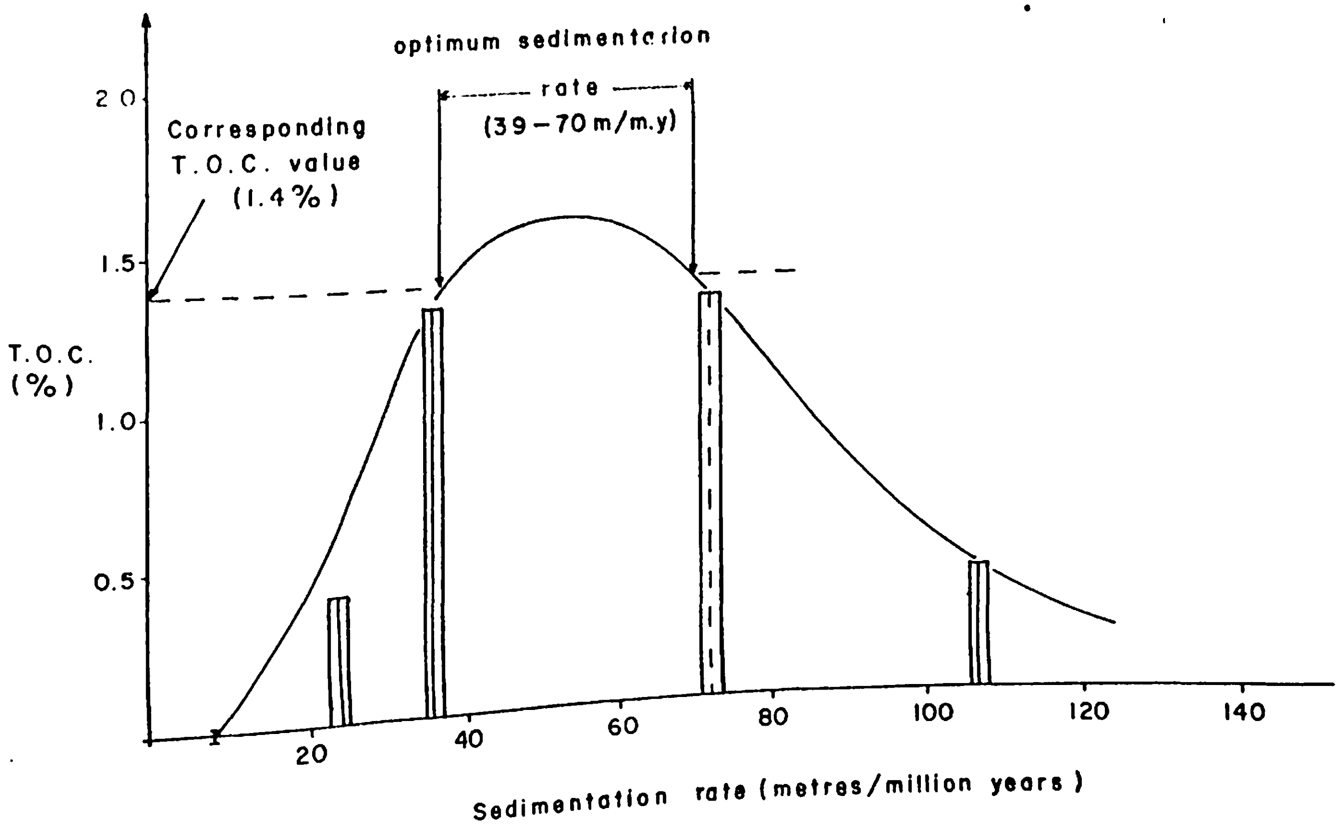

Fig. 29. T.O.C. - Sedimentation rate curve for Sirius - I well.

NDOVU – 1 WELL

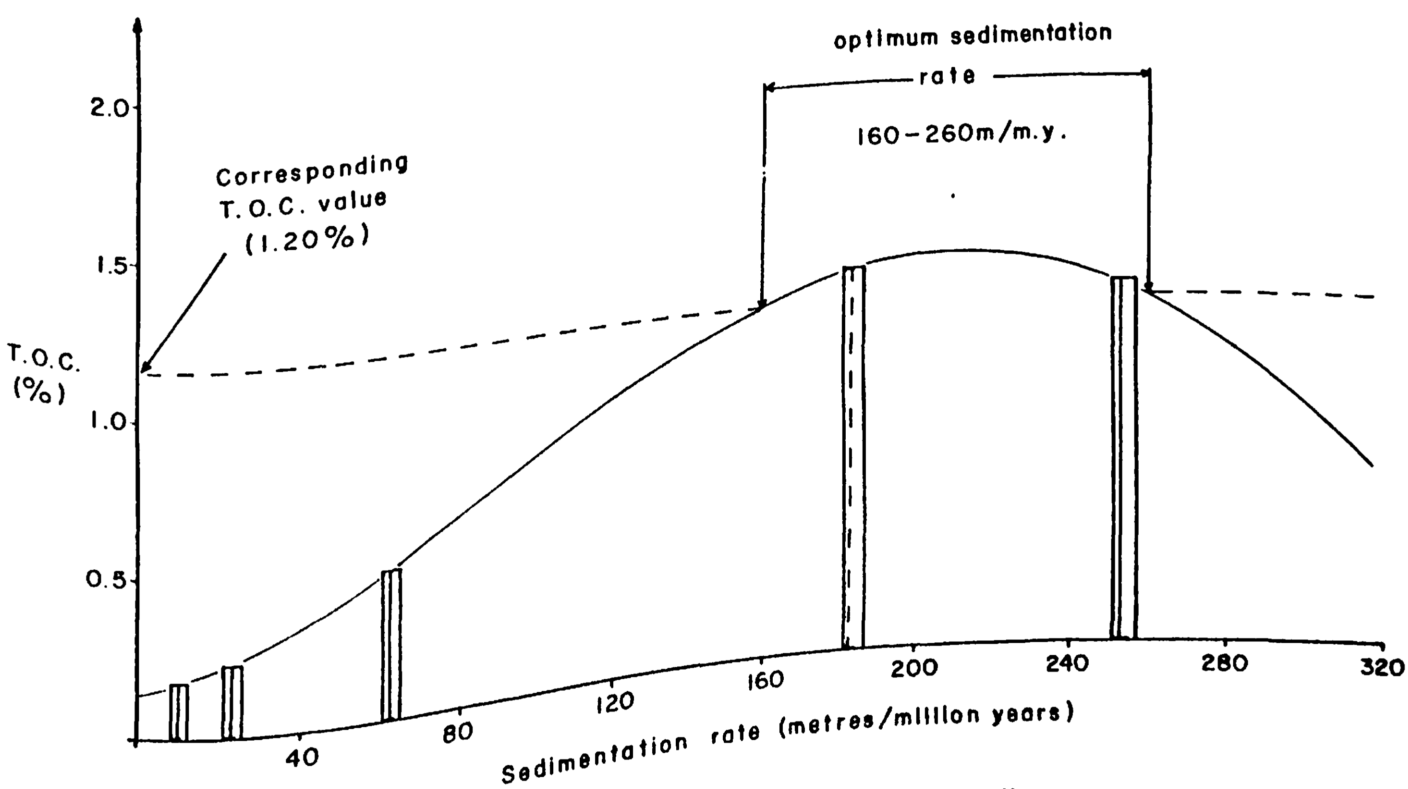

Fig. 30. T.O.C. - Sedimentation rate curve for Ndovu-I well.

ANZA - 1 WELL

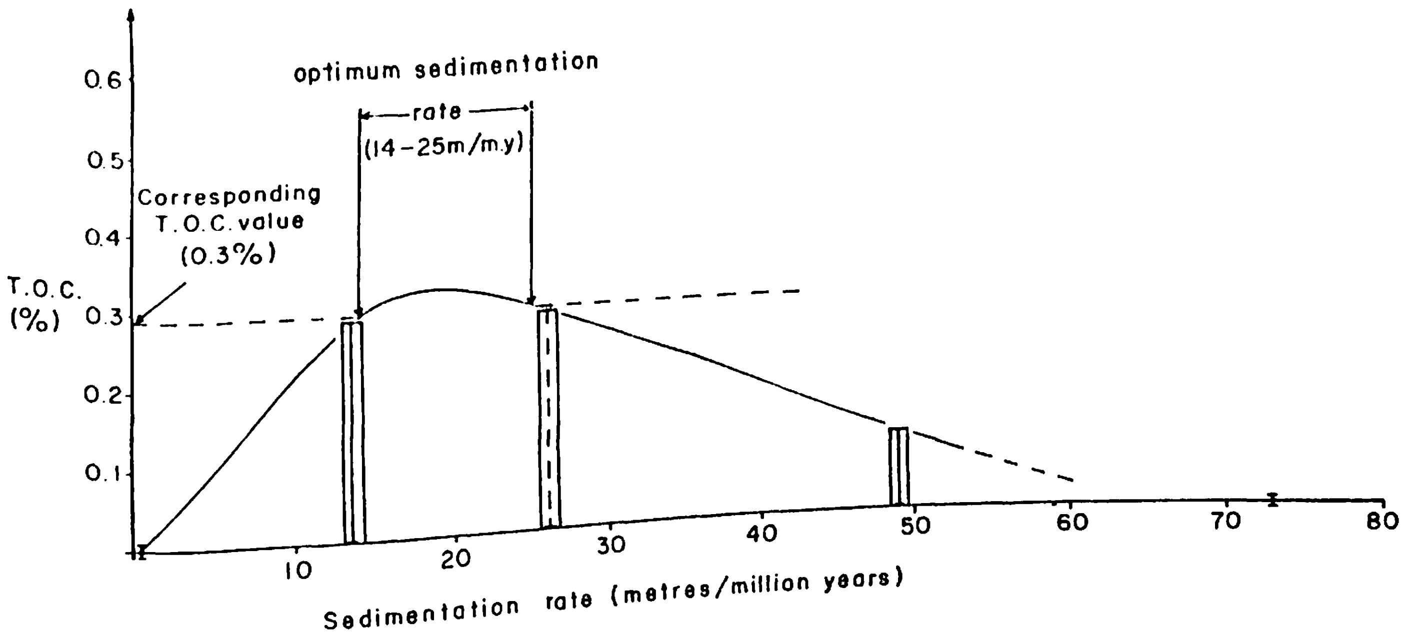

Fig. 31. T.O.C. - Sedimentation rate curve for Anza-1 well.

DUMA - 1 WELL

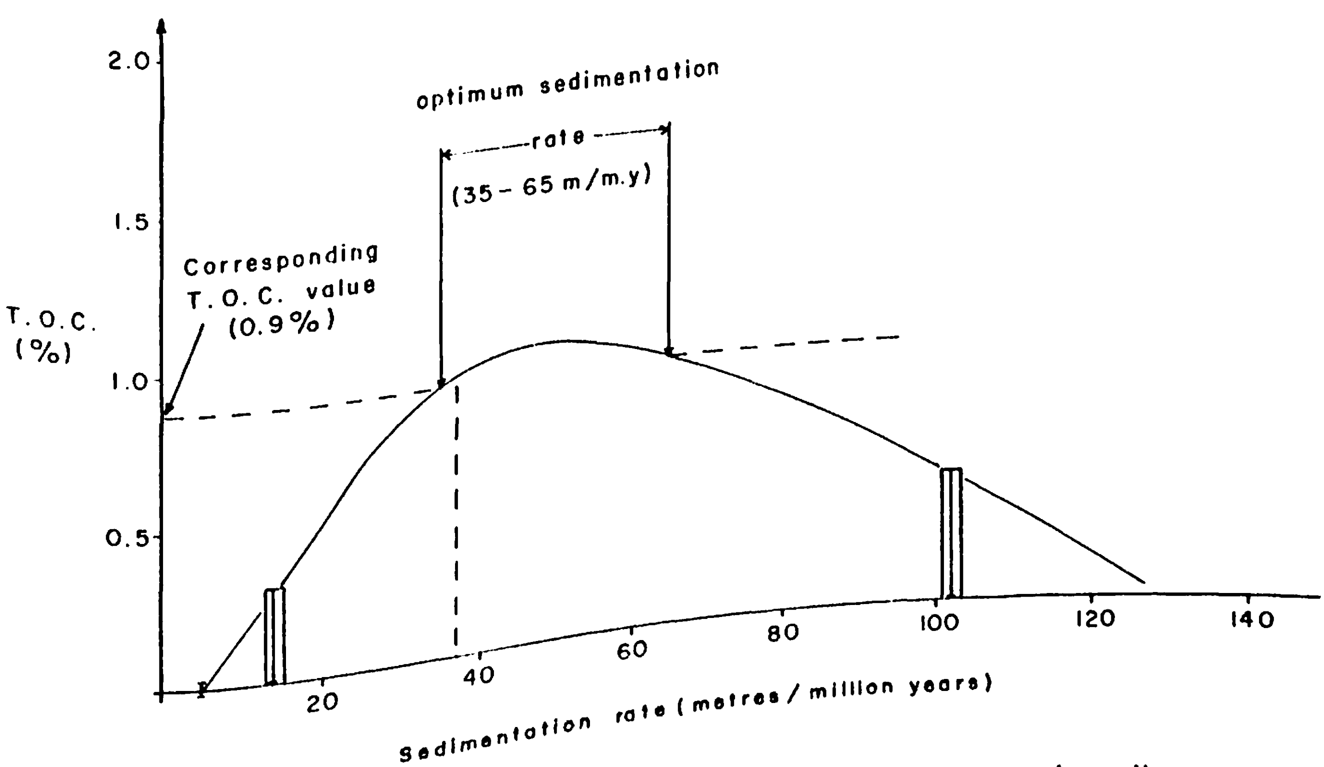

Fig. 32. T.O.C. - Sedimentation rate curve for Duma-1 well.

3.9 Sediment Types, Lithostratigraphical Zonations and Basinwide Correlations

The lithostratigraphic analysis below is based on the existing well data from the five wells in study area.

Chalbi sub-basin

Sirius-1 well bottomed out on about 60 m of limestone, overlain by 150 m of sandstone, both of which are considered to be of Neocomian to Barremian age. They are overlain by shales, sandstones and siltstones of Cenomanian and younger. Aptian-Albian sediments are missing from Sirius-1 profile, having been eroded. The TD in the adjacent Bellatrix-1 well is Cenomanian in age. The TD in the adjacent Bellatrix-1 well is Cenomanian in age based on coal beds that have been reported in this bottom section (Bosworth, 1992).

In both wells, the top of the Cretaceous (Maestrichtian age) consists of sandstone red beds and conglomerates. Thickness variations are shown in the correlation (Fig. 34). Tertiary sections in this basin are generally thick undated sandstones, basalts, sandstones and gravels.

Yamicha sub-basin

Palynological data suggest that the Tertiary/Cretaceous (Maestrichtian) boundary is at about 1470 m depth in Ndovu-1 well. The Tertiary section is however, much thicker in the southeastern flasks of the basin at 3129 m depth in the Anza-1 well. In both Ndovu-1 and Anza-1, the section above Tertiary/Cretaceous boundary is undated and there is no recorded significant lithologic break to suggest any distinctive hiatus. The upper Cretaceous (Maestrichtian) is about 260 m and 271 m thick in Ndovu-1 and Anza-1 wells respectively. This section is mainly siltstones, shales and sandstones. The section (upper Cretaceous) is considered as a deep water marine grading up the profile to brackish and lacustrine environments (Bosworth, 1992). The lower Cretaceous is at least 2537 m thick in Ndovu-1 and 262 m in Anza-1. The section consists of mainly fossiliferous shales with dinoflagellates (Anza-1 section, Fig. 14).

Intermediate Tilted Blocks Area

Duma-1 bottom out on Campanian shales, sandstones and siltstones. The upper Cretaceous (Campanian/Maestrichtian) record a marine incursion (Fig. 12) based on microfossils and traces of anhydrite. The Cretaceous is overlain by about 310 m of Tertiary sandstones, conglomerates.

The lower Cretaceous is about 2533 m with the bottom 333 m being barren and hence undated. The general lithology is mainly sandstones, shales and siltstones. It may thus be concluded that continental sedimentation dominated the Anza Graben during Cretaceous. Marine incursion occured however, at the same time as shown by the Cenomanian section in Ndovu-1 well, Maestrichtian section in Duma-1 well and in the upper Cretaceous of the Anza-1 well.

The relationship between these different sediment types and zonations described above and their depositional environments (Figures 11 to 14) with the optimum paleosedimentation rates (section 3.8) are further discussed in section 4.4.

Figure 33 summarizes the sediment types, lithological zonations and presents a basinwide correlation. The following additional facts, which discussed in section 4.2, are apparent. Thereis agood match between Ro and TTI oil windows; Ro however,tends to be most accurate as TTI is based on certain unverifiable assumptions. The Cretaceous, especially the Lower Cretaceus seems to be the most prospective. The Tertiary formations are immature in most sections except for the Anza-1 and, nearly all the wells reached TD while still within the oil window. These results are discussed in section 4.2.

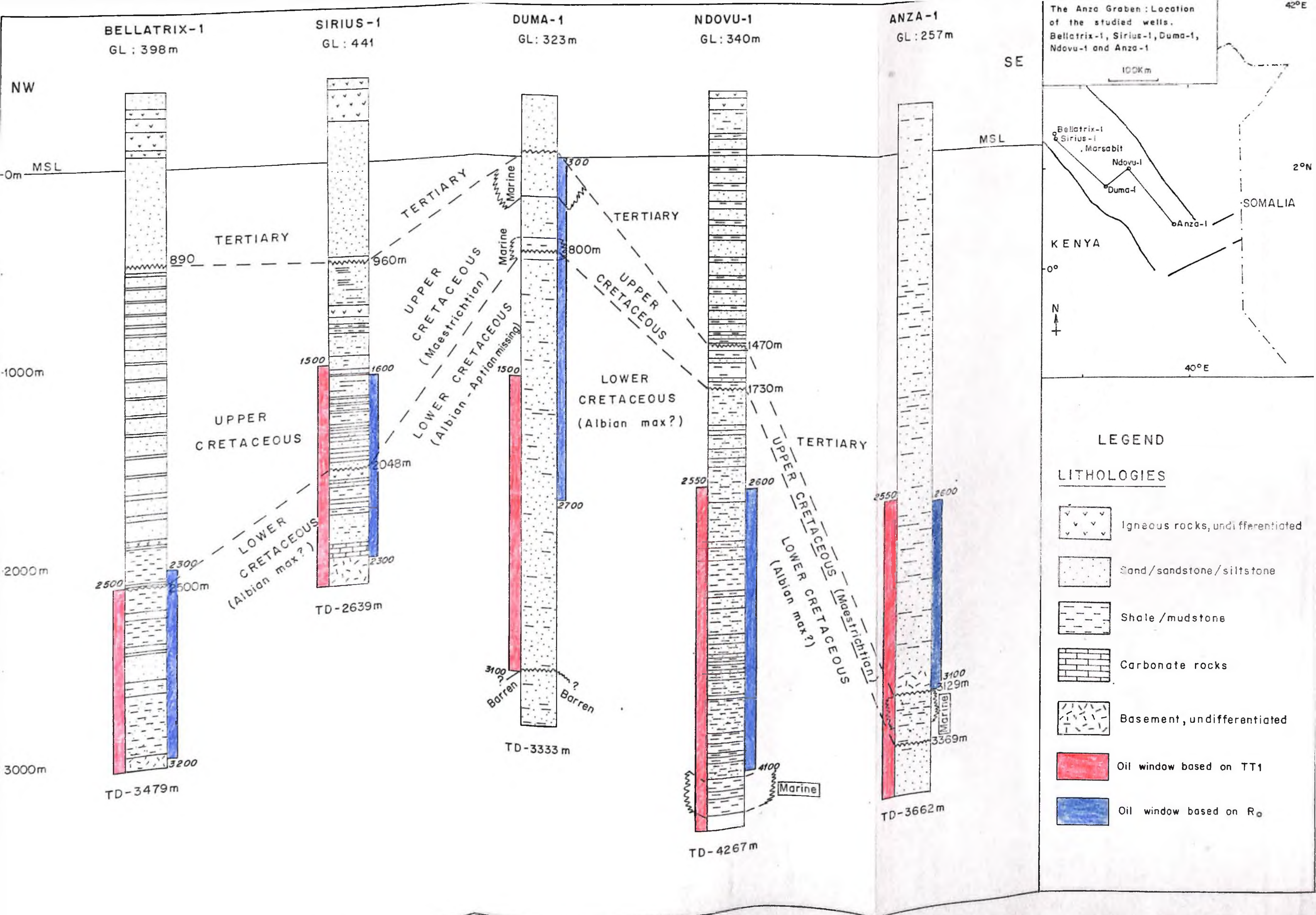

...logical zonations and basinwide correlations.

CHAPTER 4

DISCUSSION

4.1 Thermal Maturity

Bellatrix and Sirius-1 apparently have higher geothermal gradients than those in the Yamicha (Table 1) and this can be attributed to proximity to the Kenyan Rift. Structural activity associated with the Intermediate Titled blocks (Riaroh, 1992) is proposed to explain the geothermal gradient value which is slightly higher as compared to the less active south Yamicha sub-basin.

Studies conducted by Waples (1980; 1981) and Cohen (1985) have shown that high geothermal gradient and extra burial preceding uplift and erosion will normally increase maturity. These findings corroborate the TTI calculations (Table 3 to 7) based on the burial histories for Anza-1 and Ndovu-1 wells which had erosional hiatus. Also, since maturity is directly related to the amount of time spent near the maximum burial depth and temperature, the impact on maturity of the important events when they occur early in the history of the rock is much less. An implication of this finding which has also been cited by Cohen (1985) in his work is that source-rock maturity in rifted basins where high geothermal gradients are present in the early stages of basin evolution, will not be unusually high unless the source rock was deposited during the very early rifting stage.

Igneous intrusions are known to occur in the region surrounding the Chalbi sub-basin: i.e. Kulal, Chari Ache, Hurri Hills and Marsabit (Nyamweru, 1986). Their effect is however, difficult to precisely account for with maturity models as the present models have not been calibrated for such high temperatures. Furthermore, there is substantial doubt about the temperatures actually achieved in the sedimentary rocks and the rate at which thermal anomalies decay (Waples, 1985, 1992). Other sources of error include poor estimate of the amount of erosional removal, e.g. during unconformity, and poor present-day temperature data (or when past events e.g. igneous activity) created a thermal regime quite different from the present one.

4.2 Temperature-Time Index Technique

Lopatin's TTI method represents the relative timing and magnitude of episodes of deposition and erosion associated with periods of regional tectonism through the geologic past upto the present time (Waples, 1980; Guidishi *et al.*, 1985; Pitman *et al.*, 1987). The method allows one to predict both where and when hydrocarbons have been generated and at what depths liquids will be cracked to gas (Waples, 1985). It has even been suggested that maturity models are more accurate than measured data for determining the extent of petroleum generation (Yukler and Kokesh, 1984).

The hydrocarbon-generation history of the Anza sub-basin were evaluated by reconstructing the burial and thermal history of Cretaceous/Tertiary using a Lopatin technique. A time-temperature burial history model presented in Figures 23 to 27 and Tables 3 to 7 depict the thermal regime and different periods of regional tectonism that are proposed to have occurred in the sub-basins.

4.2.1 Interpretation of the TTI Results

Uncalibrated TTI values are obviously of little value unless compared in some way with measured maturity values. Table 8 below shows a correlation between TTI and hydrocarbon generation based on the most reliable present-day understanding of catagenesis and hydrocarbon formation. Different kerogen types have different oil-generation thresholds and Waples' original choice of Vitrinite Reflectance(R_o) of 0.65% as the threshold for oil-generation is almost certainly too high as recent studies by Waples(1985; 1992) have shown. Also the onset of oil generation is shown to vary from TTI = 1 for resinite to TTI = 3 for high-sulphur kerogens, TTI = 15 for Type III kerogens (Table 10). For the purposes of this study a general value of TTI = 3 (R_o = 0.5%) is taken to mark the onset of oil generation, and TTI = 180 (R_o = 1.35%) to mark the end of the oil window. These values are assumed to be representative given that the general depositional environment is mainly lacustrine for most of the wells (Fig. 11 to 14). Based on this distinction, the oil windows in each well and sub-basin have been defined as shown in Table 11.

Table 10. Correlation of TTI values with vitrinite-reflectance values and hydrocarbon generation (After, Waples,1985).

TTI	R_o	Generation	
1	0.40	Condensate from resinite	
3	0.50		
10	0.60	early	
15	0.65		
20	0.70	Oil	peak
50	0.90		
75	1.00		
180	1.35	late	
900	2.00	Wet gas	
		dry gas	

Another important assumption in the determinations was that the geothermal gradient was assumed constant for each well (Table 1), i.e. to be the same as present day gradient of the well. The surface temperature was taken as 32°C.

Table 11 and Figure 33 compare the oil windows for the basin as determined from the measured vitrinite reflectance values done by Sommer, (1990) and the TTI values in this study.

Table 11. Oil window depths in the basin: TTI results compared with R_o determinations.

	Bellatrix-1	Sirius-1	Duma-1	Ndovu-1	Anza-1
TTI(3-180)	2500-3479 (TD)	1500-2639 (TD)	1500-3100 (TD=3333)	2550-4267 (TD)	2550-3662 (TD)
R_o (0.5-1.35%)	2300-3200	1600-2300	300-2700	2600-4100	2500-3100

Depths in metres (m)

There is generally good agreement between the vitrinite reflectance and TTI values. The measured reflectance values reach the onset of oil generation R = 0.50% at a slightly shallow depth than do the calculated TTI values in Bellatrix-1 and significantly so in Duma-1 wells. This discrepancy could possibly reflect the use of low gradient (underestimated paleotemperature), underestimated erosional removal (in the case of Duma-1) or a combination of both factors (150 m is considered as the intrinsic accuracy of Lopatin's method, (Waples, 1985) meaning an error of about 150 m between the measured (R_o) and calculated maturity depths is acceptable).

4.3 T.O.C. - Optimum Sedimentation Rate Curves

Empirical relationship of percentage organic carbon and sedimentation rate from different parts of the world (including the some from giant oil fields e.g.Nagaoka Plains in Japan and Midland Plains, Texas) suggest that optimal organic carbon concentration may be found between sedimentation rates of 8-90 m/M.Y, and mid-values between 30-60 m/M.Y (Magara, 1986). Although the optimum rate of sedimentation is not always constant, thus it has to be empirically obtained and the result only applicable within the same basin or area, it is interesting to note that results obtained in this study (Table 9) compare very well with the world figures with the exception of Ndovu well.

The Ndovu well, however, happens to be sited at the flanks of the deepest section of the graben near the Lagh Boghal Fault (Fig. 4). This partly explains the high optimum sedimentation rate. Most of the sedimentation in this section of the sub-basin took place in a continental (lacustrine) environment except for the brief marine incursion in the Upper Cretaceous time (Fig. 11). High rates of sedimentation was thus apparently necessary for the preservation of the available organic matter. This suggestion is validated by the low (0.3%) T.O.C results obtained for the Anza well which is situated in the southern flanks of the same Yamicha sub-basin owing to its low sedimentation rates (14-25 m/M.Y.). In this part of the basin, as opposed to the north-western Ndovu area, the sedimentation rate was relatively small (four times lower) thus inhibiting the organic matter preservation through burial and exposing them to destruction (Table 9). In this explanation, it is noted that the environment of deposition in both cases was approximately similar, only that the marine incursion appeared in the Anza before it encroached north into the Ndovu area. This is consistent with evidence elsewhere (Cannon *et al*, 1981) concerning the sea invasion after the Gondwanaland break-up. In both cases the organic matter supply is assumed to be largely similar. The low TOC in the Anza Graben is related unproportionally to the low sedimentation rate rather than the better supply of organic matter owing to its predicted initial thicker marine profile enhancing primary productivity.

Both Bellatrix and Sirius wells in the Chalbi basin have largely similar results suggesting basinal similarity in hydrocarbon prospectivity. The optimum sedimentation rates of 39-90 (m/M.Y) largely fall within the world optimum values. With corresponding T.O.C values of 0.9 to 1.4% (Table 10), which are well above the 0.5% empirical threshold, the basin presents an interesting prospect.

In each of the five wells, the optimum organic carbon percentage (T.O.C.) decreases as the rate of sedimentation increases or decreases from this value. In this regard, it is important to note that below each curved line (Fig 29 to 32) there are many plotted points. This means that even if the rates of sedimentation were optimum, the organic matter was not always available in areas of deposition (Magara, 1986) to be preserved by the burial processes and against the inherent organic destruction mechanisms.

4.4 Optimum Paleosedimentation Rates and Sediment types

Based on the results of the optimum paleosedimentation rates for the graben, the following results (Table 12) are obtained especially when these values are associated with particular sediment types.

Table 12. Optimum paleosedimentation rates and the related sediment types.

Well Name	Optimum P/sedimentation Rate (m/M.Y)	Depth Interval (m)	Sediment types
Bellatrix-1	39-70	2300-3479 (TD)	Shales/Sandstones
Sirius-1	51-90	960-2040 (TD-2639)	Shales, Sandstones&Limestone
Duma-1	35-65	800-TD (TD-3333)	Marine shales, Anhydrite,Sandstones & Siltstones
Ndovu-1	160-260	3000-TD (4267)	Shales,Sandstones& Siltstones
Anza-1	14-25	1800-TD (3662)	Shales, Sandstones & Siltstones

These results suggest that in the entire basin, the optimum paleosedimentation rates are associated with shales, sandstones and siltstones. In Sirius-1 limestones were deposited instead of siltstones. Given that shales are the major source rocks in continental environments (and most sandstones with minor shales and siltstones) and the sandstones generally are the reservoir materials, it is apparent that when these parameters are integrated together with T.O.C.s, they suggest that potential for oil exists in this graben.

4.5 Genetic Potential, Transformation Ratio, and T_{max}

The concept in which these maturity parameters are understood and used in this study are explained in the 'Legend' to the Appendix at the end of the report.

4.5.1 Genetic Potential

The genetic potential ($S_1 + S_2$) gives a qualitative estimate of hydrocarbon resource potential. Based on the classification by Tissot and Welte (1978), a value of 6 mg/g indicate good potential, 2-6 mg/g suggest moderate hydrocarbon potential and values less than 2 mg/g indicate poor source potential.

There is moderate to good potential in Ndovu-1 at 3020-3220 m depth (1.78-25.67 mg/g) and poor potential below this depth. The above range falls within the oil window as defined by the TTI determinations. In south Yamicha in the Anza-1 well, the genetic potential is mostly below 0.1 mg/g suggesting a poor potential. This is incidentally reflected in the T.O.C.-paleosedimentation rate curve for the Anza-1 well, in which we note low paleosedimentation rate for this part of the basin resulting in low T.O.C. being preserved as opposed to the Ndovu-1 area. Duma-1 is characterized by poor, below 0.1 mg/g genetic potential for the 2500 m-TD oil window depth. In the Chalbi sub-basin, a moderate to good potential (2.0-21.0 mg/g) is observed in Sirius-1 at 1500-1940 m depth. Below this depth a poor potential is noted. The adjacent Bellatrix-1 reports a potential of less than 2 mg/g.

Related studies on genetic potential of other basins, (Pitman *et al* 1985) suggest a caution, however, that condensed polyaromatic and oxygen-rich structures characteristic of terrestrially derived type II kerogens generally have only moderate oil potential but may generate significant amounts of gas. It is also known that the quantity of oil or gas produced is a function of the dominant type of organic matter, its organic richness, thermal maturity, and the availability of migrational paths.

4.5.2 Transformation Ratio (or Production Index P.I.) and T_{max}

The Production Index (P.I.) or transformation ratio ($S_1/[S_1 + S_2]$ is also often used to assess the relative thermal maturity of organic matter and the presence of migrated hydrocarbons. A value of 0.1-0.2 marks the transition from immature to mature, ranging upto 0.4 for type III kerogen (Durand and Piratte, 1983). Unusually high P.I. generally indicate the presence of migrated hydrocarbons.

The degree of maturation may also be obtained by analysing the temperature of maximum hydrogen generation during pyrolysis (T_{max} in °C) under laboratory conditions. T_{max} values of 435-460°C have been established to correspond to peak hydrogen generation. These results are summarized in Table 13 below based on the oil window determined from TTI analyses (Tables 3 to 7 and Figures 23-27) and the data listed in Appendix A to E.

Table 13. Genetic potential, transormation ratio, T_{max} and the oil window.

	Ndovu-1	Anza-1	Duma-1	Sirius-1	Bellatrix-1
Oil window (m)	2500-TD	2550-TD	2500-3100	1500-TD	2500-TD
Genetic Potential (mg/g)	1.78-25.67 (3020-3220 m)	<0.1	<2.0	2.0-21.00 (1500-1940 m)	<2.0
Transformation Ratio = (0.1-0.2)	2500 m-TD	2480 m-TD	2420 m-TD	1900 m-TD	2620 m-TD
T_{max} (°C)	421-483	294-302	469-483	444-582	443-466

In Ndovu-1 there is an excellent match in the depth of the oil window as defined by TTI and the Transformation Ratio ($S_1/[S_1 + S_2]$) at 2500 m to TD. The T_{max} of 421-483°C falls roughly within peak range, 435-460°C.

In the Anza-1 area the transformation is observed from 2480 m-TD depth with a relatively low T_{max} of 294-302. Duma-1 records transformation into mature source rocks at 2420 m to TD. The T_{max} confirms this at 469-483°C. In the Chalbi basin, the transforms occur slightly below that predicted by the TTI at 2620 m to TD (Bellatrix-1) with an optimum T_{max} of 443-446 for this range. The adjacent Sirius-1, has the transformation at 1900 m to TD and a T_{max} of 443-582.

CHAPTER 5

SUMMARY AND CONCLUSIONS

On the whole, this study recognizes that there is an empirical relationship between paleosedimentation rate and the T.O.C. when the environment of deposition is taken into account. Optimum sedimentation rates which minimize the effects of both dilution and consumption/destruction commonly result in the most organic - rich sediments. The results of this study thus support the finding by Dow (1978) that there is an optimum rate of sedimentation for maximum concentration of organic matter. This concept can be applied as a principal mechanism in assessing any sedimentary basin. Other studies have also shown that the most organic-rich sediments are deposited in areas of high organic productivity where the supply of bottom oxygen is minimal, the water reasonably quiet and the sedimentation rate of mineral particles is intermediate. Generally therefore surface productivity is an important source of organic carbon which is lithified for preservation.

In the Chalbi sub-basin the optimum paleosedimentation rate is between 39 and 90 m/M.Y, corresponding to T.O.C. values of between 0.9 to 1.4%, and are within the range of empirical values determined for other parts of the world. When these findings are integrated with results of sediment maturity studies through burial histories, this sub-basin presents an encouraging hydrocarbon prospect area.

In the Yamicha sub-basin, it is apparent from the TTI results and the T.O.C.-paleosedimentation rate curves that relatively higher sedimentation rates (at 160-260 m/M.Y as the optimum value with a corresponding T.O.C. value of about 1.2%) are necessary for organic matter preservation. The sub-basin zone in the vicinity of Ndovu well which is the deepest zone of the basin has the most pronounced prospect at T.O.C. value of about 1.2% and a maturity value within the oil window at TD. Within approximately this same depositional environment but at reduced sedimentation rate (14-25 m/M.Y) the southern flanks of the Yamicha sub-basin where Anza well is situated, the preservation potential diminishes nearly four times giving a corresponding T.O.C.

value of 0.3%, well below the required minimum value of 0.5%. Maturity studies (T.T.I. from burial curves) also show these values to fall within the oil window. These results suggest a reduced prospect in the southwestern flanks of the Yamicha sub-basin, whereas the prospect is enhanced towards the deeper zones of the sub-basin towards the northwest as represented by the Ndovu well results.

The optimum paleosedimentation rates are characterised by mainly shales, sandstones and siltstones in the entire basin. Shales are normally the source rocks and sandstones are reservoirs rocks. Limestones (found in Sirius-1) may also act as source and reservoir rocks. These results further suggest enhanced hydrocarbon potential in the basin covered by the study.

From the TTI determinations, the oil window is shown to occur between 2500 m to TD for Bellatrix-1 well and from 1500 m to TD for Sirius-1 both in the Chalbi sub-basin. The oil window runs from 2500 m to TD (Ndovu-1) and 2550 m to TD (Anza-1), in the Yamicha sub-basin. The intermediate Tilted Blocks Area (Duma-1) has the oil window between 2500-3100 m depth. These empirical results compare very favourably with independent determinations based on T_{max}, genetic potentials and the transformation ratios listed in appendix A to E.

CHAPTER 6

REFERENCES

Amoco Kenya (1988). Final Well Report. Bellatrix-1, Kenya.

Amoco Kenya (1988). Final Well Report. Sirius-1, Kenya.

Beicip (1984). Petroleum potential of Eastern Kenya. Unpublished report to the Ministry of Energy, Kenya.

Beicip (1985). Petroleum potential of Ethiopia. Unpublished report to the Ministry of Mines and Energy, Ethiopia, p 14-17.

Bosworth, W. and Morley, C. (1992). Structural evolution of the Anza Rift, Kenya, based on reflection seismic data. Tectonophysics KRISP Volume 1992 (in press).

Bosellini, A. (1986). East Africa continental margins. Geology, Vol. 14 pp 76-78, U.S.A.

Brooks, J. (1981). Organic maturation of sedimentary organic matter and petroleum exploration - A review, In: J.Brooks (ed.) Organic Maturation Studies and Fossil Fuel Exploration. Academic Press, U.K. p 1-37.

Cannon, R.T.; Siambi-Simiyu, W.H.N. and Karanja, F.M. (1981). The proto-Indian Ocean and a probable Paleozoic/Mesozoic triradial rift system in East Africa. Earth and Planetary Science Letters, 52, Elsevier Sc. Publ., p 419-426.

Chenot, D. (1987). Gravity and magnetic data interpretation, Kenya. Block 9. TOTAL CFP, Paris. 18 p.

Cohen, C.W. (1985). Role of fault rejuvenation in hydrocarbon accumulation and structural evolution of Reconcavo Basin, northeastern Brazil. AAPG, Vol. 69, pp 65-76.

De Cruz, M. and Milliped, P. (1988). Palynology and depositional environments, Ndovu-1 well. In: Ndovu-1 Laboratory Studies - TEP/DE/LAB. TOTAL Kenya.

Dindi, E.W., (1992). Geophysical studies of the Anza Graben, North Eastern Kenya. Unpublished PhD Thesis, University of Nairobi. 191 p.

Dow, W.G. (1978). Petroleum source beds on continental slopes and rises. AAPG. 62., pp 1584-1606.

Durand, B., and Paratte, M.,(1983). Oil potential of coals: A geochemical approach, In: J. Brooks, ed., Petroleum Geochemistry and Exploration of Europe: Geological Society Special Publication 12., pp 255-265.

Gazette of Kenya, Vol. XXXIX, dated March 2nd 1937.

Gazette of Kenya No. 613 (1938) official.

Gazette of Kenya, Vol. XL dated July 29th 1938.

Guidishi, T.M.; Kendall, C.G. St. C.; Lerche, I.; Toth, D.J.; Yarzab, R.F. (1985). Basin Evaluation using burial calculations: An overview. A.A.P.G. Bulletin Vol. 69 No. 1, pp 92-105.

Joubert, P. (1960). Geology of the Mandera-Damassa area. Rept. No. 48. Geol. Surv. Kenya. Nairobi, 65 p.

Joubert, P. (1963). Geology of the Wajir - Wajir Bor area, Geol. Surv. Kenya. Nairobi, 44 p.

Magara, K. (1986). Geological Models of Petroleum Entrapment. Elsevier Applied Sc. Publ., 328p.

Matheson, F.J. (1971). Geology of the Garba Tula area. Rept. No. 88. Geol. Surv. Kenya Nairobi. 30 p.

Miller, J.B. (1973). Geologic study of the Garissa-Wajir area, related to the Chevron Oil Licence, Kenya. Unpublished Report. 19 p.

Nyamweru, C.K. (1986). Late Quarternary environments in the Chalbi Basin, Kenya: Sedimentary and geomorphological evidence. Document No. 2595 g GEMS PAC Information Sciences No. 4. UNEP, Nairobi. 37 p.

Pitman, J.K.; Franczyk, K.J.; Anders, D.E. (1987). Marine and nonmarine gas-bearing rocks in Upper Cretaceous Blackhawk and Neslen Formations, Eastern Uinita Basin, Utah: Sedimentology diagenesis, and source rock potential. AAPG Bull. Vol. 71 pp 76-94.

Rabinowitz, P.D. and Falvey, D. (1982). Salt diapirs bordering the continental margin of northern Kenya and Somalia. Science, Vol. 215 AAAS.

Riaroh, D.R.O. (1992). Listhostratigraphy of Duma-1 well: Implications as to the depositional history and petroleum geology of the Intermediate Tilted Blocks, central Anza Graben, N.E. Kenya. Internal Report, Ministry of Energy, Kenya.

Reeves, C.V.; Karanja, F.M. and MacLeod, (1986). Geophysical evidence for a failed Jurassic rift and tripple junction in Kenya. Earth and Planetary Science Letters, 81. Elsevier Sc. Publ. pp 299-311.

Ronov, A.B. (1958). Organic carbon in sedimentary rocks (in relation to the presence of petroleum). Geochemistry 5, pp 510-36.

Schull, T.J. (1988). Rift basins of interior Sudan: Petroleum exploration and discovery. AAPG Bulletin Vol. 72 No. 10.

Selley, R.C. (1985). Elements of Petroleum Geology. W.H. Freeman Publ., New York 179 p.

Sommer, F. (1990). Petrography, diagenesis and thermal evolution of the Anza Basin, Kenya. TOTAL CFP, Paris. 9 p.

Tepma Kenya (1988). Ndovu-1, Geological Final Report. 36 p.

Tepma Kenya (1989). Geological Final Report, Duma-1, Block 9, Kenya. 23 p.

Thompson, A.O. and Dodson, R.G. (1958). Geology of the Derkali-Melka Murri area. Rept. No. 43, Geol. Surv. Kenya. Nairobi 35 p.

Thompson, A.O. and Dodson, R.G. (1960). Geology of the Bur Mayo-Tarbaj area. Rept. No. 47, Geol. Surv. Kenya. Nairobi 49 p.

Tissot, B.P. and Welte, D.H. (1978). Petroleum Formation and Occurrence. Spring-Verlag Publ., New York. 527p.

UNESCO/C.C.G.M. (1971). Tectonic map of Africa. UNESCO, Paris.

Waples, W.D. (1980). Time and temperature in petroleum formation. Application of Lopatin's method to petroleum exploration. AAPG, Bul. Vol. 64 No. 6. pp 916-926.

Waples, W.D. (1981). Organic Geochemistry for Exploration Geologists. Colorado School of Mines, Burgess Publ. Co. CEPCO Division. pp 95-106.

Waples, W.D. (1985). Geochemistry in Petroleum Exploration. IHRDC, Boston 232 p.

Waples, W.D. (1992). The art of maturity modeling. Part 1: Finding a satisfactory geologic model and, Part 2: Alternative models and sensitivity analysis. AAPG. Vol. 76 No. 1 pp 31-46 and pp 47-66.

Yukler, M.A. and Kokesh, F. (1984). A review of models used in petroleum resource estimation and organic geochemistry. In: J. Brooks and D. Welte (eds.). Advances in Petroleum Geochemistry, Vol. 1. London, Academic Press, pp 813-826.

7 APPENDICES

Geochemical Data Listing for the five wells used in this study.

Appendix A. Geochemical Data Listing for Ndovu-1
(Yamicha sub-basin).

Appendix B. Geochemical Data Listing for Duma-1
(Intermediate Tilted Blocks sub-basin).

Appendix C. Geochemical Data Listing for Anza-1
(Yamicha sub-basin).

Appendix D. Geochemical Data Listing for Bellatrix-1
(Chalbi sub-basin).

Appendix E. Geochemical Data Listing for Sirius-1
(Chalbi sub-basin).

LEGEND

T.O.C. = Total Organic Carbon (weight % of rock).

S_1 = Quantity of organic matter existing in the rocks as free or adsorbed hydrocarbons (kg of hydrocarbons - free and thermo-vaporizeable - per ton of rock = oil.

S_2 = Quantity of hydrocarbons and hydrocarbon-like compounds released from the rocks at pyrolytic temperatures (250°C) (=kg of hydrocarbons (cracking of kerogen) per ton of rock → kerogen.

S_1+S_2 = Original genetic potential plus residual genotic potential. A value of 2 mg/g is considered minimum for oil source rocks.

P.I. = Production Index, $S_1/(S_1+S_2)$ = Transformation ratio or index of maturation. With respect to hydrocarbon generation, transition from immature to mature is about 0.1.

T_{max} = Temperature at the maximum hydrocarbon (S_2) generation during pyrolysis; measures prior thermal history. Transition from immature to mature is about 440°C.

APPENDIX A

Geochemical Data Listing for

Ndovu-1 (Yamicha Sub-basin)

Ndovu-1

Depth (m)	TOC (%)	S_1 (mg/g)	S_2 (mg/g)	S_1+S_2 (mg/g)	PI $S_1/(S_1+S2$	T_{max}
500	0.00	0.00	0.00	0.00	0.00	291
520	0.00	0.00	0.03	0.00	0.00	199
540	0.00	0.00	0.04	0.04	0.00	235
560	0.00	0.00	0.01	0.01	0.00	220
580	0.00	0.00	0.00	0.00	0.00	240
600	0.00	0.00	0.01	0.01	0.00	245
620	0.00	0.00	0.01	0.01	0.00	265
640	0.00	0.00	0 01	0.01	0.00	252
660	0.00	0.00	0.00	0.00	0.00	242
680	0.00	0.01	0.05	0.06	0.17	247
700	0.00	0.00	0.00	0.00	0.00	238
720	0.01	0.09	0.00	0.09	1.00	236
740	0.01	0.00	0.00	0.00	0.00	283
760	0.01	0.00	0.00	0.00	0.00	244
780	0.01	0.00	0.00	0.00	0.00	242
800	0.00	0.00	0.00	0.00	0.00	242
820	0.01	0.02	0.05	0.07	0.29	257
840	0.04	0.03	0.11	0.14	0.21	256
860	0.05	0.02	0.06	0.08	0.25	248
880	0.02	0.00	0.00	0.00	0.00	258
900	0.01	0.00	0.00	0.00	0.00	258
920	0.08	0.00	0.01	0.01	0.00	286
940	0.12	0.00	0.03	0.03	0.00	308
960	0.12	0.00	0.04	0.04	0.00	334
980	0.12	0.00	0.02	0.02	0.00	333
1000	0.32	0.00	0.15	0.00	0.00	351
1020	0.13	0.00	0.07	0.07	0.00	365
1040	0.26	0.00	0.11	0.11	0.00	385
1060	0.08	0.00	0.01	0.01	0.00	333
1080	0.10	0.00	0.02	0.02	0.00	317
1100	0.10	0.00	0.04	0.04	0.00	326
1120	0.10	0.00	0.09	0.09	0.00	362
1140	0.18	0.00	0.16	0.16	0.00	383
1160	0.12	0.00	0.14	0.00	0.00	281
1180	0.27	0.01	0.15	0.16	0.06	336
1200	0.15	0.00	0.04	0.04	0.00	340
1220	0.27	0.01	0.09	0.10	0.10	289
1240	0.22	0.00	0.11	0.11	0.00	281
1260	0.34	0.01	0.21	0.22	0.05	302
1280	0.11	0.00	0.02	0.02	0.00	285
1300	0.22	0.00	0.10	0.10	0.00	296
1320	0.35	0.01	0.27	0.28	0.04	318
1340	0.08	0.01	0.07	0.08	0.11	297
1360	0.12	0.01	0.05	0.06	0.17	377
1380	0.14	0.01	0.11	0.12	0.08	368
1400	0.17	0.01	0.06	0.07	0.14	292
1420	0.23	0.01	0.10	0.11	0.09	359
1440	0.14	0.00	0.00	0.00	0.00	290

A(ii)

1460	0.10	0.01	0.07	0.08	0.12	280
1480	0.42	0.00	0.20	0.20	0.00	340
1500	0.36	0.00	0.11	0.11	0.00	300
1520	0.12	0.00	0.22	0.22	0.00	334
1540	0.24	0.00	0.09	0.09	0.00	302
1560	0.31	0.02	0.52	0.54	0.04	369
1580	0.12	0.00	0.04	0.04	0.00	311
1600	0.21	0.00	0.08	0.08	0.00	341
1620	0.16	0.00	0.04	0.00	0.00	307
1640	0.08	0.00	0.03	0.03	0.00	272
1660	0.18	0.00	0.07	0.07	0.00	325
1680	0.13	0.00	0.05	0.05	0.00	283
1700	0.09	0.00	0.09	0.09	0.00	280
1720	0.19	0.01	0.14	0.15	0.07	300
1740	0.32	0.04	0.22	0.26	0.15	359
1760	0.41	0.30	0.29	0.59	0.51	316
1780	0.10	0.02	0.13	0.15	0.13	314
1800	0.09	0.00	0.02	0.02	0.00	259
1820	0.08	0.01	0.06	0.07	0.14	279
1840	0.16	0.00	0.06	0.06	0.00	326
1860	0.22	0.00	0.04	0.04	0.00	362
1880	0.26	0.04	0.12	0.16	0.25	344
1900	0.08	0.00	0.00	0.00	0.00	251
1920	0.08	0.01	0.04	0.05	0.20	228
1940	0.21	0.08	0.13	0.21	0.38	264
1960	0.12	0.00	0.00	0.00	0.00	240
1980	0.09	0.00	0.01	0.01	0.00	246
2000	0.04	0.00	0.00	0.00	0.00	244
2020	0.07	0.01	0.01	0.02	0.50	226
2040	0.05	0.00	0.02	0.02	0.00	362
2060	0.08	0.01	0.01	0.02	0.50	255
2080	0.09	0.00	0.02	0.02	0.00	254
2100	0.08	0.00	0.03	0.03	0.00	270
2120	0.10	0.00	0.02	0.02	0.00	237
2140	0.14	0.00	0.03	0.03	0.00	252
2160	0.12	0.00	0.05	0.05	0.00	290
2180	0.12	0.00	0.03	0.03	0.00	304
2200	0.28	0.00	0.22	0.22	0.00	298
2220	0.23	0.00	0.06	0.06	0.00	285
2240	0.19	0.00	0.05	0.05	0.00	224
2260	0.22	0.00	0.02	0.02	0.00	304
2280	0.15	0.00	0.13	0.14	0.07	234
2300	0.18	0.01	0.16	0.17	0.06	255
2320	0.17	0.01	0.01	0.01	0.00	222
2340	0.12	0.00	0.08	0.10	0.20	304
2360	0.04	0.02	0.01	0.01	0.00	247
2380	0.16	0.00	0.05	0.05	0.00	282
2400	0.15	0.00	0.09	0.11	0.18	259
2420	0.11	0.02	0.05	0.08	0.38	247
2440	0.07	0.03	0.01	0.01	0.00	202
2460	0.09	0.00	0.01	0.01	0.00	275
		0.00				

A(iii)

2480	0.18	0.00	0.06	0.06	0.00	319
2500	0.25	0.01	0.11	0.12	0.08	421
2520	0.17	0.02	0.11	0.13	0.15	382
2540	0.33	0.02	0.22	0.24	0.08	379
2560	0.46	0.04	0.27	0.31	0.13	294
2580	0.15	0.00	0.09	0.09	0.00	335
2600	0.15	0.01	0.14	0.15	0.07	309
2620	0.39	0.31	0.35	0.66	0.47	397
2640	0.21	0.11	0.17	0.28	0.39	437
2660	0.63	0.04	0.32	0.36	0.11	432
2680	0.65	0.01	0.58	0.59	0.02	430
2700	0.60	0.19	0.40	0.59	0.32	374
2720	0.57	0.09	0.37	0.46	0.20	414
2740	0.63	0.24	0.64	0.88	0.27	416
2760	0.40	0.06	0.32	0.38	0.16	412
2780	0.79	0.10	0.69	0.79	0.13	418
2800	0.69	0.19	0.69	0.88	0.22	364
2820	0.64	0.17	0.53	0.70	0.24	410
2840	0.72	0.16	0.65	0.81	0.20	398
2860	0.8	0.31	0.85	1.16	0.27	385
2880	0.85	0.12	0.83	0.95	0.13	417
2900	1.03	0.07	1.01	1.08	0.06	444
2920	1.01	0.16	1.10	1.26	0.13	413
2940	0.89	0.12	0.87	0.99	0.12	428
2960	1.37	0.18	1.37	1.55	0.12	428
2980	1.30	0.12	1.19	1.31	0.09	434
3000	1.18	0.08	1.19	1.27	0.06	444
3020	1.31	0.07	1.71	1.78	0.04	425
3040	0.92	0.10	0.90	1.00	0.10	407
3060	1.56	0.18	1.23	1.41	0.13	441
3080	2.03	0.13	2.71	2.84	0.05	447
3100	2.59	0.24	3.19	3.43	0.07	381
3120	1.41	0.11	1.42	1.53	0.07	427
3140	1.55	0.63	3.16	3.79	0.17	442
3160	0.82	0.06	0.84	0.90	0.07	430
3180	0.99	0.06	1.35	1.41	0.04	428
3200	10.85	0.59	25.08	25.67	0.02	444
3220	6.96	0.34	15.64	15.98	0.02	446
3240	0.56	0.07	0.48	0.55	0.13	415
3260	0.61	0.10	0.48	0.58	0.17	436
3280	0.64	0.03	0.52	0.55	0.05	451
3300	0.91	0.04	0.59	0.63	0.06	450
3320	0.85	0.10	1.02	1.12	0.09	448
3340	0.64	0.06	0.51	0.57	0.11	450
3360	0.65	0.08	0.54	0.62	0.13	448

A(iv)

3380	0.88	0.19	0.69	0.88	0.22	453
3400	0.75	0.11	0.68	0.79	0.14	449
3420	0.89	0.09	0.80	0.89	0.10	451
3440	0.98	0.06	0.88	0.94	0.06	452
3460	0.88	0.09	0.76	0.85	0.11	439
3480	0.84	0.04	0.65	0.69	0.06	454
3500	0.97	0.05	0.71	0.76	0.07	453
3520	0.84	0.06	0.55	0.61	0.10	458
3540	0.95	0.04	0.78	0.82	0.05	453
3560	0.78	0.09	0.49	0.58	0.16	430
3580	0.95	0.10	0.77	0.87	0.11	423
3600	1.01	0.06	0.74	0.80	0.08	453
3620	0.84	0.05	0.51	0.56	0.09	458
3640	0.90	0.06	0.70	0.76	0.08	436
3660	0.84	0.07	0.56	0.63	0.11	456
3680	0.78	0.06	0.49	0.55	0.11	457
3700	0.84	0.06	0.59	0.65	0.09	457
3720	0.85	0.08	0.72	0.80	0.10	457
3740	0.87	0.06	0.71	0.77	0.08	457
3760	0.83	0.06	0.56	0.62	0.10	459
3780	0.81	0.05	0.45	0.50	0.10	460
3800	0.84	0.05	0.57	0.62	0.08	468
3820	1.05	0.08	0.73	0.81	0.10	459
3840	1.03	0.05	0.53	0.58	0.09	462
3860	0.96	0.04	0.32	0.36	0.11	468
3880	1.21	0.05	0.46	0.51	0.10	448
3900	1.02	0.08	0.69	0.77	0.10	464
3920	0.84	0.07	0.56	0.63	0.11	466
3940	0.74	0.08	0.48	0.56	0.14	473
3960	0.77	0.10	0.71	0.81	0.12	454
3980	1.00	0.06	0.58	0.64	0.09	475
4000	0.76	0.09	0.56	0.65	0.14	474
4020	0.83	0.06	0.54	0.61	0.10	480
4040	0.91	0.08	0.60	0.68	0.12	484
4060	0.86	0.07	0.65	0.72	0.10	475
4080	0.54	0.04	0.33	0.37	0.11	485
4100	0.83	0.08	0.56	0.64	0.13	475
4120	0.77	0.10	0.52	0.62	0.16	479
4140	0.77	0.07	0.50	0.57	0.12	475
4160	0.75	0.06	0.41	0.47	0.13	475
4180	0.86	0.05	0.42	0.47	0.11	478
4200	0.73	0.05	0.42	0.47	0.11	471
4220	0.78	0.03	0.43	0.46	0.07	470
4240	0.74	0.06	0.54	0.60	0.10	468
4260	0.60	0.03	0.26	0.29	0.10	483

APPENDIX B

Geochemical Data Listing for

Duma-1 (Intermediate Tilted Blocks Sub-Basin)

Duma-1

Depth (m)	TOC (%)	S_1 (mg/g)	S_2 (mg/g)	S_1+S_2	PI $S_1/(S_1+S2$	T_{max}
520	0.41	0.00	0.19	0.19	0.00	446
540	0.54	0.01	0.41	0.42	0.02	444
560	0.42	0.00	0.28	0.28	0.00	445
580	0.12	0.00	0.05	0.05	0.00	448
600	0.31	0.00	0.20	0.20	0.00	444
620	0.38	0.08	0.29	0.37	0.22	444
640	0.54	0.01	0.47	0.48	0.02	435
660	0.25	0.00	0.15	0.15	0.00	443
680	0.28	0.00	0.17	0.17	0.00	444
700	0.12	0.00	0.05	0.05	0.00	419
720	0.33	0.01	0.29	0.30	0.03	445
740	0.13	0.00	0.05	0.05	0.00	320
760	0.29	0.00	0.15	0.15	0.00	451
780	0.26	0.00	0.25	0.25	0.00	450
800	0.15	0.00	0.09	0.09	0.00	446
820	0.23	0.00	0.15	0.15	0.00	447
840	0.33	0.00	0.22	0.22	0.00	447
860	0.71	0.04	0.79	0.83	0.05	446
880	1.01	0.03	1.75	1.60	0.02	444
900	1.00	0.09	1.60	1.69	0.05	443
920	0.44	0.02	0.70	0.72	0.03	446
940	0.42	0.02	0.54	0.56	0.04	443
960	0.48	0.03	0.55	0.58	0.05	446
980	0.49	0.04	0.59	0.63	0.06	446
1000	0.53	0.03	0.55	0.58	0.05	445
1020	0.55	0.03	0.54	0.57	0.05	445
1040	0.41	0.02	0.32	0.34	0.06	446
1060	0.50	0.02	0.42	0.44	0.05	445
1080	0.22	0.00	0.14	0.14	0.00	447
1100	0.62	0.05	0.75	0.80	0.06	445
1120	0.29	0.02	0.19	0.21	0.10	449
1140	0.34	0.02	0.27	0.29	0.07	448
1160	0.33	0.01	0.27	0.28	0.04	448
1180	0.39	0.02	0.42	0.44	0.05	445
1200	0.28	0.01	0.28	0.29	0.03	449
1220	0.19	0.00	0.14	0.14	0.00	450
1240	0.31	0.01	0.24	0.25	0.04	446
1260	0.45	0.02	0.31	0.33	0.06	451
1280	0.30	0.01	0.17	0.18	0.06	449
1300	0.14	0.00	0.06	0.06	0.00	454
1320	0.25	0.01	0.15	0.16	0.06	453
1340	0.25	0.00	0.16	0.16	0.00	443
1360	0.25	0.00	0.17	0.17	0.00	450
1380	0.36	0.00	0.28	0.28	0.00	447
1400	0.35	0.01	0.25	0.26	0.03	447
1420	1.04	0.10	1.07	1.17	0.09	447

B(ii)

1440	1.11	0.13	1.26	1.39	0.09	450
1460	0.19	0.00	0.10	0.10	0.00	453
1480	0.41	0.03	0.54	0.57	0.05	448
1500	0.82	0.08	1.36	1.94	0.04	447
1520	0.19	0.00	0.07	0.07	0.00	462
1540	0.15	0.00	0.07	0.07	0.00	444
1560	0.11	0.00	0.14	0.14	0.00	432
1580	0.25	0.01	0.21	0.22	0.05	438
1600	0.20	0.01	0.23	0.24	0.04	452
1620	0.16	0.01	0.17	0.18	0.06	451
1640	0.45	0.04	0.66	0.70	0.06	451
1660	0.29	0.01	0.34	0.35	0.03	453
1680	0.23	0.02	0.36	0.38	0.05	451
1700	0.37	0.03	0.57	0.60	0.05	454
1720	0.68	0.07	1.04	1.11	0.06	454
1740	0.28	0.21	0.33	0.54	0.39	469
1760	0.43	0.05	0.76	0.81	0.06	456
1780	0.40	0.01	0.31	0.32	0.03	454
1800	1.41	0.31	3.40	3.71	0.08	457
1820	0.34	0.11	0.52	0.63	0.17	456
1840	0.50	0.11	0.81	0.92	0.12	455
1860	0.52	0.05	0.99	1.04	0.05	455
1880	0.29	0.00	0.37	0.37	0.00	457
1900	0.44	0.02	0.59	0.61	0.03	454
1920	0.33	0.01	0.30	0.31	0.03	457
1940	0.47	0.04	0.69	0.73	0.05	433
1960	0.58	0.06	0.52	0.58	0.10	460
1980	0.35	0.02	0.20	0.22	0.09	460
2000	0.48	0.04	0.35	0.39	0.10	458
2020	0.53	0.04	0.50	0.54	0.07	458
2040	0.33	0.02	0.22	0.24	0.08	461
2060	0.70	0.08	0.46	0.54	0.15	463
2080	0.58	0.08	0.52	0.60	0.13	459
2100	0.26	0.08	0.17	0.25	0.32	462
2120	0.26	0.04	0.21	0.25	0.16	460
2140	0.50	0.10	0.54	0.64	0.16	460
2160	0.54	0.16	0.76	0.21	1.11	461
2180	0.54	0.12	0.52	0.64	0.19	443
2200	0.21	0.00	0.10	0.10	0.00	442
2220	0.55	0.07	0.58	0.65	0.11	459
2240	0.62	0.14	0.59	0.73	0.19	456
2260	0.77	0.14	0.74	0.88	0.16	459
2280	0.48	0.06	0.31	0.37	0.16	467
2300	1.13	0.19	1.73	1.92	0.10	461
2320	0.99	0.19	1.03	1.22	0.16	470
2340	0.10	0.00	0.05	0.00	0.05	115
2360	0.14	0.00	0.06	0.06	0.00	432
2400	0.30	0.01	0.17	0.18	0.06	461
2420	0.35	0.02	0.23	0.25	0.08	474
2440	0.57	0.06	0.34	0.42	0.15	444
2460	0.42	0.04	0.26	0.30	0.13	474
2480	0.52	0.06	0.44	0.50	0.12	465
2500	0.34	0.02	0.22	0.24	0.08	469

B(iii)

2520	0.34	0.03	0.23	0.26	0.12	470
2540	0.32	0.03	0.20	0.23	0.13	473
2560	0.47	0.04	0.26	0.30	0.13	473
2580	0.51	0.06	0.34	0.40	0.15	473
2600	0.48	0.07	0.38	0.45	0.16	474
2620	0.47	0.05	0.29	0.34	0.15	476
2640	0.47	0.09	0.33	0.42	0.21	473
2660	0.81	0.35	0.89	1.24	0.28	465
2680	0.51	0.09	0.40	0.49	0.18	474
2700	0.61	0.12	0.45	0.57	0.21	474
2720	0.47	0.06	0.38	0.44	0.14	456
2740	0.56	0.11	0.43	0.54	0.20	467
2760	0.35	0.07	0.21	0.28	0.25	475
2780	0.24	0.03	0.18	0.21	0.14	443
2800	0.38	0.05	0.22	0.27	0.19	482
2820	0.27	0.03	0.12	0.15	0.20	482
2840	1.02	0.27	0.53	0.80	0.34	485
2860	0.57	0.11	0.22	0.33	0.33	466
2880	0.15	0.00	0.04	0.04	0.00	407
2900	0.31	0.03	0.13	0.16	0.19	450
2920	0.13	0.00	0.03	0.03	0.00	392
2940	0.57	0.10	0.27	0.37	0.27	489
2960	0.10	0.00	0.01	0.01	0.00	166
2980	0.17	0.01	0.07	0.08	0.13	474
3000	0.49	0.06	0.18	0.24	0.25	499
3020	0.14	0.00	0.05	0.05	0.00	428
3040	0.89	0.06	0.31	0.37	0.16	486
3060	0.50	0.03	0.15	0.18	0.17	501
3080	0.17	0.00	0.03	0.03	0.00	340
3100	0.33	0.01	0.13	0.14	0.07	471
3120	0.65	0.01	0.13	0.14	0.07	521
3140	0.17	0.01	0.05	0.06	0.17	235
3160	0.40	0.01	0.08	0.09	0.11	511
3180	0.36	0.01	0.07	0.08	0.13	510
3200	0.47	0.01	0.11	0.13	0.15	517
3220	0.47	0.02	0.10	0.11	0.09	520
3240	0.52	0.01	0.80	0.08	0.00	520
3260	0.60	0.00	0.13	0.14	0.07	485
3280	0.55	0.01	0.12	0.13	0.08	498
3300	0.71	0.01	0.24	0.26	0.08	486
3320	0.37	0.02	0.06	0.06	0.00	463
3333	0.59	0.00	0.08	0.08	0.00	484
		0.00				

APPENDIX C

Geochemical Data Listing for

Anza-1 (Yamicha Sub-basin)

Anza-1

Depth (m)	TOC (%)	S_1 (mg/g)	S_2 (mg/g)	S_1+S_2	S_1/S_1+S_2	Tmax
1820	0.01	0.02	0.03	0.05	0.04	311
1840	0.21	0.25	1.07	1.32	0.19	348
1860	0.00	0.02	0.00	0.02	1.00	256
1880	0.01	0.03	0.02	0.05	0.60	211
1900	0.02	0.02	0.04	0.06	0.33	216
1920	0.01	0.01	0.01	0.02	0.50	212
1940	0.01	0.00	0.00	0.00	0.00	195
1960	0.03	0.00	0.03	0.03	0.00	232
1980	0.05	0.01	0.03	0.04	0.25	244
2000	0.09	0.04	0.18	0.22	0.18	269
2020	0.08	0.02	0.09	0.11	0.18	282
2040	0.03	0.03	0.05	0.08	0.38	233
2060	0.06	0.05	0.11	0.16	0.31	291
2080	0.05	0.07	0.20	0.27	0.26	312
2100	0.03	0.01	0.02	0.03	0.33	317
2120	0.07	0.06	0.18	0.24	0.25	312
2140	0.06	0.09	0.15	0.24	0.38	140
2160	0.57	0.08	0.33	0.41	0.20	286
2180	0.12	0.19	0.32	0.51	0.37	302
2200	0.05	0.02	0.10	0.12	0.17	306
2220	0.11	0.23	0.35	0.58	0.40	315
2240	0.05	0.02	0.11	0.13	0.15	318
2260	0.04	0.01	0.02	0.03	0.33	243
2280	0.05	0.00	0.01	0.01	0.00	210
2300	0.06	0.00	0.08	0.08	0.00	346
2320	0.06	0.02	0.12	0.14	0.14	364
2340	0.04	0.00	0.03	0.03	0.03	294
2360	0.03	0.00	0.01	0.01	0.00	261
2380	0.06	0.01	0.07	0.08	0.13	398
2400	0.19	0.08	0.29	0.37	0.22	445
2420	0.00	0.00	0.11	0.11	0.00	488
2440	0.00	0.00	0.12	0.12	0.00	414
2460	0.00	0.00	0.10	0.10	0.00	411
2480	0.01	0.02	0.16	0.18	0.11	446
2500	0.02	0.02	0.13	0.15	0.13	455
2520	0.01	0.01	0.06	0.07	0.14	339
2540	0.00	0.03	0.07	0.10	0.30	294
2560	0.01	0.06	0.11	0.17	0.35	303
2580	0.00	0.02	0.07	0.09	0.22	337
2600	0.00	0.02	0.07	0.09	0.22	320
2630	0.00	0.01	0.07	0.08	0.13	362
2640	0.00	0.02	0.01	0.03	0.67	296
2660	0.00	0.03	0.02	0.05	0.60	300
2680	0.00	0.07	0.06	0.13	0.54	234
2700	0.04	0.09	0.22	0.31	0.29	338
2720	0.01	0.10	0.06	0.16	0.63	270
2740	0.03	0.12	0.03	0.15	0.80	262

C(ii)

Depth (m)	TOC (%)	S_1 (mg/g)	S_2 (mg/g)	S_1+S_2	S_1/S_1+S_2	Tmax
2760	0.08	0.25	0.30	0.55	0.45	300
2780	0.14	0.77	0.46	1.23	0.11	324
2800	0.16	0.56	0.36	0.92	0.61	287
2820	0.11	0.51	0.23	0.74	0.69	252
2840	0.45	0.19	0.07	0.26	0.73	251
2860	0.03	0.08	0.04	0.12	0.62	269
2880	0.04	0.14	0.06	0.20	0.70	291
2900	0.05	0.09	0.07	0.16	0.56	268
2920	0.02	0.12	0.06	0.18	0.67	310
2940	0.06	0.25	0.10	0.35	0.71	282
2960	0.05	0.33	0.09	0.42	0.79	292
2980	0.05	0.17	0.08	0.25	0.68	252
3000	0.15	0.23	0.17	0.40	0.58	249
3020	0.07	0.27	0.13	0.40	0.68	365
3040	0.01	0.15	0.02	0.17	0.88	228
3060	0.05	0.24	0.06	0.30	0.80	236
3080	3.82	4.07	28.62	32.69	0.12	334
3100	0.01	0.29	2.30	2.59	0.11	318
3120	0.44	0.19	0.97	1.16	0.16	321
3140	0.08	0.10	0.14	0.24	0.42	261
3160	0.16	0.09	0.32	0.41	0.22	289
3180	0.48	0.10	0.74	0.84	0.12	284
3200	0.33	0.12	0.32	0.44	0.27	353
3220	0.15	0.03	0.11	0.14	0.21	264
3240	0.87	0.13	1.31	0.44	0.30	299
3260	0.15	0.01	0.11	0.12	0.08	294
3280	0.37	0.04	0.64	0.68	0.06	299
3300	0.42	0.05	0.99	1.04	0.05	338
3320	0.05	0.01	0.03	0.04	0.25	312
3340	0.17	0.04	0.20	0.24	0.17	365
3360	0.14	0.02	0.19	0.21	0.10	297
3380	0.08	0.01	0.12	0.13	0.08	322
3400	0.03	0.00	0.01	0.00	0.00	253
3420	0.06	0.00	0.15	0.15	0.00	308
3440	0.08	0.01	0.07	0.08	0.13	261
3460	0.02	0.00	0.02	0.02	0.00	232
3480	0.06	0.03	0.10	0.13	0.23	266
3500	0.08	0.07	0.40	0.47	0.15	340
3520	0.04	0.02	0.09	0.11	0.18	290
3540	0.23	0.03	0.15	0.18	0.17	332
3560	0.04	0.04	0.13	0.17	0.24	317
3580	0.14	0.08	0.28	0.36	0.22	353
3600	0.11	0.02	0.13	0.15	0.13	341
3620	0.08	0.04	0.08	0.12	0.33	289
3640	0.06	0.03	0.07	0.10	0.30	302
3660	0.03	0.02	0.38	0.40	0.05	284

APPENDIX D

Geochemical Data Listing for

Bellatrix-1 (Chalbi Sub-basin)

Bellatrix-1

Depth (m)	TOC (%)	S_1 (mg/g)	S_2 (mg/g)	S_1+S_2	S_1/S_1+S_2	Tmax
1380	0.00	0.00	0.03	0.03	0.00	349
1400	0.00	0.00	0.03	0.03	0.00	461
1420	0.00	0.00	0.02	0.02	0.00	616
1440	0.00	0.00	0.01	0.01	0.00	296
1800	0.04	0.00	0.10	0.00	0.00	586
1820	0.02	0.00	0.04	0.07	0.00	502
1840	0.01	0.00	0.02	0.02	0.00	298
1860	0.00	0.00	0.05	0.05	0.00	506
1880	0.03	0.00	0.04	0.04	0.00	439
1900	0.03	0.00	0.04	0.04	0.00	308
1920	0.11	0.00	0.19	0.19	0.00	429
1940	0.05	0.00	0.09	0.09	0.00	436
1960	0.09	0.00	0.08	0.08	0.00	451
2080	0.09	0.00	0.08	0.08	0.00	354
2100	0.07	0.00	0.07	0.00	0.00	470
2140	0.01	0.00	0.00	0.00	0.00	0
2160	0.06	0.00	0.01	0.01	0.00	196
2180	0.06	0.00	0.03	0.03	0.00	485
2200	0.03	0.00	0.01	0.01	0.00	387
2220	0.24	0.00	0.13	0.13	0.00	443
2240	0.63	0.00	0.58	0.58	0.00	439
2260	1.65	0.02	3.12	3.14	0.01	442
2280	4.58	0.11	10.65	10.76	0.01	438
2300	0.49	0.00	0.39	0.39	0.00	443
2320	0.40	0.00	0.30	0.30	0.00	445
2340	0.35	0.01	0.19	0.20	0.05	446
2360	0.40	0.01	0.18	0.19	0.05	446
2380	0.43	0.02	0.20	0.22	0.09	445
2400	0.58	0.02	0.29	0.31	0.06	442
2420	0.68	0.02	0.42	0.44	0.05	446
2440	0.87	0.02	0.63	0.65	0.03	444
2460	0.82	0.02	0.63	0.65	0.03	445
2480	0.61	0.02	0.44	0.46	0.04	442
2500	0.59	0.03	0.33	0.36	0.08	443
2520	0.73	0.02	0.41	0.43	0.05	445
2540	0.63	0.01	0.31	0.32	0.03	448
2560	0.64	0.01	0.35	0.36	0.03	449
2580	0.63	0.01	0.39	0.40	0.03	448
2600	0.58	0.02	0.50	0.52	0.04	449
2620	0.33	0.02	0.23	0.25	0.08	448
2640	0.84	0.08	1.66	1.74	0.05	450
2660	0.44	0.03	0.32	0.35	0.09	449
2680	0.30	0.03	0.17	0.20	0.15	440
2700	0.34	0.03	0.17	0.20	0.15	450
2720	0.86	0.06	0.49	0.55	0.11	449
2740	0.66	0.05	0.43	0.48	0.12	446
2760	0.60	0.06	0.45	0.51	0.12	449

D(ii)

Depth (m)	TOC (%)	S_1 (mg/g)	S_2 (mg/g)	S_1+S_2	S_1/S_1+S_2	Tmax
2780	0.81	0.07	0.89	0.96	0.07	447
2800	0.54	0.04	0.61	0.65	0.06	453
2820	0.64	0.04	0.61	0.65	0.06	451
2840	0.53	0.02	0.42	0.44	0.05	451
2860	0.49	0.01	0.26	0.27	0.04	452
2880	0.14	0.00	0.06	0.06	0.00	309
2900	0.15	0.00	0.06	0.06	0.00	298
2920	0.31	0.04	0.48	0.52	0.08	318
2940	0.28	0.06	0.35	0.41	0.15	453
2960	0.39	0.09	0.23	0.32	0.28	454
2980	0.14	0.07	0.06	0.13	0.54	457
3000	0.46	0.11	0.33	0.44	0.25	303
3020	0.89	0.17	1.15	1.32	1.13	453
3040	0.30	0.04	0.20	0.24	0.17	461
3060	0.19	0.01	0.12	0.13	0.08	482
3080	0.17	0.02	0.14	0.16	0.13	457
3100	1.23	0.25	1.53	1.78	0.14	458
3120	0.37	0.07	0.40	0.47	0.15	459
3140	0.51	0.10	0.43	0.53	0.19	459
3160	1.44	0.50	2.24	2.74	0.18	454
3180	0.33	0.08	0.33	0.41	0.20	461
3200	0.56	0.19	0.76	0.95	0.20	461
3220	0.70	0.16	0.67	0.83	0.19	462
3240	0.45	0.07	0.40	0.47	0.15	467
3260	0.66	0.16	0.69	0.85	0.19	463
3280	1.50	0.02	2.10	2.12	0.01	433
3300	0.39	0.08	0.67	0.75	0.11	463
3320	0.37	0.08	0.32	0.40	0.20	467
3340	0.33	0.03	0.27	0.30	0.10	460
3360	0.34	0.06	0.30	0.09	0.67	467
3380	0.42	0.05	0.24	0.29	0.17	465
3400	0.34	0.05	0.31	0.36	0.14	460
3420	0.37	0.08	0.36	0.44	0.18	465
3440	0.51	0.11	0.43	0.54	0.20	466

APPENDIX E

Geochemical Data Listing for

Sirius-1 (Chalbi Sub-basin)

Sirius-1

Depth (m)	TOC (%)	S_1 (mg/g)	S_2 (mg/g)	S_1+S_2	S_1/S_1+S_2	Tmax
1460	0.08	0.00	0.21	0.21	0.00	445
1480	0.51	0.12	9.54	9.66	0.01	444
1500	1.34	0.10	8.76	8.86	0.01	509
1520	0.74	0.06	3.77	3.83	0.02	446
1540	0.19	0.01	0.28	0.29	0.03	501
1560	1.47	0.07	8.99	9.06	0.01	445
1580	2.06	0.12	14.24	14.36	0.01	444
1600	1.69	0.10	10.34	10.44	0.01	444
1620	3.19	0.24	21.07	21.31	0.01	444
1640	1.08	0.08	4.83	4.91	0.02	444
660	1.19	0.08	5.11	5.19	0.02	446
1680	2.60	1.15	16.61	17.76	0.06	444
1700	1.65	0.13	8.04	8.17	0.02	441
1720	2.09	0.15	13.84	13.99	0.01	446
1740	2.37	0.17	14.40	14.57	0.01	444
1760	1.04	0.11	4.68	4.79	0.02	447
1780	1.42	0.16	7.10	7.26	0.02	445
1800	1.38	0.11	6.23	6.34	0.02	445
1820	1.47	0.16	6.63	6.79	0.02	443
1840	1.12	0.11	4.81	4.92	0.02	444
1860	0.90	0.05	2.66	2.71	0.02	445
1880	0.78	0.05	2.46	2.51	0.02	448
1900	0.76	0.08	2.01	2.09	0.04	443
1920	0.85	0.06	1.87	1.93	0.03	447
1940	1.85	0.26	9.77	10.03	0.03	447
1960	0.42	0.07	0.73	0.80	0.09	442
1980	0.66	0.08	1.09	1.17	0.07	444
2000	0.64	0.09	1.02	1.11	0.08	444
2020	0.86	0.11	1.30	1.41	0.08	443
2040	0.81	0.09	1.09	1.18	0.08	443
2060	0.88	0.10	1.25	1.35	0.07	443
2080	0.68	0.08	0.54	0.62	0.13	445
2100	0.52	0.08	0.62	0.70	0.11	443
2180	0.31	0.02	0.12	0.14	0.14	439
2200	0.54	0.05	0.29	0.34	0.15	459
2220	0.48	0.03	0.26	0.29	0.10	447
2240	0.58	0.05	0.41	0.46	0.11	436
2260	0.36	0.02	0.18	0.20	0.10	459
2280	0.57	0.03	0.53	0.56	0.05	445
2300	0.76	0.08	0.63	0.71	0.11	443
2320	0.65	0.08	2.47	2.55	0.03	446
2340	0.45	0.03	0.49	0.52	0.06	448
2360	0.66	0.09	0.98	1.07	0.08	445
2380	0.42	0.03	0.26	0.29	0.10	498
2400	0.16	0.01	0.09	0.10	0.10	453
2420	0.21	0.01	0.21	0.22	0.05	447
2440	0.09	0.02	0.07	0.09	0.22	442

E(ii)

2460	0.45	0.05	0.58	0.63	0.08	411
2480	0.35	0.04	0.31	0.35	0.11	441
2500	0.35	0.02	0.75	0.77	0.03	444
2520	0.08	0.01	0.08	0.09	0.11	522
2530	0.04	0.01	0.04	0.05	0.20	582